University of Nevada

Reno

Geology, Geochemistry, and Alteration of the Seligman and Monte Cristo Stocks, White Pine Mining District, White Pine County, Nevada

A thesis submitted in partial fulfillment of the requirements for the degree of Master of Science in Geology

by

Mines Library
University of Nevada - Reno
Reno, Nevada 89557-0044

Thomas R. Putney

August, 1985

MINES
LIBRARY
Thesis
1986

The thesis of Thomas R. Putney is approved:

L. F. Larson

Thesis Advisor

L. F. Larson

Department Chairman

John E. Nellor

Dean, Graduate School

University of Nevada

Reno

August, 1985

ACKNOWLEDGEMENTS

I wish to thank Phillips Petroleum Company - Minerals Division which provided funding for analytical work, and access to geologic data from the Mt. Hamilton project. Bob Forest of Phillips' Reno office, first suggested the possiblility of doing a thesis at Mt. Hamilton, and arranged for my summer employment there in 1981. Steve Jones, project geologist at Mt. Hamilton and fellow graduate student, was extremely helpful in providing base maps and unpublished geologic data, and in imparting to me some of his extensive knowledge of the Mt. Hamilton deposit.

Union Carbide - Metals Division allowed access to and sampling of drill core from the Monte Cristo area.

I am grateful to the members of my thesis committee for their help during the project. Dr. L.T. Larson provided useful suggestions on improving the thesis, and at various times provided additional impetus to finish the project. Dr. M.J. Hibbard helped with the petrographic study and Dr. Dan Taylor provided assistance with the statistical analysis.

Dr. and Mrs. Kendall Jones graciously provided food and lodging during my stays in Ely in the summers of 1982 and 1983.

Numerous graduate students, including Glenn

Gierzycki, Joe Graney, Carl Frost, and Phil Jackson, provided friend- ship and lively discussions of ore deposits and more mundane subjects. Dr. Don Hudson provided the basic computer programs used in the thesis, and stimulating discussions of hydrothermal alteration. Terry Sprecher graciously provided a much-needed "short course" in word-processing. I am especially grateful to Marla Osborne for her moral and technical support and encouragement throughout the project.

Finally, I would like to thank my parents for their support and encouragement in everything I have done.

ABSTRACT

The Seligman and Monte Cristo stocks are small, Cretaceous, granodioritic to granitic plutons which produced calcic exoskarns and associated tungsten-molybdenum mineralization in the Cambrian carbonates they intruded. The stocks are the surface expression of a much larger granodioritic intrusive body. Age dates are inconclusive, but the Monte Cristo stock is inferred to be younger than the Seligman stock, based on the spatial distribution of plagioclase-pyroxene endoskarn in the Seligman stock.

Rock types associated with the Seligman stock include granodiorite, granite, aplite, dacite porphyry, quartz monzodiorite and diorite. Intrusives associated with the Monte Cristo stock include granite porphyry, granodiorite porphyry, and rhyodacite porphyry. Variations in major and trace element chemistry, between the intrusive rock types, are related to the degree of magmatic differentiation and the affects of later hydrothermal alteration in the rocks.

The Seligman stock exhibits characteristics, such as equigranular texture and endoskarn development, which are typical of plutons which are associated with tungsten skarn deposits, whereas the Monte Cristo stock exhibits porphyritic texture, intense stockwork quartz veining, and potassic alteration which are more typical of plutons associated with porphyry copper or molybdenum deposits.

TABLE OF CONTENTS

LIST OF ILLUSTRATIONS

Figures

Figures

Figures

Plates

Plates In Pocket

LIST OF TABLES

INTRODUCTION

LOCATION AND ACCESS

The Seligman-Monte Cristo area is in the western part of the White Pine Mining District, in White Pine County, Nevada (Figure 1), and encompasses all or parts of Sections 8, 9, 10, 15, 16, 17, 20, 21, and 22, in Township 16N, Range 57E. The area is on the west flank of Pogonip Ridge, about 4 air miles west of the abandoned town of Hamilton and 36 air miles west of Ely. Access to the general area is via a county-maintained gravel road which turns south from U.S. Highway 50 about 48 miles west of Ely and 35 miles east of Eureka.

The Seligman area proper is accessed via an unimproved road which turns off to the southeast from the county maintained road about 8.5 miles south of Highway 50 and extends up Seligman Canyon. The study area is criss-crossed by drill roads which connect the Seligman Canyon road with Monte Cristo Canyon (Plate 1). Elevations in the area range from 7400 feet at the range front to over 10,700 feet at Mt. Hamilton, and the area is generally inaccessible to vehicles from November to May due to heavy snowfall.

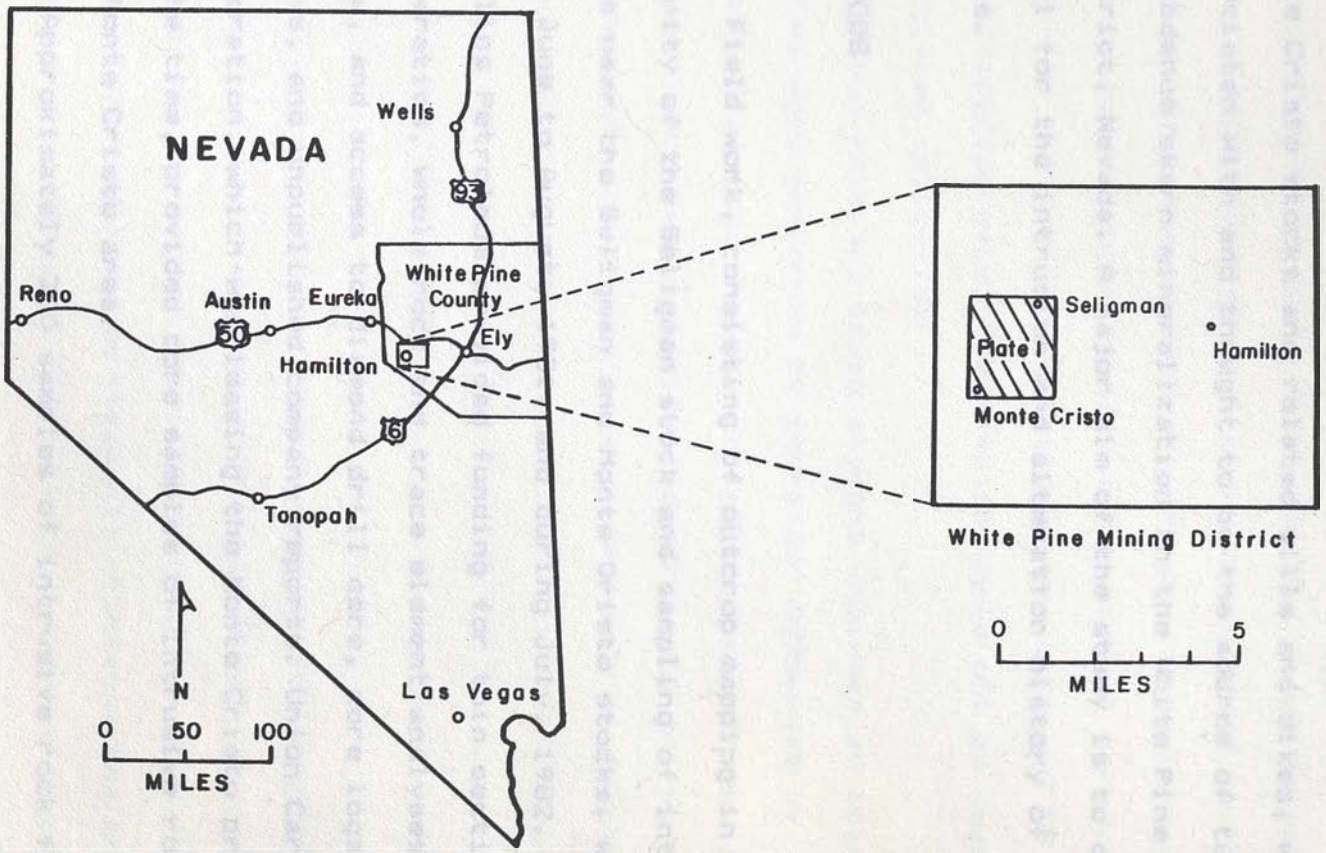

Fig. 1. Map showing location of White Pine Mining District and Seligman - Monte Cristo area.

PURPOSE

The purpose of this thesis is to describe the geology, alteration, and geochemistry of the Seligman and Monte Cristo stocks and related sills and dikes, which are associated with and thought to be the source of tungsten-molybdenum skarn mineralization in the White Pine mining district, Nevada. A major aim of the study is to develop a model for the intrusion and alteration history of these rocks.

METHODS

Field work, consisting of outcrop mapping in the vicinity of the Seligman stock and sampling of intrusive rocks near the Seligman and Monte Cristo stocks, was done from June to August, 1981, and during July, 1982. Phillips Petroleum provided funding for thin section preparation, whole rock and trace element analyses, K-Ar dates, and access to diamond drill core, core logs, assays, and unpublished company reports. Union Carbide Corporation, which was leasing the Monte Cristo property at the time, provided core samples of intrusive rock from the Monte Cristo area.

Approximately 300 samples of intrusive rock from outcrops and drill core were studied in thin section, to

determine primary and alteration mineralogy, using standard petrographic techniques. The majority of these (210) were from core holes drilled by Phillips around the Seligman stock, whereas 25 samples were from holes drilled in and around the Monte Cristo stock. About 40 samples of contact metamorphosed wall rock were studied in thin section. Selected samples of intrusive rock were point counted to determine primary modal mineral percentages, and x-ray diffraction techniques were utilized in the identification of minerals which could not be readily identified optically.

Whole rock and trace element analyses of intrusive samples were performed by Barringer Resources by inductively-coupled plasma emission spectroscopy. Computer programs were used to calculate norms and petrologic indices, and to perform cluster analysis on geochemical data .

CLIMATE AND VEGETATION

Climate in the study area ranges from mid-latitude steppe in the valley west of Pogonip Ridge, to subhumid continental at higher elevations (Houghton and others, 1975). The mid-latitude steppe is characterized as semiarid with adequate rainfall to support sagebrush, various grasses, dwarf pinyon and juniper trees, whereas

the subhumid zone is characterized by mountain mahogany, quaking aspen, and pine. Bristlecone pines occur near the top of Pogonip Ridge. Summers are generally mild with maximum July temperatures averaging less than 84 degees F., whereas winters are severe; minimum January temperatures average 12 to 20 degrees F. and higher elevations receive 40 to 80 inches of snow per year (Houghton and others, 1975).

HISTORY AND PREVIOUS STUDIES

The history of the White Pine mining district has been discussed by several authors, including Larsh (1909), Humphrey (1960), Jackson (1963), and Hose and others (1976). Most of the production has been from the silver and lead-silver belts which are shown on Figure 2. About 22 million dollars worth of silver was produced between 1865 and 1886 from shallow, high grade cerargyrite deposits in brecciated Guilmette Limestone on Treasure Hill (Hose and others,1976). The high grade silver ore was discovered on Treasure Hill in 1867, and by 1869 there were more than 25,000 people in the district. The shallow ores were depleted by 1872 and exploration failed to locate significant extensions of the ore at depth. By 1885, when a fire destroyed the town of Hamilton, silver mining on Treasure Hill had virtually ended.

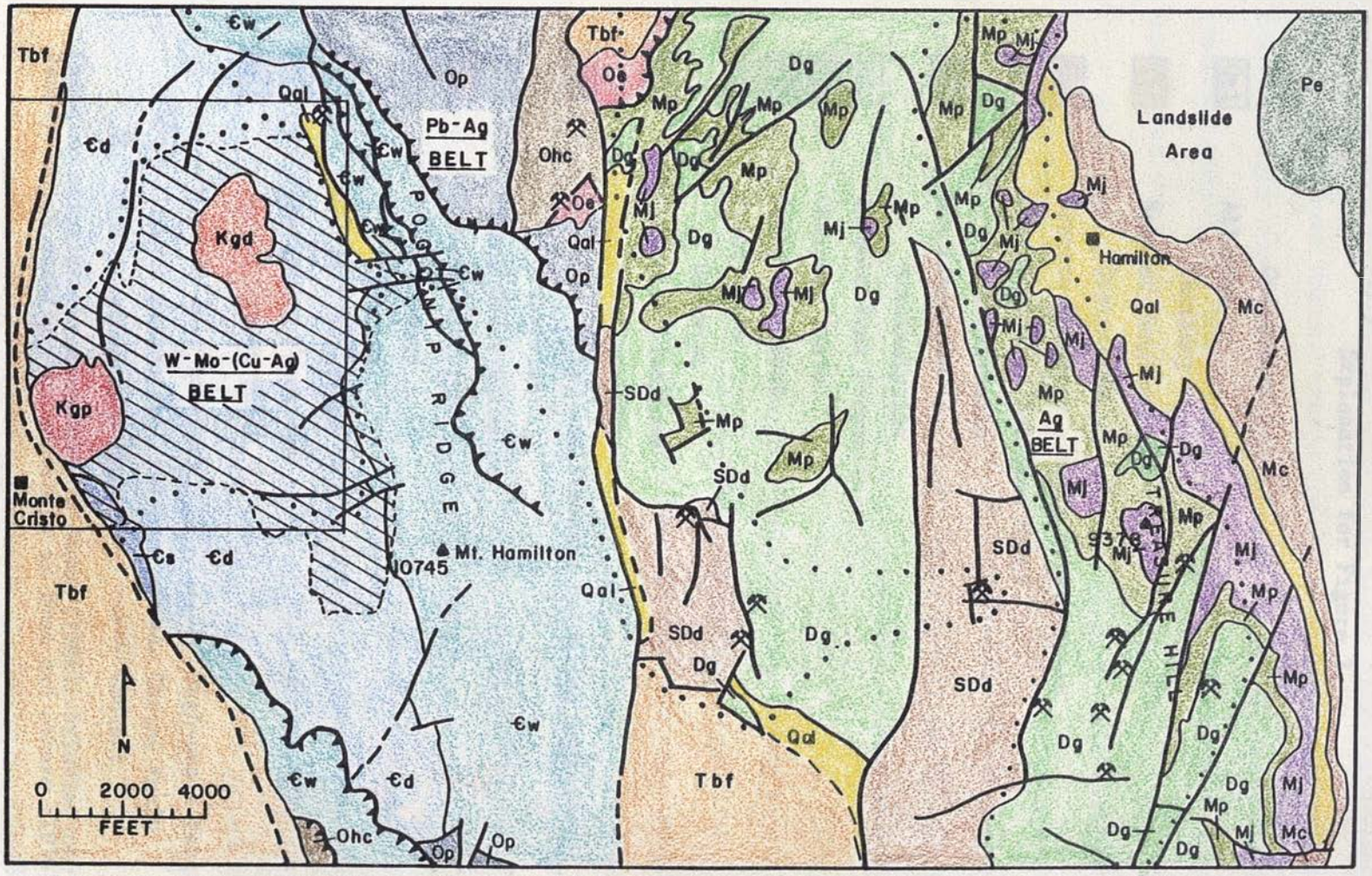

Fig. 2. Generalized geologic map of White Pine Mining District, showing location of mineral belts and outline of thesis area. Modified from Humphrey (1960). Explanation on following page.

Explanation for Figure 2.

Quaternary

Qal — Alluvium

Tertiary

Tbf — Belmont Fanglomerate

Cretaceous

Kgp — Granite Porphyry - Monte Cristo Stock

Kgd — Granodiorite - Seligman Stock

Pennsylvanian

Pe — Ely Limestone

Mississippian

Mdp — Diamond Peak Formation

Mc — Chainman Shale

Mj — Joana Limestone

Mp — Pilot Shale

Devonian

Dg — Guilmette Limestone

Silurian-Devonian

SDd — Laketown, Sevy, and Simonson Dolomites Undivided

Ordovician

Ohc — Hanson Creek Dolomite

Oe — Eureka Quartzite

Op — Pogonip Group

Cambrian

Cw — Windfall Formation

Cd — Dunderburg Formation

Cs — Secret Canyon Shale

····· Mineral belt boundary

Contact metamorphic aureole

Mine or group of mines

— - - — High-angle fault

Thrust fault

Contact

Cambrian stratigraphy according to Jones (1984); Silurian to Pennsylvanian stratigraphy according to Hose and others (1976)

Production from the district since 1886 has been from the lead-silver belt, where lead-silver replacement ore bodies occur near steep faults and low-angle bedding plane faults, mostly in the Hanson Creek, Lone Mountain and Guilmette Formations (Hose and others, 1976).

Minor production of silver by reworking of dumps has occurred sporadically since the times of major mining activity, and an unspecified, but probably minor amount of tungsten was produced from the Monte Cristo area (Tungsten-Molybdenum-Copper Belt) in 1954 (Hose and others, 1976).

Exploration activity in the district since the 1950's has been mostly concentrated in the vicinity of the Seligman and Monte Cristo stocks. Copper was the original exploration target, but more recently tungsten-molybdenum and precious metal mineralization associated with skarn surrounding the two stocks has been investigated. At present (1985) the area around the Seligman stock is claimed by Phillips Petroleum Company, and the Monte Cristo area is controlled by Umont Mining Company. Phillips has drilled over 60 core and rotary holes in the Seligman area since 1972, and a like number of holes have been drilled within and peripheral to the Monte Cristo stock by several companies since the 1950's.

The geology and ore deposits of the White Pine mining district have been described by several authors. Hague

(1870) first described the general geology of the district and the cerargyrite deposits on Treasure Hill. Larsh (1909) published a map of the district, including the Seligman-Monte Cristo area, and first noted the apparent zoned nature of the district from copper in the west to lead and silver in the east. Keys (1955) described the occurrence of lead-silver mineralization at the Mary Ellen mine.

Humphrey (1960) did the first detailed study of the district. He described the stratigraphy, structure, and ore deposits, and mapped all accessible mine workings. Papers by Hewitt and others (1965) and Smith (1970) describe the occurrence of silver-bearing black calcite at Treasure Hill.

Sonnevil (1979) studied the development of skarn surrounding the Monte Cristo stock, and included brief descriptions of the intrusive rocks. Jones (1984) described skarn mineralization surrounding the Seligman stock with emphasis on silver sulfosalt veins which occur in and near the stock. In addition to published reports, several Phillips company reports and maps have been utilized in this study.

REGIONAL GEOLOGY AND STRUCTURE

The Seligman-Monte Cristo area is on the west flank of Pogonip Ridge, a faulted block which lies just west of the northern end of the White Pine Range. The White Pine Range is a north-trending block-faulted mountain range which extends from northeastern Nye County into southwestern White Pine County. The lithologic sequence in the range consists of up to 23,000 feet of Paleozoic carbonates and clastics which are overlain by up to 15,000 feet of Tertiary volcanic and sedimentary rocks (Moores and others, 1968).

Cambrian to Devonian carbonates and minor clastics were deposited in miogeosynclinal environments, and are part of the eastern carbonate assemblage which forms the lower plate of the Roberts Mountain Thrust in central Nevada (Stewart, 1980). The study area is about 25 miles east of the leading edge of the thrust, which was emplaced during the Late Devonian - Early Mississippian Antler Orogeny. Post Antler deposition in the area is represented by Mississippian clastics and carbonates and Pennsylvanian - Permian carbonates which were deposited in the Antler foreland basin to the east of the orogenic belt (Stewart, 1980).

Tertiary ash flow tuffs, flows, and clastic sedimentary rocks overlie the Paleozoic sequence, and

occur predominantly in the southern part of the range.

Mesozoic intrusive activity in the White Pine Range is represented by two small Cretaceous stocks of granodioritic to granitic composition which intrude Cambrian carbonates in the Seligman-Monte Cristo area. These stocks are part of an east-west trending belt of isolated, Early Cretaceous plutons of intermediate composition, which extends from Ely to Eureka (Hose and others, 1976). This belt includes a dacite porphyry stock in the Pancake Range, 10 miles west of the study area, and the monzonite porphyries associated with copper deposits in the Robinson district, 30 miles to the east. Tertiary intrusive activity is represented by three small quartz monzonitic to granitic stocks which intrude Paleozoic carbonates at the southern end of the White Pine Range.

The structure of the northern, central, and southern portions of the White Pine Range has been discussed by Humphrey (1960), Tracy (1980), and Moores and others (1968), respectively. In general, two major deformational episodes have affected the range. The first episode in Late Mesozoic to Early Tertiary time produced broad north to northeast-trending folds and high-angle faults, and local thrust faults in the Paleozoic rocks. This episode was probably responsible for doming of lower Paleozoic rocks on Pogonip Ridge and the formation of high-angle faults which localized ore deposits in the silver and

lead-silver belts in the White Pine mining district (Humphrey, 1960). Doming on Pogonip Ridge may be a result of intrusion of the Seligman and Monte Cristo stocks in Early Cretaceous time.

The second major deformation probably occurred in late Tertiary time as a result of basin and range extension, which uplifted the White Pine Range and Pogonip Ridge along high-angle normal faults. Low-angle detachment faults, which emplaced younger rocks over older rocks in the central and southern White Pine Range probably resulted from gravity sliding associated with uplift of the range (Moores and others, 1968; Tracy, 1980).

LOCAL STRATIGRAPHY

Sedimentary rocks in the Seligman-Monte Cristo area consist of Middle to Upper Cambrian interbedded limestones, shales and siltstones. Contact metamorphism and metasomatism, associated with the intrusion of the Seligman and Monte Cristo stocks, have converted these rocks to calc-silicate skarn, hornfels, and marble at intrusive contacts and for distances of as much as 5,000 feet away from intrusive outcrops (Figure 2 and Plate 1).

Metamorphism, faulting and poor exposure have generally prevented the development of a detailed stratigraphic sequence based on surface outcrops. Humphrey (1960) correlated the sedimentary rocks on Pogonip Ridge with the Cambrian section in the Eureka mining district, 30 miles to the west. Subsequent work by Jones (1984), based primarily on drill core logging and additional fossil data, has refined the stratigraphy of the area. The following description of the stratigraphic section is based largely on that of Jones (1984) with additional data for the Monte Cristo area from Sonnevil (1979). The generalized stratigraphy of the area is shown on Figure 2.

Formations present in the study area include the Middle Cambrian Eldorado Dolomite, Geddes Limestone, and Secret Canyon Shale, and the Upper Cambrian Dunderburg Shale and Windfall Formation. Surface exposure is limited

to the top part of the Secret Canyon Shale and younger formations. The Eldorado Dolomite and Geddes Limestone are present only in the subsurface, where they have been intersected in drill holes greater than 2,000 feet deep peripheral to the Monte Cristo stock. All of these units were defined and described by Nolan and others (1956) from their type area, the Eureka mining district.

The Eldorado Dolomite is the oldest unit present in the study area. The Eldorado consists of gray to white, medium to coarse grained dolomitic marble, which commonly contains serpentine veinlets and stockwork pyrite-magnetite veinlets where it has been intersected in drill hole PH-56 (Plates 1 and 3). The total thickness of this unit is unknown, but about 500 feet of it is present at the bottom of PH-56, and as much as 650 feet of it has been drilled south of the Monte Cristo stock (Sonnevil, 1979).

The Geddes Limestone overlies the Eldorado Dolomite and consists of massive limestone, which is typically brecciated and silicified. Drilling has indicated that its thickness varies from 6 to 195 feet south of the Monte Cristo stock (Sonnevil, 1979), and from 20 to 80 feet north of the stock (Jones, 1984). This unit is assigned to the Geddes based on its lithology and stratigraphic position between dolomitic marble and overlying interbedded siltstone and limestone of the Secret Canyon

Shale. Hose and others (1976) consider the Eldorado Dolomite and Geddes Limestone to be correlative with the Pole Canyon Limestone in the southern White Pine Range and elsewhere in White Pine County.

The Middle Cambrian Secret Canyon Shale consists of 1,600 to 1,700 feet of interbedded limestone and siltstone, which has been variably metamorphosed to calc-silicate hornfels, skarn, and marble. Jones (1984) has divided the Secret Canyon into two members; an upper wavy-bedded member consisting of alternating thin layers of limestone and siltstone which have been converted to marble and pyroxene hornfels, respectively, and a lower evenly bedded silty member. Two shaly siltstone beds, ranging in thickness from 10 to 100 feet, which have been converted to biotite hornfels, are present in the Secret Canyon, and have been used as marker beds for correlating between drill holes (Jones, 1984).

In the Eureka district, Nolan and others (1956) described a thick-bedded dolomite, overlying the Secret Canyon Shale, which he assigned to the Hamburg Dolomite. This dolomite has not been observed in the Seligman-Monte Cristo area, where the Secret Canyon is overlain by 1,300 to 1,500 feet of interbedded limestone and calcareous siltstone which has been assigned to the Upper Cambrian Dunderburg Shale by Jones (1984) on the basis of lithology and fossil data. The Secret Canyon as defined by Jones in

the study area may include Middle to early Upper Cambrian rocks which are correlative with the Hamburg Dolomite. Rocks equivalent to the Secret Canyon Shale and Hamburg Dolomite have been assigned to the Lincoln Peak Formation in the southern White Pine Range (Moores and others, 1968).

The Dunderburg Shale is 265 feet thick in the Eureka district, where it overlies the Hamburg Dolomite. Jones (1984) estimated that the Dunderburg was 1,300 to 1,500 feet thick in the study area, where it conformably overlies the Secret Canyon Shale. This apparent thickening of the Dunderburg may have occurred at the expense of the Hamburg Dolomite, a situation which has been noted in the southern Ruby Mountains, about 50 miles north of the study area, where the Dunderburg is 1,200 to 1,400 feet thick (Hose and others, 1976).

Jones divided the Dunderburg into four members, which he identified in drill core, but which could not be correlated with surface exposures. Member 1 consists of about 500 feet of alternating 1 to 2 inch beds of silty limestone and calcareous siltstone. This member is typically altered to skarn or marble in the contact aureole. Member 2 is made up of about 220 feet of calcareous siltstone with local silty limestone beds, and has been metamorphosed to pyroxene hornfels with local garnet-pyroxene beds. Member 3 consists of 450 to

500 feet of silty limestone, alternating with 1 to 3 inch thick limestone beds, which is typically altered to garnet-pyroxene skarn with local pyroxene hornfels. The uppermost member, Member 4, is 100 to 300 feet thick and consists of calcareous siltstone and shale which has been converted to pyroxene hornfels and biotite hornfels, respectively.

Rocks of the Windfall Formation, which were originally assigned to the Goodwin Formation by Humphrey (1960) in the White Pine district, conformably overly the Dunderburg Shale, and consist of about 800 feet of thin-bedded limestone, overlain by over 700 feet of massive dolomite. Nolan and others (1956) recommended the use of the name Windfall Formation for Upper Cambrian rocks which overlie the Dunderburg Shale in the Eureka District, instead of Goodwin Formation, which includes a large thickness of Ordovician strata in its type area. The Windfall Formation forms the top of Pogonip Ridge, east of the study area, and also marks the upper stratigraphic limit of contact metamorphism associated with the Seligman-Monte Cristo intrusive system. Rocks near the base of the Windfall have been weakly metamorphosed to marble and hornfels.

The youngest units present in the study area are the Belmont Fanglomerate and Quaternary alluvium. The Belmont Fanglomerate is a Tertiary gravel which was deposited west

of the White Pine Fault during the uplift of Pogonip Ridge. This unit is over 1,200 feet thick near Monte Cristo and consists of unsorted limestone pebbles and cobbles and granitic debris (Humphrey, 1960). Alluvium occurs as local gravel deposits in Seligman Canyon.

LOCAL STRUCTURE

The structure of the study area has been described by Humphrey (1960), Sonnevil (1979), and Jones (1984). Pre-Tertiary structure is dominated by north-trending folds and reverse faults, whereas Tertiary deformation is represented by high-angle, generally north-trending normal faults.

The Seligman and Monte Cristo stocks were emplaced in the west flank of Pogonip Ridge, which is an elongated domal uplift with its center near the Seligman stock (Humphrey, 1960). In the vicinity of the two stocks carbonate wall rocks have been deformed into north to northeast-trending anticlinal and synclinal folds (Plate 1). Sonnevil (1979) inferred that these folds predated the intrusion of the stocks, based on the presence of two reverse faults north of the Monte Cristo stock which cut a fold and intersect, but do not offset the stock. Intrusion of the stocks may have domed the metasediments and produced dips of 10 to 60 degrees in these rocks near intrusive contacts.

Tertiary structures include north-south and east-west trending normal faults, which were probably active during the formation of the Basin and Range province in late Tertiary time. Humphrey (1960) estimated that 8,000 to 15,000 feet of vertical displacement occurred along the

White Pine Fault during the uplift of Pogonip Ridge. Fault displacements on Pogonip Ridge (Seligman Area) were estimated by Jones (1984) to range from 100 to 500 feet.

INTRUSIVE ROCKS

The Seligman and Monte Cristo stocks are small Cretaceous plutons, exposed about 3,500 feet apart (Plate 1), which are the surface expression of an apparently much larger intrusive system. Diamond drilling in skarn surrounding the stocks has enabled the development of a partial three dimensional view of the intrusive system, which is shown in Plates 2 and 3.

The stocks are similar in age (see section on age dates below), but they have marked differences in texture and alteration. Sills and dikes are present in the subsurface, and locally at the surface, peripheral to both stocks. Sills predominate, probably due to the distinctly bedded nature of the carbonate wall rocks, but locally dikes invade wall rock along fractures and may contain wall rock inclusions.

The following descriptions of intrusive rocks are based on field observations and petrographic study of drill core and surface samples. Petrographic features of intrusive rocks identified in this study are presented in Tables 1 and 2. Intrusive rocks are named according to Streckheisen (1973,1979), based on modal analysis of thin sections by point counting or estimation of primary mineral percentages. Determination of primary mineral percentages has been complicated by multiple stages of

alteration which have affected virtually all intrusive rocks in the study area. In particular, estimates of modal percentages of dacite porphyry sills, which are present in the subsurface between the stocks, are speculative due to intense alteration of the groundmass constituents of these rocks. Anorthite content of plagioclase was estimated, where possible, by measuring extinction angles on albite twins according to the Michel-Levy method. Alteration has commonly obliterated twinning in plagioclase, allowing only occasional determination of An content.

SELIGMAN STOCK AND RELATED INTRUSIVES

The Seligman stock is a northwest-trending elongate body of predominantly granodiorite composition, which has a surface exposure of about 3,600 by 2,000 feet (Plate 1). Outcrops of the stock are typically highly weathered except where they have been invaded by quartz veins. Areas of intense stockwork quartz veining in the stock are generally limited to a northwest-trending zone, as shown in Plate 1. A plot of the elevation of the top of the main intrusive body (Plate 2) indicates that the Seligman stock is the surface expression of a larger northwest-trending body of granodiorite. Granodiorite which is very similar in texture and mineralogy to the Seligman stock has been intersected in the bottom of drill hole U-52, and

TABLE 1 PETROGRAPHIC CHARACTERISTICS OF THE SELIGMAN STOCK AND RELATED INTRUSIVES

Rock Type	Texture	Modal Percentages and Mineral Characteristics						
		Plagioclase	K-Feldspar	Quartz	Biotite	Hornblende	Accessories	Opaques
Hbl-Bi Granodiorite	equigran-slightly porphyritic	36-50 % .5-3 mm sub-euhed zoned An45-55-An25-35 myrmekite alb, carls, per twinning	8-18 % .2-3 mm anhed intergran-oikycrystic min carls twinning	20-32 % .1-1 mm (intergran) 2-7 mm (phenos) an-subhed	7-16 % .2-.5 mm (flakes) 1-5 mm (books)	tr-7 % .5-3 mm sub-euhed prisms, intergrown w/ biotite	tr-2 % sphene apatite zircon	0-3 % pyrite magnetite
Hbl-Bi Granite	equigran, porphyritic	27-42 % .5-2 mm sub-euhed zoned An45-An30 myrmekite alb, carls, per twinning	20-45 % .5-6 mm anhed intergran-oikycrystic min grid twinning .1-.2 mm (gran grdmass in porphyry)	14-38 % .5-1 mm (intergran) 2-7 mm (phenos) .05-.2 mm (gran grdmass in porphyry)	4-11 % .5-5 mm (books)	1-8 % 1-5 mm sub-euhed prisms, intergrown w/ biotite	tr-1.5 % sphene apatite zircon	0-1 % pyrite magnetite
Quartz Monzodiorite, Diorite	equigran.	43-73 % .5-3 mm sub-euhed zoned An48-An30 alb, carls twinning	3-10 % .2-3 mm anhed intergran untwinned	3-10 % .5-3 mm anhed intergran	10-20 % .5-5 mm books	5-16 % .7-3 mm prisms, intergrown w/ biotite	1-3 % sphene apatite	tr-5 % pyrite magnetite
Bi Dacite Porphyry	porphyritic	30-50 % 1-7 mm (phenos) zoned An42-48 cores alb, carls twinning .2-.4 mm (grdmass)	15-25 % .1-.5 mm (gran grdmass) untwinned	20-35 % .1-.5 mm (grdmass) 1-5 mm (phenos)	5-10 % 1-4 mm books	0-5 % .5-2 mm subhed prisms	tr sphene apatite	0-1 % pyrite magnetite
Aplite	equigran	15-30 % .2-2 mm zoned sub-euhed An9-13 cores alb, carls myrmekite	30-75 % .1-.5 mm anhed granular carls, grid twinning granophyric .5-4 mm anhed oikycrystic carls, grid twinning microperth	15-40 % .2-.5 mm anhed granular .2-2 mm anhed granophyric	0-5 % 1-3 mm books	tr-2 % 1-3 mm euhed prisms	tr sphene apatite	0-1 % pyrite
Pegmatite	pegmatitic	10-20 % 1-4 mm alb, carls twinning altered	40-60 % 1 mm-1.3 cm anhed granophyric	30-40 % .2-5 mm anhed granophyric	0 %	0 %	0 %	0 %

may be a buried extension of this body.

Sills and dikes, ranging in composition from granodiorite to granite, with local dacite porphyry, quartz monzodiorite, diorite, and aplite, have been intersected in drill holes surrounding the stock at horizontal distances as much as 1,800 feet from the exposed stock. At the surface, aplite dikes and sills are only present in a narrow zone near the stock contacts.

Hornblende Biotite Granodiorite

Hornblende biotite granodiorite forms the majority of the exposed Seligman stock and also occurs as sills and dikes, ranging from .5 to 60 feet thick in the subsurface. In drill holes the thickness of sills and dikes generally decreases with distance from the stock. Granodiorite in drill core is generally light gray to white, with dark brown biotite and hornblende phenocrysts. At the surface the rock is stained to a yellow-brown color due to oxidation of disseminated pyrite. Granodiorite is medium-grained, equigranular to slightly porphyritic, and consists of plagioclase surrounded by quartz and K-feldspar, with disseminated biotite and hornblende.

Where it is least altered, plagioclase is typically subhedral to euhedral and has albite, carlsbad and pericline twinning and oscillatory zonation. An content of

plagioclase typically ranges from An 45-55 in the cores of crystals to An 25-35 at the rims. Locally where plagioclase is in contact with K-feldspar, crystal rims have myrmekitic overgrowths of vermicular quartz and oligoclase. Plagioclase is generally partially to totally altered to clinozoisite, epidote, sericite, calcite, and/or prehnite.

K-feldspar in granodiorite is anhedral, fine to medium grained and generally untwinned. It ranges from fine grained intergrowths with quartz, which partially surround plagioclase, to medium grained optically continuous oikycrysts which completely surround plagioclase and rounded quartz grains (Figures 3 and 4). K-feldspar is usually dusty looking, resulting from weak kaolinitic alteration, and is locally replaced by sericite.

Biotite occurs mostly as subhedral to euhedral books and fine grained flakes disseminated throughout the rock. Biotite commonly contains inclusions of magnetite, pyrite, sphene and apatite, and is usually partially altered to chlorite and epidote, and locally to sericite and iron oxides. Hornblende occurs as discrete euhedral crystals and as subhedral intergrowths with biotite. Hornblende is generally fresh, but it is locally altered to chlorite and calcite.

Quartz occurs primarily as anhedral crystals

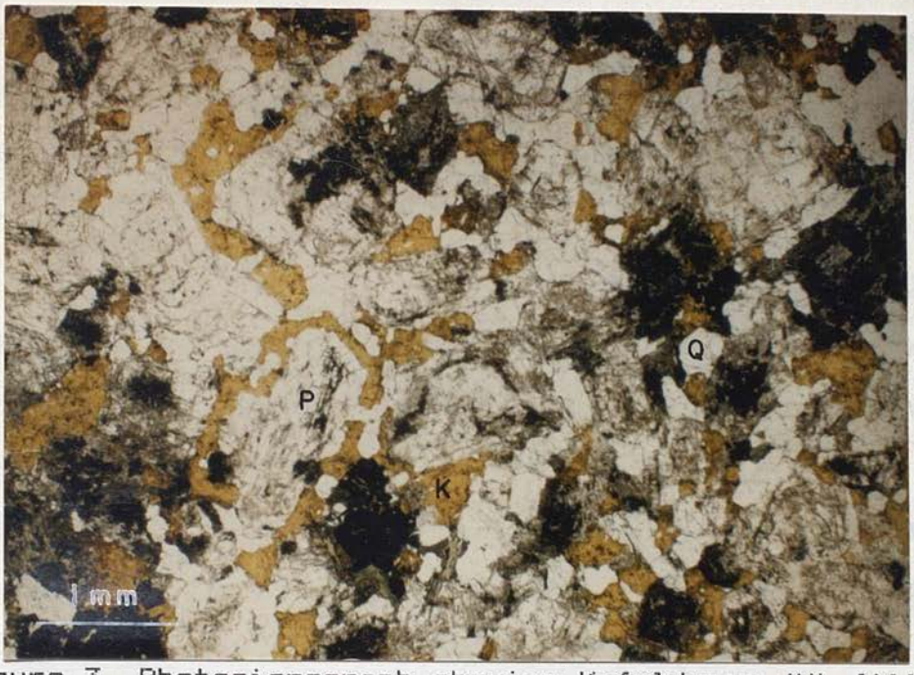

Figure 3. Photomicrograph showing K-feldspar (K) filling in around plagioclase (P) and quartz (Q) in hornblende biotite granodiorite. Sample is stained for K-feldspar. Uncrossed nicols. (Sample P64-3, 1016 ft.)

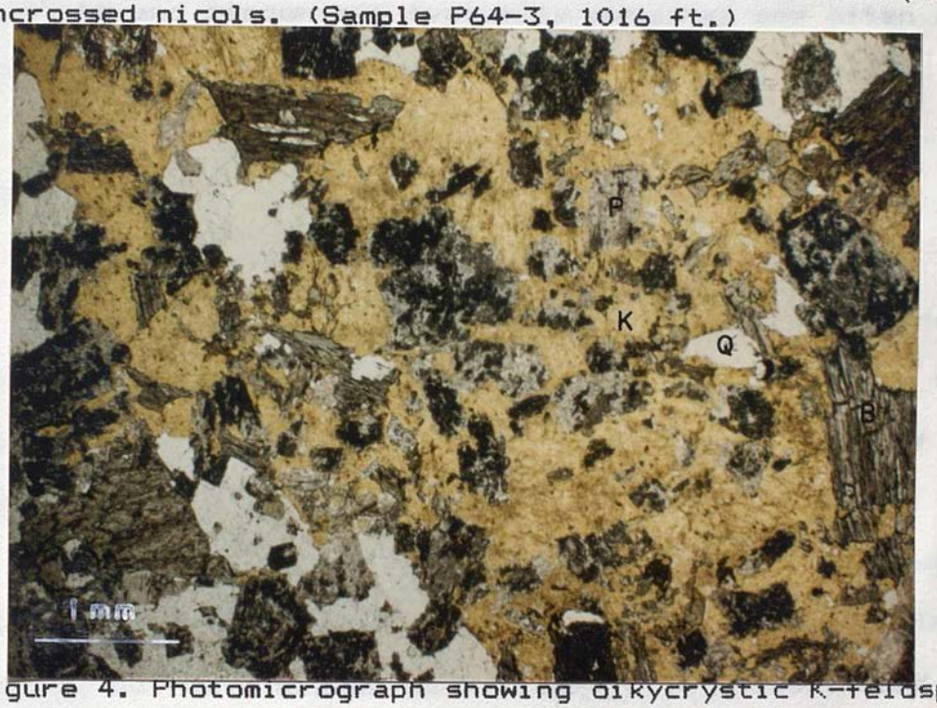

Figure 4. Photomicrograph showing oikycrystic K-feldspar (K) surrounding altered plagioclase (P), biotite (B), and quartz (Q) in hornblende biotite granodiorite. Sample stained for K-feldspar. Uncrossed nicols. (Sample P28-4, 1218 ft.)

intergranular to plagioclase, and as scattered blocky to rounded phenocrysts. Phenocrysts are typically slightly strained and often contain fine grained euhedral plagioclase inclusions within their rims.

Accessory minerals in granodiorite include pyrite, magnetite, sphene, apatite, and minor zircon. Pyrite is the most abundant opaque mineral and is present in most samples as fine grained cubes and anhedral masses disseminated through the rock. Pyrite is locally rimmed by epidote and may be intergrown with magnetite. Magnetite is present in many samples as discrete anhedral crystals which are sometimes rimmed by chlorite or sphene. Sphene, apatite and zircon are typically euhedral and often are closely associated with mafics.

Hornblende Biotite Granite

Hornblende biotite granite occurs in the subsurface as sills and dikes as much as 44 feet thick, and at the surface as a porphyritic border near the contacts of the Seligman stock.

The sills and dikes exhibit textures and mineralogy which are similar to that of the granodiorite described above, but have higher percentages of K-feldspar and hornblende, and less plagioclase. K-feldspar is generally oikycrystic and coarser grained than in the granodiorite

and locally displays grid twinning typical of microcline. No cross-cutting relationships were observed between granite and granodiorite, but granite sills and dikes may have been emplaced slightly later than the main body of granodiorite, based on geochemistry which suggests that they crystallized from a more differentiated melt.

Porphyritic granite is present at the surface within 100 feet of the stock contact (samples SI-7 and SI-14 on Plate 1), and differs from the granite described above, only by having a porphyritic texture. The rock consists of 1 - 7 mm. phenocrysts of plagioclase, quartz, biotite, and hornblende in a fine-grained matrix of granular quartz and K-feldspar. This rock probably formed as a chilled margin on the Seligman stock. Its relatively fine-grained groundmass is probably a result of more rapid cooling of the magma at the margins of the stock where it was in contact with cooler wall rock.

Quartz Monzodiorite and Diorite

Rocks of diorite to quartz monzodiorite composition occur as local zones within granodiorite sills and as a dike at the bottom of drill hole PH-51. These rocks are distinguished by their high percentage of mafic minerals (Table 1, Figure 5). Texturally they are very similar to

Figure 5. Drill core specimens of diorite (left; sample P51-10, 2047 ft.) and quartz monzodiorite (right; sample P27-3, 741 ft.).

granodiorite, but they have much more plagioclase and much less K-feldspar and quartz. No cross-cutting relationships between these rocks and granodiorite have been observed, but these rocks may represent local emplacement of less differentiated magma from the deeper parts of the magma chamber during the crystallization of the Seligman stock, as is suggested by their geochemistry (see section on geochemistry below).

Aplite and Pegmatite

Aplite ranges from fine to medium grained and occurs as narrow dikes, chilled margins on dikes and sills, and as zones within thick granodiorite and granite sills.

Fine grained aplite is present as dikes, .5 to 2 feet thick, which cut granodiorite and pyroxene hornfels near the stock contacts, and as narrow borders on 2 to 6 inch thick pegmatite dikes. Aplite dikes typically have a narrow zone of granophyric quartz and K-feldspar adjacent to wall rock, which grades into a granular mosaic of K-feldspar, quartz, and albite (Figure 6). Pegmatite dikes, which occur in the eastern surface contact zone of the stock and in drill hole PH-22, are typically zoned from fine grained aplite adjacent to wall rock, to a zone of granophyric quartz and K-feldspar, to a core of coarse grained K-feldspar, quartz and albite (Figure 7).

Figure 6. Photomicrograph of narrow aplite dike in granodiorite showing zonation from granophyric quartz-K-feldspar (GP) at margin to granular quartz-K-feldspar (GR) in center of dike. Crossed nicols. (Sample SD-1A)

Figure 7. Hand specimen of aplite-pegmatite dike (sample SD-2) showing zonation from fine-grained aplite (A) next to wall rock, to granophyric quartz-K-feldspar (GP), to pegmatite (P) in the center of the dike.

K-feldspar in fine grained aplite is anhedral and commonly displays grid twinning and/or carlsbad twinning. Plagioclase is subhedral and commonly totally altered to sericite, but locally has albite and carlsbad twinning and myrmekitic overgrowths on crystal rims. Hornblende occurs in minor amounts as euhedral prismatic crystals.

Medium grained aplite occurs as zones within thick sills of granite or granodiorite in drill holes PH-10 and PH-22, and is typified by its high percentage of K-feldspar relative to quartz and plagioclase, and its general lack of primary mafic minerals. A distinctive feature of this rock is its tendency to contain granular pyroxene (Figure 8) or coarse grained garnet, which are interpreted to be alteration minerals which formed due to an influx of calcium from adjacent wall rocks. These aplitic zones may represent areas of accumulation of potassium-enriched late stage melt.

Biotite Dacite Porphyry

Biotite dacite porphyry sills and dikes, 1 to 11 feet thick, have only been observed in drill core from drill holes PH-11, PH-13, PH-15, and PH-54, all of which are southwest of the exposed Seligman stock (Plate 1.). Dacite porphyry is medium to dark gray-green with white phenocrysts, and is distinguished from granodiorite by its

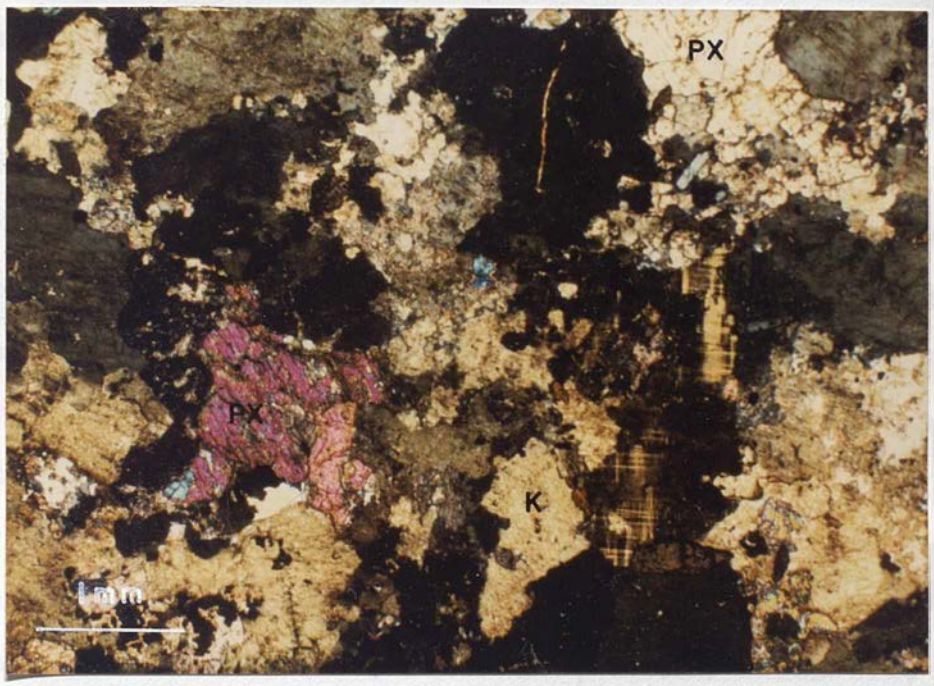

Figure 8. Photomicrograph of altered aplite showing clinopyroxene (PX) in stained K-feldspar (K). Note grid twinning in K-feldspar. Crossed nicols. (Sample P22-6, 976 ft.)

porphyritic texture (Figure 9). The rock consists of plagioclase, minor biotite and quartz phenocrysts in a fine grained granular to slightly sutured groundmass of quartz, K-feldspar, and plagioclase. Generally intense alteration of the groundmass of the rock to sericite, clinozoisite, epidote, or chlorite prevents an accurate determination of the primary mineral percentages of this rock (Figure 10).

In drill core from PH-11 and PH-54, dacite porphyry dikes, 1 to 3 feet thick, cut hornblende biotite granodiorite at angles of 20 to 70 degrees. The contacts between the intrusives are sharp and there appears to be no flow alignment of mafics in either rock type. In PH-13 and PH-15 dacite porphyry occurs as sills in pyroxene hornfels.

Their occurrence in drill holes near the Seligman stock suggests that dacite porphyry sills and dikes are related to this stock, although they are texturally more similar to the Monte Cristo stock. These rocks apparently post date the Seligman stock, and may be the first indication of a shift in the locus of intrusive activity to the southwest, and the onset of conditions which produced porphyritic textures in the Monte Cristo stock and associated dikes and sills.

Figure 9. Drill core specimens of dacite porphyry. Specimen at left (sample P54-7, 1783 ft.) contains quartz-epidote-pyrite veinlet, and specimen at right (P13-2, 1655 ft.) contains quartz-pyrite-molybdenite veinlet.

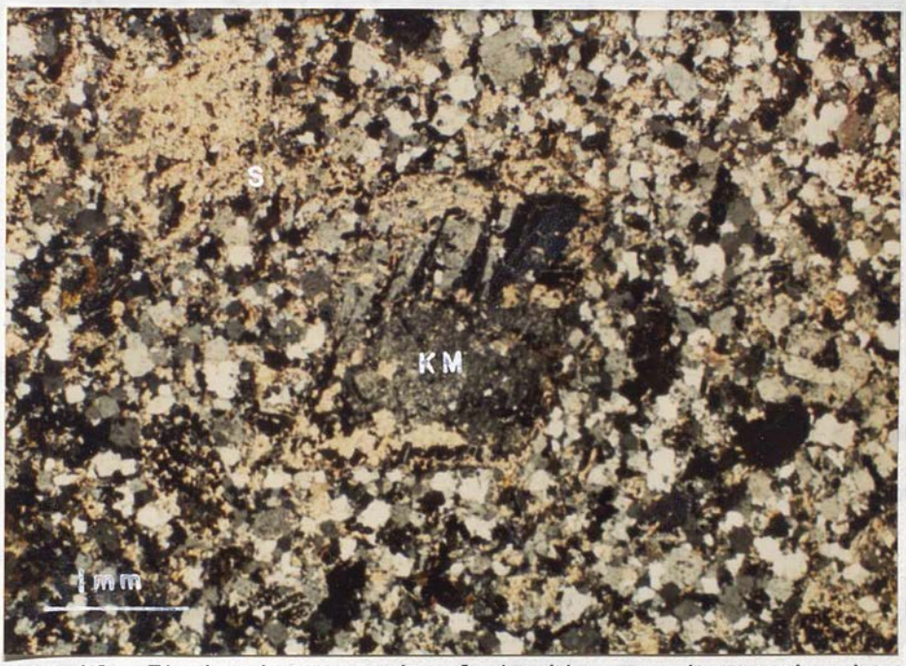

Figure 10. Photomicrograph of dacite porphyry showing alteration of groundmass to sericite (S) and alteration of plagioclase phenocryst (P) to kaolinite and montmoriillonite (KM). Crossed nicols. (Sample P13-2, 1655 ft.)

MONTE CRISTO STOCK AND RELATED INTRUSIVES

The Monte Cristo stock is a roughly circular body of biotite granite porphyry which has an exposed diameter of approximately 2400 feet (Plate 1). The stock forms a topographic high due to the presence of intense stockwork quartz veining (Figure 11), which has made its outcrop resistant to erosion. The stock may be a northwest-trending intrusive offshoot from the buried Seligman stock, but no connection between the two stocks has been intersected in drilling to date (Plates 2 and 3). Although drill hole data is limited, the Monte Cristo stock appears to be a steep-walled pipe-like body, which is inclined to the southeast. Drill hole PH-56, between the Seligman and Monte Cristo stocks and less than 800 feet from the northeast outcrop edge of the Monte Cristo stock, and which is over 3,000 feet deep, failed to intersect the main intrusive body.

Sills and dikes of granite porphyry and granodiorite porphyry are present in the subsurface in skarn and hornfels, peripheral to the Monte Cristo stock, and biotite hornblende rhyodacite sills are present at the surface near the stock outcrop (Plate 1).

Petrographic characteristics of intrusives from the Monte Cristo area are shown in Table 2.

Figure 11. Outcrop of Monte Cristo stock (granite porphyry) showing stockwork quartz veining.

TABLE 2 PETROGRAPHIC CHARACTERISTICS OF THE MONTE CRISTO STOCK AND RELATED INTRUSIVES

Rock Type	Texture	Modal Percentages and Mineral Characteristics						
		Plagioclase	K-Feldspar	Quartz	Biotite	Hornblende	Accessories	Opaques
Bi Granite Porphyry	porphyritic	20-40 % 1-5 mm phenos sub-euhed zoned An45-An30 alb, carls, per twinning	17-55 % .1-.5 mm gran grdmass 1-3 mm anhed min phenos carls twinning	20-40 % .05-.4 mm gran grdmass 1-10 mm an-euhed phenos	5-15 % .2-.7 mm (flakes) 1-5 mm (books)	0-3 % .2-2 mm subhed prisms	tr-1 % sphene apatite	tr-1 % pyrite magnetite
Biotite Granodiorite Porphyry	porphyritic	35-60 % 1-7 mm phenos sub-euhed zoned An50-An35 alb, carls, per twinning	15-25 % .1-.5 mm gran grdmass untwinned	20-30 % .1-.3 mm gran grdmass 1-5 mm anhed phenos	5-15 % .2-.5 mm (flakes) 1-5 mm (books)	0-5 % .2-3 mm sub-euhed prisms	tr-1 % sphene apatite	tr-1 % pyrite magnetite
Bi-Hbl Rhyodacite Porphyry	porphyritic	20-30 % 1-6 mm phenos sub-euhed zoned An35-40 core alb, carls twinning	27-60 % .05-.1 mm gran grdmass untwinned	20-30 % .05+.1 mm gran grdmass 1-5 mm anhed phenos	2-5 % 1-3 mm books	5-16 % .1-4 mm sub-euhed prisms	tr-1 % sphene apatite	0-1 % pyrite magnetite

Biotite Granite Porphyry

Biotite granite porphyry forms the surface exposure of the Monte Cristo stock, and is also present in the subsurface as sills and dikes 5 to 260 feet thick. Intense stockwork quartz-K-feldspar and quartz-sericite veining has obscured the original composition of this rock, but it is classified as a granite based on modal mineral percentages (Table 2). Surface outcrops of the stock are light gray to white, and contain up to 70 % quartz veins (Figure 12). Sonnevil (1979) identified several different generations of quartz veins, and noted that 3 to 10 different quartz vein attitudes could be measured on a given stock outcrop.

Texturally, biotite granite porphyry resembles the other porphyrytic rocks in the study area, and consists of plagioclase, quartz, and biotite phenocrysts in a fine grained groundmass of granular K-feldspar and quartz (Figure 13). Plagioclase is commonly totally altered to sericite, and may be partially altered to clinozoisite, calcite, K-feldspar, or kaolinite. K-feldspar is fresh or weakly altered to kaolinite and sericite, and biotite is altered to sericite, chlorite, epidote, or calcite.

Intensity of quartz veining and associated potassic alteration (secondary K-feldspar) appears to decrease away from the exposed Monte Cristo stock, and the original

Figure 12. Hand specimens of quartz-veined granite porphyry from the Monte Cristo stock. From left, samples MI-1, MI-5, and MI-4.

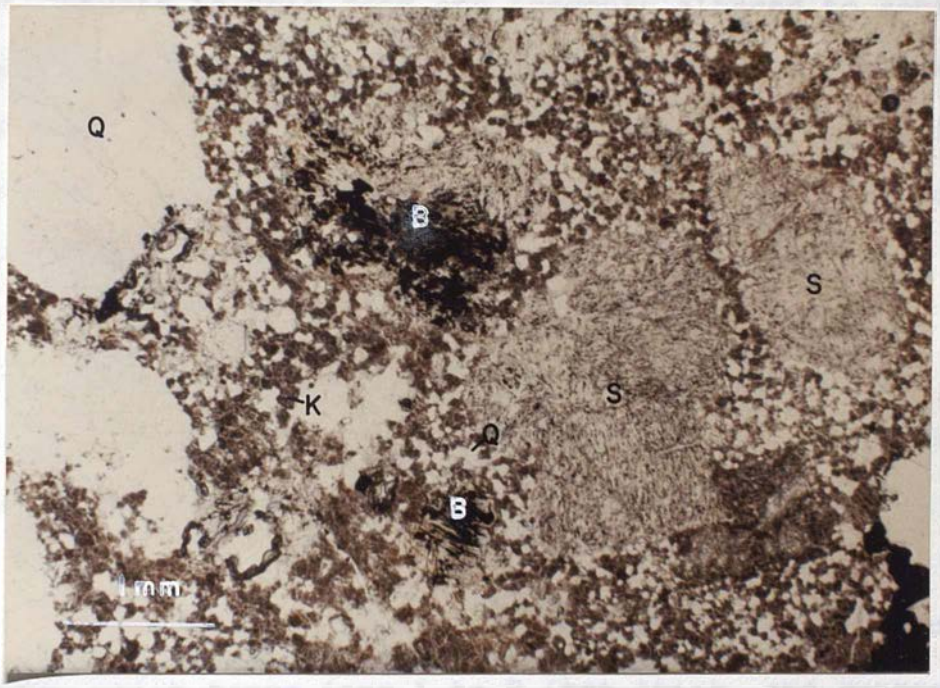

Figure 13. Photomicrograph showing sericitized plagioclase (S) and biotite (B) phenocrysts with quartz (Q) phenocrysts in fine-grained groundmass of quartz (Q) and K-feldspar (K) of biotite granite porphyry. Uncrossed nicols. (Sample MI-10)

composition of the stock may be represented by granodiorite porphyry which is present in the subsurface peripheral to the stock.

Biotite Granodiorite Porphyry

Biotite granodiorite porphyry occurs as sills and dikes 5 to 50 feet thick in drill holes U-23, U-41, U-47, U-50, and U-51 (Plate 1). This rock is texturally very similar to biotite granite porphyry, but has more plagioclase, less primary K-feldspar, and is only locally altered to secondary K-feldspar (Table 2). Plagioclase phenocrysts in this rock are commonly altered to sericite, kaolinite, clinozoisite and epidote, and groundmass K-feldspar is generally altered to kaolinite and sericite. Biotite and hornblende are altered to chlorite, epidote, and calcite.

Biotite granodiorite porphyry may represent the pre-alteration equivalent of biotite granite porphyry.

Biotite Hornblende Rhyodacite Porphyry

Biotite hornblende rhyodacite porphyry sills and dikes, which range from 1 to 9 feet thick, are exposed within skarn and hornfels peripheral to the Monte Cristo stock (Plate 1), and occur in the upper 500 feet of drill

hole PH-56. These rocks are generally intensely altered, obscuring their primary mineralogy.

In hand specimen, the freshest samples are fine-grained dark gray to green, with white and pink plagioclase phenocrysts and abundant subparallel prismatic hornblende crystals and scattered biotite books and quartz phenocrysts. Where the rock has been intensely altered, the porphyritic texture is preserved, but the groundmass is typically light gray-green (Figure 14).

Rhyodacite porphyry is texturally similar to granite and granodiorite porphyry associated with the Monte Cristo stock, except that its groundmass is more fine-grained. The rock consists of plagioclase, hornblende, biotite, and minor quartz phenocrysts in a fine-grained granular groundmass of quartz and K-feldspar (Figure 15). Locally potassic alteration has produced K-feldspar which replaces the groundmass and plagioclase phenocrysts ; in some cases the groundmass consists of calcic plagioclase, which probably replaced original groundmass K-feldspar and quartz, and hornblende has been pseudomorphically replaced by clinopyroxene. Sericitic alteration of the groundmass and plagioclase phenocrysts, and alteration of plagioclase to pink clinozoisite (thulite) are also common in these rocks.

The proximity of biotite hornblende rhyodacite porphyry outcrops to the Monte Cristo stock and the

Figure 14. Photograph of sericitic alteration front in rhyodacite porphyry in the vicinity of drill hole PH-56.

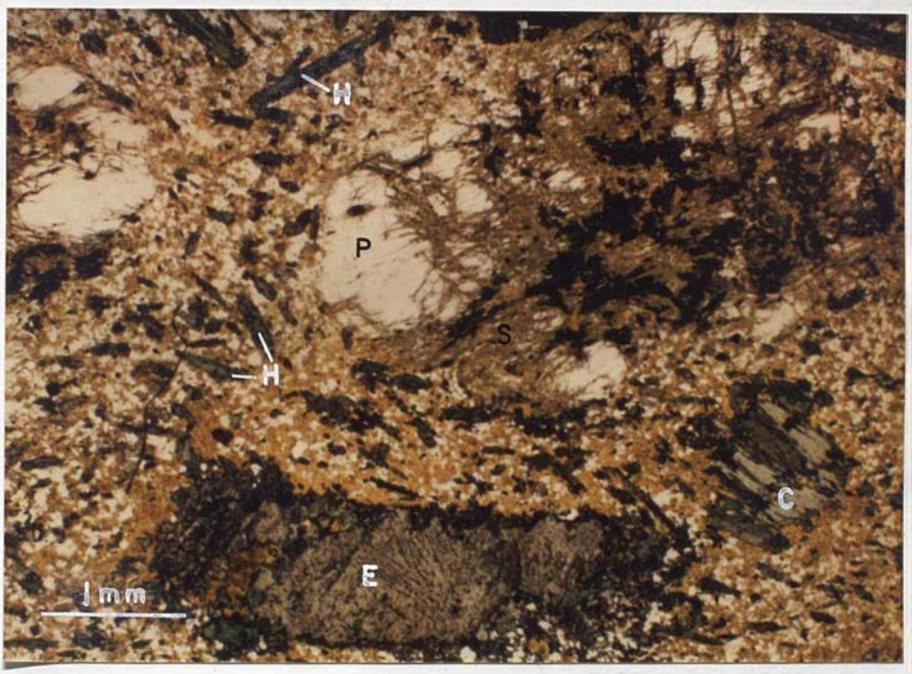

Figure 15. Photomicrograph of altered rhyodacite porphyry showing plagioclase phenocryst (P) partially altered to sericite (S), biotite altered to epidote (E) and chlorite (C), and fresh hornblende (H) in groundmass of quartz and K-feldspar (stained yellow). Uncrossed nicols. (Sample MD-5)

textural similarity of rhyodacite porphyry to granite porphyry suggests that these rocks are related. There is some indirect evidence that rhyodacite porphyry was emplaced prior to the Monte Cristo stock; the sills are altered to K-feldspar and locally to sericite, alteration types which are well-developed in the Monte Cristo stock, suggesting that they were altered by the same fluids which altered the Monte Cristo stock, presumably during its emplacement. Age relationships between rhyodacite porphyry and dacite porphyry associated with the Seligman stock are unknown due to a lack of cross-cutting relationships.

SEQUENCE OF EMPLACEMENT

The inferred sequence of emplacement of the intrusives in the study area from oldest to youngest is: 1) Seligman stock (hornblende biotite granodiorite and porphyritic granite) and quartz monzodiorite, diorite, granodiorite, granite sills and dikes 2) aplite-pegmatite dikes 3) biotite dacite porphyry sills and dikes 4) biotite hornblende rhyodacite porphyry sills and dikes 5) Monte Cristo stock (biotite granite porphyry) and granodiorite porphyry and granite porphyry sills and dikes.

Cross-cutting relationships were only observed between dacite porphyry and granodiorite and between

aplite and granodiorite. The relative ages of the other intrusives are inferred and based on spacial relations and similarities in texture and alteration.

AGE DATES

Age dates of intrusive rocks from the Seligman-Monte Cristo area have been reported by several authors, including Adair and Stringham (1960), Armstrong (1970), Edwards and McLaughlin (1972), and Sonnevil (1979). These dates and those obtained in this study are presented in Table 3. Reported K-Ar dates have been recalculated using tables provided by Dalrymple (1979) which incorporate new decay and abundance constants.

Recalculated K-Ar dates for biotite from both stocks yield a bracket of 92.7+2 to 104.5+4 m.y. for intrusion of the stocks, indicating that they are Early Cretaceous in age. All K-Ar dates on biotite from the study area should be viewed as minimum ages, because of the ubiquitous alteration of biotite to chlorite, which probably caused Ar loss from the biotite. There is also the possibility that the intrusion of the later of the two stocks may have 'reset' the biotite in the stock which crystallized first.

Biotite dated in this study contained minor amounts of chlorite (probably less than 5 % as estimated from examination of thin sections of the dated samples).

TABLE 3. RADIOMETRIC AGE DATES OF INTRUSIVE ROCKS FROM THE SELIGMAN-MONTE CRISTO AREA

ROCK TYPE	LOCATION	METHOD	MINERAL DATED	DETERMINED BY	REFERENCE	REPORTED AGE (m.y.)	RECALCULATED AGE (m.y.)
Hbl Bi Grd	Seligman Stock	K-Ar	Biotite (30% Chlor.)	R.L. Armstrong	Armstrong (1970)	90.4±2	92.7±2
Hbl Bi Grd	Seligman Stock (Sample SD-3)	K-Ar	Biotite (<5% Chlor.)	Geochron Lab	This Study	102±4	104.5±4
Hbl Bi Grd	Subsurface Hole U-52	K-Ar	Biotite	Geochron Lab	Sonnevil (1979)	104±8	106.6±8
Hbl Bi Grd	Seligman Stock	Pb-α	Not Reported	R.J. Roberts	Adair and Stringham (1960)	128±15	----
Bi Grn Porph	Monte Cristo Stock Hole U-11	K-Ar	Biotite (<5% Chlor.)	Geochron Lab	This Study	98.7±3.6	101.2±3.6
Qtz Monz (Bi Grn)	Monte Cristo Stock Hole U-9	K-Ar	Biotite (Altered)	Shell Research	Edwards and McLaughlin (1972)	94±5.4	96.4±5.4
		"	Muscovite	"	"	113±4.8	115.8±4.8
		Rb-Sr	Biotite	"	"	86±73	----
		"	Muscovite	"	"	75±58	----
Qtz Monz Porph (Dacite Porph)	Subsurface Hole U-6	K-Ar	Biotite (Chlorite)	Shell Research	Edwards and Mclaughlin (1972)	140±8	143.4±8

However, biotite dated in earlier studies appears to have contained significant amounts of chlorite (Table 3), and these dates are generally significantly younger than dates obtained in this study. The reason for the markedly higher date on 'quartz monzonite porphyry' from south of the Monte Cristo stock is unknown.

Rb-Sr dates on biotite and muscovite are of little use due to their large error brackets. The Pb-alpha date from the Seligman stock is significantly higher than the K-Ar dates, a situation which is relatively common in dated plutons in the eastern Great Basin (Armstrong,1970).

In summary, the K-Ar dates suggest that the stocks were emplaced over a period of less than 10 million years, and that the Monte Cristo stock may be younger than the Seligman stock. However the affects of alteration and multiple intrusions may have introduced significant errors in these dates.

DEPTH AND STYLE OF EMPLACEMENT

Estimates of sedimentary cover during emplacement of the Seligman and Monte Cristo stocks range from 20,000 to 27,000 feet (6.1 to 8.2 km.). These figures were obtained by compiling thickness estimates for Paleozoic rocks in the study area from Humphrey (1960) and Jones (1984), and in western White Pine County from Langenheim and others

(1973) and Hose and others (1976). The maximum estimate includes 5,000 feet of Mesozoic rocks which have been mapped in Eureka and Elko Counties, but which have not been mapped near the study area.

The stocks exhibit textures and alteration which suggest differing cooling histories and possibly emplacement into different levels of the crust.

The Seligman stock is essentially equigranular and contains virtually no potassic alteration and only relatively minor stockwork quartz veining. Late stage potassium-enriched melt in this stock apparently crystallized as oikycrystic K-feldspar which surrounds previously formed plagioclase, and as minor aplite-pegmatite dikes and aplitic zones in sills. Textures in the Seligman stock suggest that it cooled at a relatively slow rate and there was no violent release of potassium-rich late stage fluid. This stock possesses features which are typical of plutons associated with tungsten skarn deposits, and which are believed to have crystallized at depths of 6 to 10 km (Newberry and Einaudi, 1981).

The Monte Cristo stock possesses a porphyritic texure and is characterized by potassic alteration and intense fracturing and stockwork quartz veining, features which are typical of plutons associated with porphyry copper and molybdenum deposits, which are believed to have crystallized at depths as shallow as 1 to 2 km. (Titley

and Beane, 1981). This stock apparently crystallized in two stages; crystalization of medium to coarse grained plagioclase phenocrysts, followed by crystallization of a fine grained 'quenched' groundmass of granular quartz and K-feldspar. Relatively violent separation of potassium-silica-rich aqueous fluid from the remaining melt may have been responsible for the extensive fracturing of the stock and the emplacement of quartz-K-feldspar veins.

If the structural and stratigraphic interpretations of Jones (1984) and Sonnevil (1979) are correct, there is no evidence to suggest that the stocks were emplaced into significantly different levels of the crust. The Monte Cristo stock was apparently emplaced into the lower part of the Dunderburg Shale, and the Seligman stock was emplaced slightly higher into the Dunderburg. It does not appear likely that the Monte Criso stock is a faulted-off portion of a higher part of the Seligman stock, as faults intersected in drilling have relatively minor displacements (probably not more than 500 feet (Jones, 1984)). Thus, a difference in level of emplacement is probably not responsible for the observed differences between the stocks.

The observed differences between the two stocks may be a result of differing water contents in the melts from which they crystallized. A significantly higher water content in the melt that produced the Monte Cristo stock

could have caused the melt to become saturated in water at an earlier stage of crystallization than the Seligman stock. Separation of the aqueous phase, so-called retrograde boiling, due to cooling and crystallization of the magma to the point of aqueous phase saturation, could have produced the fine-grained 'quenched' groundmass and intense fracturing and potassic alteration observed in this stock. However, the estimated depth of emplacement for the stock (6-8 km.), appears to be rather high for the intensity of fracturing that is present. Burnham and Ohmoto (1980) noted that the intensity of fracturing which could be produced by retrograde boiling decreases rapidly with depth (pressure). Moderate to intense fracturing is most likely to occur in plutons which are emplaced at depths between 1 and 6 km.

CONTACT METAMORPHISM AND SKARN FORMATION

Contact metamorphism and metasomatism, resulting from the intrusion of the Seligman and Monte Cristo stocks, has converted interbedded limestone, calcareous siltstone and shale to calc-silicate hornfels, marble and calcic exoskarn. Plate 1 shows the distribution of these rocks in the study area. This map was compiled from an unpublished map by Brand (1980), and maps by Sonnevil (1979), which cover the area surrounding the Monte Cristo stock. Additional mapping of intrusive rocks by the author in the vicinity of the Seligman stock and northeast of the Monte Cristo stock, is also included.

Metamorphism and alteration in the contact aureole of the Seligman and Monte Cristo stocks have been described in some detail by Jones (1984) and Sonnevil (1979). Sonnevil identified three stages of skarn formation in the wall rock surrounding the Monte Cristo stock, beginning with an anhydrous stage dominated by the formation of garnet and pyroxene, followed by two hydrous stages, dominated by epidote-actinolite and chlorite-rich assemblages. Jones identified a similar sequence of skarn formation associated with the Seligman stock; an early anhydrous stage, which produced garnet-pyroxene and wollastonite skarn, biotite and pyroxene hornfels, and marble, followed by hydrous alteration of previously-

formed skarn to epidote, actinolite, chlorite and biotite, and finally a period of hydrothermal alteration which oxidized and altered sulfides deposited in earlier stages.

The sequence of skarn formation in the study area as described above is very similar to the generalized sequence of skarn formation described by Einaudi and others (1981). This sequence proceeds from an early stage of prograde, anhydrous metamorphism associated with the intrusion of a pluton, to a period of metasomatic skarn formation characterized by the production of anhydrous calc-silicates, resulting from the release of hydrothermal fluid from the crystallizing pluton, and finally to a stage of hydrous alteration of previously formed assemblages and deposition of sulfides as temperatures declined in the contact aureole.

The following descriptions of metamorphic rocks and skarn in the study area are based on the observations of the author and the work of Sonnevil (1979) and Jones (1984).

PROGRADE METAMORPHIC ROCKS AND SKARN

Marble

Marble occurs at the outer margins of the contact aureole where it grades into gray interbedded calcareous

siltstone and limestone. It is light green to white and consists of lenses and beds of recrystallized calcite interbedded with laminated layers which contain fine-grained clinopyroxene and local bladey wollastonite. At the surface, differential weathering has caused the laminated beds to stand out in relief against marble lenses and beds which are more susceptible to weathering.

The bleached white color of the marble is probably the result of the driving-off of carbon, which is a common constituent in the unaltered limestone, during contact metamorphism. Rising temperatures caused by the intrusion of the stocks probably caused the recrystallization of calcite, and the formation of clinopyroxene and wollastonite by reactions between quartz and magnesian(?) calcite which were probably present in the original rock.

Hornfels

Two major types of hornfels, biotite and clino-pyroxene hornfels, are present, although they are not differentiated on Plate 1.

Biotite hornfels is a dense, fine-grained, light gray to dark brown rock which is composed of predominantly biotite and quartz. Tremolite was observed in biotite hornfels in the Monte Cristo area (Sonnevil, 1979), but was only observed as fracture fillings in hornfels near

the Seligman stock.

Clinopyroxene hornfels forms the bulk of outcrops adjacent to the Seligman stock and replaces biotite hornfels in the Monte Cristo area (Sonnevil, 1979). This rock is pale green and is typically finely laminated. The major constituents of the rock are fine-grained granular clinopyroxene and quartz with lesser amounts of clinozoisite. Clinozoisite is often pink in hand specimen, indicating the presence of trace amounts of manganese.

Biotite hornfels probably formed from the metamorphism of shale, whereas clinopyroxene hornfels may have formed from metamorphism of calcareous siltstone or by replacement of biotite hornfels during skarn formation.

Hornfels/Skarn

Clinopyroxene hornfels with interbedded garnet-pyroxene skarn occurs adjacent to the Seligman stock, and also to the south and southeast of the stock (Plate 1). This unit consists of laminated pyroxene hornfels with lenses and beds of medium to coarse-grained garnet-pyroxene skarn.

Pyroxene hornfels is very similar to that described above and probably was originally laminated calcareous siltstone. Skarn layers, which probably replaced original limestone layers in the rock, consist of interlocking

garnet crystals, typically with inclusions of fine-grained clinopyroxene. Garnet is typically euhedral where it projects into quartz-filled vugs, and ranges from isotropic to strongly anisotropic with concentric zoning and sector twinning. No compositional data is available on this garnet but it probably belongs to the grandite series. Clinopyroxene occurs as stubby to rounded fine-grained crystals disseminated in garnet or quartz-rich zones.

It is unknown whether this rock formed as a result of isochemical metamorphism or metasomatism. Comparison between whole rock analyses of altered and unaltered equivalents of this rock would provide an answer to this question.

Garnet-Pyroxene Skarn

Garnet-pyroxene skarn is the major host for tungsten-molybdenum mineralization in the Seligman-Monte Cristo area. It is present at the surface adjacent to both stocks, and extends out along bedding for distances of over 5,000 feet from the Monte Cristo stock (Plate 1). Surface exposures of skarn associated with the Seligman stock are much less extensive than those apparently associated with the Monte Cristo stock, but drilling has indicated the presence of more extensive skarn development

in the subsurface between the two stocks. Sonnevil (1979) attributed the extensive development of skarn southeast of the Monte Cristo stock to lateral movement of metasomatic fluid along limestone-siltstone interbeds which probably dipped into the intrusive. This skarn development could also be related to a possible southeastern at depth extension of the Seligman stock as shown on Plate 2.

Garnet-pyroxene skarn consists of medium to coarse-grained medium to dark brown garnet with lesser amounts of fine to medium-grained clinopyroxene and quartz. Bedding laminations are locally preserved in skarn, but where metasomatism was most intense, bedding features have been obliterated by the growth of coarse-grained garnet.

Garnet in skarn ranges from isotropic to anisotropic and occurs as subhedral to euhedral interlocking crystals and as euhedral crystals in quartz. Garnet in skarn near the Monte Cristo area belongs to the grossularite-andradite series and ranges in composition from 20-30 mole percent andradite near marble to 50-90 mole percent in the bulk of the skarn (Sonnevil, 1979). Sonnevil determined that these garnets were zoned in their aluminum, iron, and manganese contents. Similar compositional data for garnet from the Seligman area is not available, but it is assumed that the garnet belongs to the grandite series.

Clinopyroxene occurs as granular crystals embedded in garnet and optically-continuous quartz. Microprobe

analyses of pyroxene from the Monte Cristo area indicate that it belongs to the diopside-hedenbergite-johannsenite series, and that it is zoned with respect to magnesium, iron, and manganese (Sonnevil, 1979).

Fine to medium-grained scheelite locally occurs as disseminated anhedral grains in quartz and garnet, and as grains attached to the rims of, or embaying, euhedral garnets. Molybdenite occurs locally in garnet-pyroxene skarn, but most molybdenite appears to be more closely related to hydrous alteration of skarn than the formation of the skarn itself.

Garnet-pyroxene skarn probably resulted from the metasomatic replacement of pre-existing marble and hornfels by hydrothermal fluids, which emanated from the two stocks during the later stages of their crystallization. The extensive development of skarn southeast of the Monte Cristo stock may indicate that this stock produced a much larger volume of hydrothermal fluid during its crystallization than the Seligman stock did. Assuming that the two stocks were not emplaced at the same time, some skarn at depth between the stocks may have been affected by hydrothermal solutions from both stocks. Detailed study of skarn intersected in drill holes between the stocks may provide clues to the affects of multiple intrusions on skarn formation.

Retrograde Alteration

Retrograde alteration of prograde skarn involves the replacement of anhydrous minerals such as garnet and pyroxene by hydrous minerals such as epidote, actinolite, and chlorite, and probably occurred as temperatures declined during cooling of the stocks. The hydrous assemblages are commonly confined to veinlets and vugs in the prograde rocks. Deposition of pyrite, chalcopyrite, molybdenite, and magnetite is commonly associated with this stage of alteration.

Two alteration zones mapped by Sonnevil (1979) and shown on Plate 1 are associated with this stage of alteration. The epidote-actinolite zone is characterized by the replacement of hornfels by clinozoisite, actinolite, chlorite, and white mica and by the presence of abundant quartz-pyrite and quartz-magnetite veins with epidote and actinolite selvages in skarn. Sonnevil observed quartz-K-feldspar veins in the epidote-actinolite zone adjacent to the Monte Cristo stock, and inferred that this hydrous alteration may be related to potassic alteration in the stock. In the gossan zone, original limestone beds consist of magnetite, pyrite, and quartz, with minor chlorite, actinolite, and epidote. Sonnevil believed that this zone resulted from surface leaching of original high sulfide skarn.

Hydrous alteration also occurs in skarn and hornfels surrounding the Seligman stock, but it appears to be less intense at the surface than that associated with the Monte Cristo stock, and does not constitute a mappable unit. In Seligman rocks garnet is commonly replaced or veined by epidote, chlorite, and/or biotite, and may contain vugs which contain quartz, actinolite and chlorite. Clinopyroxene generally alters to calcite or actinolite. Jones (1984) noted that chalcopyrite, pyrite, and molybdenite were often associated with hydrous alteration of prograde skarn near the Seligman stock.

Jasperoid

Jasperoid has been described by Sonnevil (1979) in the Monte Cristo area, and also occurs peripheral to the Seligman stock (Plate 1). In the Monte Cristo area, jasperoid occurs in tremolitic limestone and skarn, commonly along faults. In general the rock consists of very fine-grained quartz which is typically iron oxide stained and brecciated.

Jasperoid crops out near the Seligman stock as linear zones of silicified, iron oxide stained and brecciated hornfels. Near the stock contact these rocks contain stockwork quartz veins and bull quartz veins up to 3 feet thick. These silicified bodies appear to have similar

attitudes to zones of quartz-sericite-sulfide veins which occur within the stock, and they may have been emplaced at the same time.

Jasperoid also occurs in the subsurface in the Geddes limestone near its contact with the Eldorado Dolomite, as encountered in drill hole PH-56 (Plate 3).

ALTERATION OF INTRUSIVE ROCKS

All intrusives in the Seligman-Monte Cristo area have been altered to some extent. The alteration types present include potassic, sericitic, propylitic, argillic and endoskarn.

No well-defined spacial zonation of alteration assemblages was observed in the study area. Alteration types typically overprint each other, and several types may be present within a single sample. Where alteration minerals are associated with veinlets, cross-cutting relationships may indicate the relative ages of the alteration types, but where alteration is weak and alteration minerals are disseminated in the primary minerals, the relative ages of the alteration types usually cannot be determined with certainty.

POTASSIC ALTERATION

Potassic alteration is defined as the replacement or veining of original rock constituents by K-feldspar or biotite. This type of alteration was observed in granite porphyry associated with the Monte Cristo stock, and in biotite hornblende rhyodacite sills north of this stock.

In biotite granite porphyry this alteration type occurs as medium grained K-feldspar selvages on quartz

veins, which cut the fine-grained quartz-K-feldspar groundmass and plagioclase phenocrysts of the rock, and as local veinlets of fine-grained biotite which occur in areas which are apparently flooded by K-feldspar (Figures 16 and 17). The intensity of quartz-K-feldspar veining appears to decrease away from the Monte Cristo stock; secondary K-feldspar was rarely observed in samples of granodiorite porphyry sills and dikes peripheral to the stock. Although biotite granite porphyry commonly contains quartz veins with sericite selvages which generally postdate K-feldspar alteration (Sonnevil, 1979), K-feldspar is usually not altered to sericite in this rock.

Potassic alteration in rhyodacite porphyry sills involves partial to total replacement of plagioclase phenocrysts and possibly groundmass quartz, and is not associated with quartz veins. In the most extreme example (Figure 18), the entire groundmass of the rock consists of granular K-feldspar, and original plagioclase phenocrysts are pseudomorphically replaced by K-feldspar. Original plagioclase phenocrysts are represented by rectangular arrangements of sericite which has replaced zones in plagioclase. Where alteration is less intense, K-feldspar locally partially replaces plagioclase phenocrysts and the groundmass of the rock contains significant amounts of quartz. Solutions which produced potassic alteration in rhyodacite may have originated from the Monte Cristo

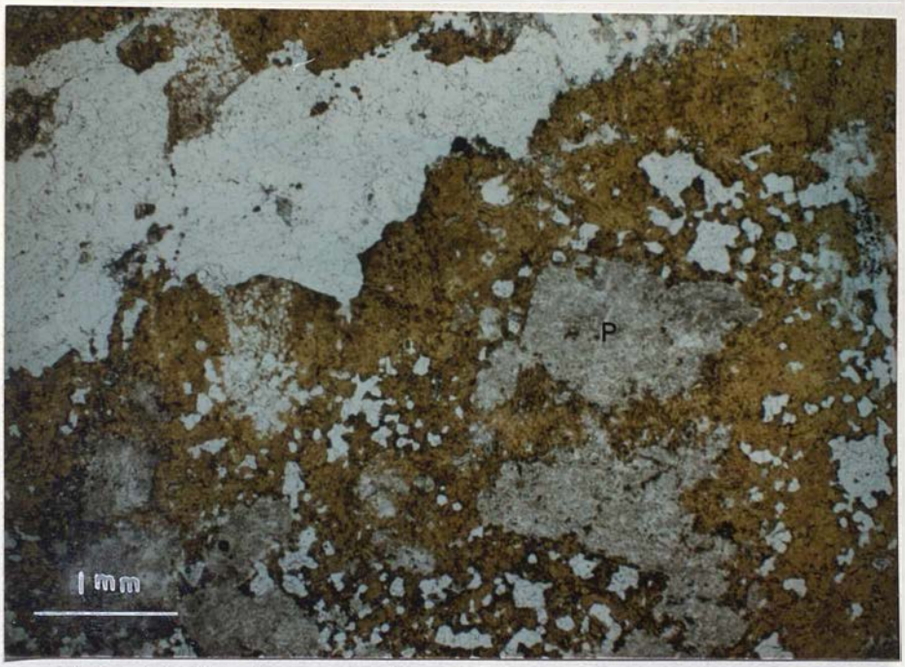

Figure 16. Photomicrograph of K-feldspar selvage (stained yellow) on quartz veinlet flooding groundmass and cutting sericitically altered plagioclase phenocryst (P) in biotite granite porphyry. Uncrossed nicols. (Sample MI-4)

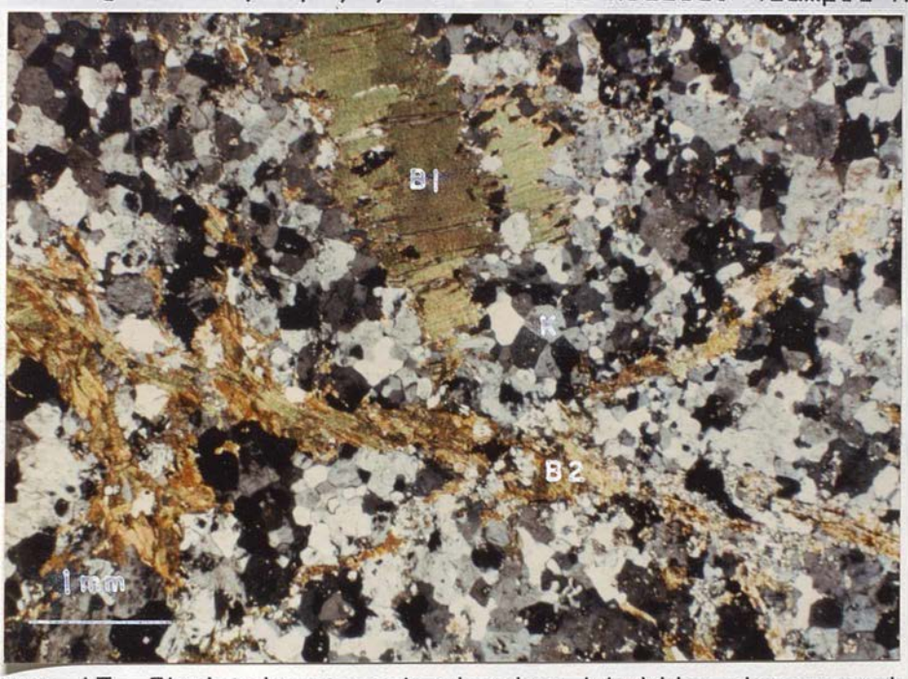

Figure 17. Photomicrograph showing biotite phenocryst (B1) and secondary biotite veinlets (B2) cutting K-felspar (K) in granite porphyry. Crossed nicols. (Sample U11-3, 1039 ft.)

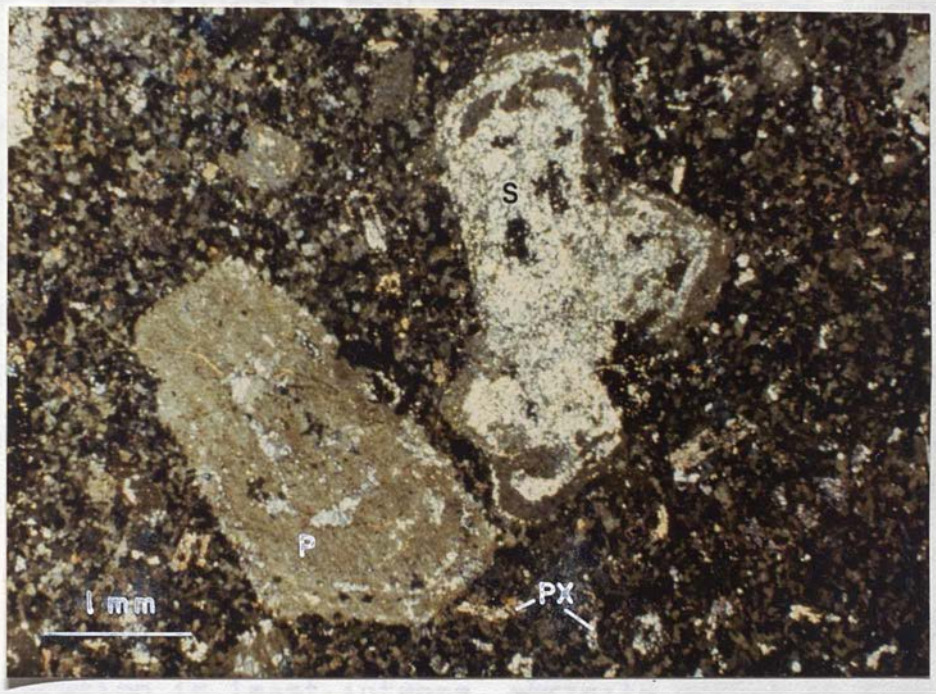

Figure 18. Photomicrograph showing replacement of plagioclase phenocrysts by K-feldspar (stained yellow-green) in rhyodacite porphyry. Original zones in plagioclase (P) indicated by arrangement of sericite (S). Groundmass consists of K-feldspar and clinopyroxene (PX) which has replaced hornblende. Crossed nicols. (Sample MD-3)

stock.

SERICITIC ALTERATION

Sericitic alteration refers to the replacement of primary rock constituents (plagioclase, K-feldspar, and biotite) by fine to medium-grained white mica. Limited x-ray diffraction analyses of sericite from the study area indicate that it is well-ordered muscovite, probably the 2M (two-layer monoclinic) polytype, and not illite. This determination is based on the presence of a well-defined, sharp 001 peak on x-ray patterns. As shown in Carroll (1970), the 001 peak of illite is not as intense and is commonly ragged and more diffuse than that associated with muscovite.

Sericitic alteration of varying intensity has affected all intrusive rocks in the study area. Where alteration is least intense, sericite occurs as fine-grained flakes replacing cores or zones in plagioclase, whereas K-feldspar is unaffected. Where alteration is intense, commonly along margins of quartz-sulfide veins, all primary minerals except quartz are altered to sericite (Figure 19).

Zones of intense sericitic alteration in the Seligman stock range from 1 to 2 inch selvages on isolated quartz-sulfide veins to zones which extend up to 500 feet from

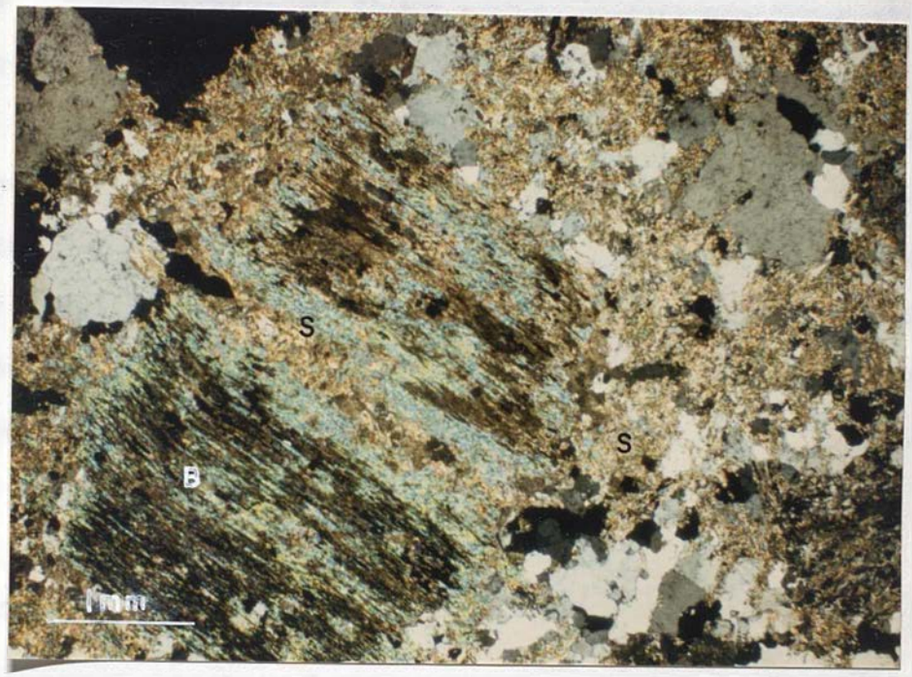

Figure 19. Photomicrograph showing intense sericitic alteration of granodiorite. Sericite (S) has totally replaced plagioclase and K-feldspar, and has partially replaced a biotite phenocryst (B). Crossed nicols. (Sample 33-1, 813 ft.)

quartz-sulfosalt veins and stockwork quartz-pyrite veins, which cut the stock at the surface.

Porphyritic sills in the subsurface appear to have been highly susceptible to sericitic alteration, which commonly obscures the original mineralogy of the groundmass. Sericite is locally interleaved with chlorite in the groundmass of these rocks, suggesting that it may have replaced biotite.

As noted by Sonnevil (1979), quartz-pyrite veins with sericite selvages generally postdate quartz-K-feldspar veins in the Monte Cristo stock, but K-feldspar appears to be stable with respect to sericite in the stock. Sericite generally replaces plagioclase phenocrysts and biotite in the main body of the stock.

PROPYLITIC ALTERATION

Propylitic is a term generally applied to alteration assemblages which contain epidote and/or chlorite (Meyer and Hemley, 1967). The propylitic assemblage in the intrusives of the study area is characterized by the replacement of mafic minerals by chlorite and epidote, and the replacement of plagioclase by clinozoisite, zoisite, and/or epidote. Disseminated alteration of this type leaves the original texture of the rock intact, and

typically coexists with weak sericitic alteration. Minerals of the propylitic assemblage also occur in, and as selvages on, quartz-pyrite±molybdenite veinlets in most of the intrusives.

Cores and zones of plagioclase in almost all samples examined are altered to zoisite, clinozoisite, and locally epidote. Zoisite occurs as fine-grained almost opaque patches in the cores of plagioclase crystals, and often displays patchy anomalous blue interference colors. This fine-grained material may also contain clinozoisite and epidote. In hand specimen, altered patches in plagioclase are often pink in color, which is typical of thulite (manganiferous zoisite) or piemontite (manganiferous epidote-clinozoisite). However, this material does not display strong yellow-pink pleochroism, typical of thulite and piemontite, in thin section.

Chlorite ranges from colorless to strongly pleochroic from pale to dark green, and commonly partially replaces biotite and hornblende along cleavages, and forms rims on disseminated magnetite grains. Biotite is typically more intensely altered than hornblende, and is often totally replaced by chlorite. Strongly yellow-green pleochroic epidote commonly coexists with chlorite in altered biotite books, and to a lesser extent in hornblende, and also rims disseminated pyrite.

Epidote and clinozoisite, associated with quartz-

pyrite veinlets, occur intergrown with quartz in the veins and as selvages which replace all primary minerals, except quartz and some K-feldspar, in the walls of the vein (Figure 20). The most intense example of this type of alteration in the study area was observed in granite(?) porphyry sills at depths greater than 1900 feet in hole PH-56, where the rock has been invaded by stockwork chlorite and quartz-epidote-pyrite±chlorite±molybdenite veinlets. Disseminated molybdenite in endoskarns southwest of the Seligman stock is commonly rimmed by clinozoisite, suggesting that its depósition is related to some propylitic alteration (Figure 21).

Quartz-sulfide veinlet-related epidote and chlorite alteration of intrusive rocks in the study area may be correlative with hydrous alteration and sulfide deposition in altered prograde skarns. Sonnevil (1979) and Jones (1984) mention the common association of molybdenite with retrograde hydrous alteration in skarn associated with both stocks. No direct link between this type of alteration and mineralization in skarn and that present in the intrusives has been observed, but the similarities in mineralogy suggest that the same fluids altered skarn and intrusive rocks, possibly at the same time.

Figure 20. Photomicrograph showing epidote (E) replacing groundmass and plagioclase phenocryst (P) in rhyodacite porphyry. Crossed nicols. (Sample MD-5)

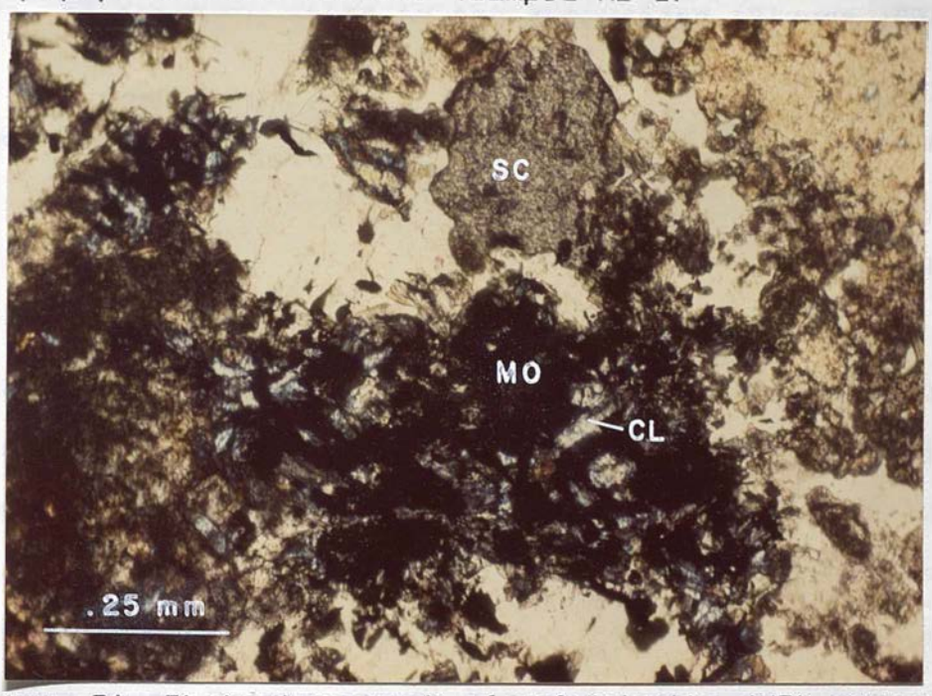

Figure 21. Photomicrograph of molybdenite (MO) surrounded by clinozoisite (CL), with scheelite (SC) and quartz (Q) in plagioclase-pyroxene endoskarn. Crossed nicols. (Sample P51-2, 1813 ft.)

ARGILLIC ALTERATION

Argillic alteration is defined as alteration of plagioclase or K-feldspar to kaolinite and/or montmorillonite. This type of alteration does not occur in a well-defined zone, but appears to be most intense in the Monte Cristo area.

Weak kaolinitic alteration, producing a dusty appearance in K-feldspar, is present in most samples which were examined, and is the most common occurrence of this alteration type. Kaolinite also occurs as fibrous crystals with montmorillonite and illite in plagioclase phenocrysts in sericitically altered dacite porphyry and granite porphyry sills in the subsurface (Figure 10).

In the most intense form of argillic alteration, kaolinite occurs as patchy replacements of K-feldspar and plagioclase, and as .1 to .2 mm. wide veinlets which cut all alteration types and primary minerals in the rock (Figure 22). Kaolinite in these rocks occurs as very fine grained (.01 to .015 mm.) granular crystals with very low first order interference colors. Calcite and sericite locally surround patches of kaolinite, and calcite also occurs within some of the kaolinite veinlets. Relatively intense argillic alteration of this type is most common in the Monte Cristo stock, but has also been observed in granodiorite from drill holes PH-45 and PH-48.

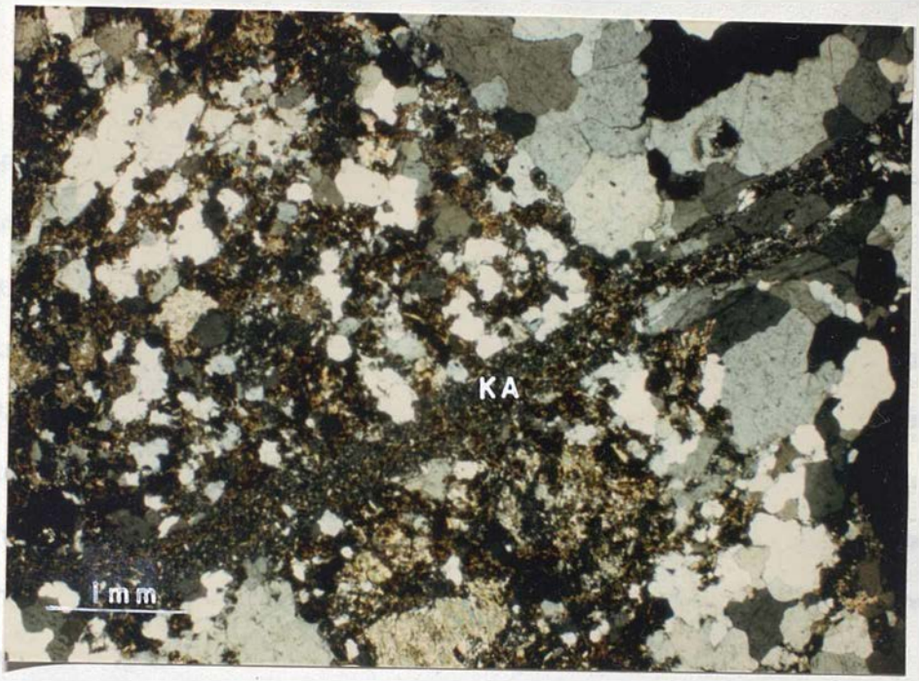

Figure 22. Photomicrograph of kaolinite veinlet (KA) cutting groundmass and quartz vein in granite porphyry. Crossed nicols. (Sample U11-2, 814 ft.)

Argillic alteration appears to post date the other alteration types, at least where it is confined to veinlets. Weak argillic alteration of K-feldspar in surface samples may be a result of surface weathering.

ENDOSKARN

Endoskarn, which forms by the metasomatic replacement of igneous rocks by calcium-rich fluids, is a common form of alteration in sills and dikes related to the Seligman stock, and locally occurs near the stock contact in the subsurface. Endoskarn development in the Monte Cristo stock appears to be much less common, although it was observed in two samples of rhyodacite porphyry north of this stock. Like the prograde exoskarns, described earlier, endoskarns have been variably altered to hydrous mineral assemblages.

The general characteristics of endoskarns have been discussed by Einaudi and Burt (1982). They noted that endoskarn is common in districts where metasomatic fluids used dike-limestone contacts as conduits, and where the dominant fluid flow was into the pluton or upward along its contacts with carbonates, rather than outward from the pluton. Endoskarn is generally absent from skarns associated with porphyry copper plutons. The general lack of endoskarn in the Monte Cristo stock may be a result of its porphyry copper-like style of emplacement.

The field and petrographic characteristics of the various endoskarns are described below, and their chemistry is discussed in a later section.

Epidote-Quartz Endoskarn

Epidote-quartz endoskarn occurs at the margins of some granodiorite and granite sills in drill holes PH-18 and PH-36, and as a small body within the Seligman stock near its contact with pyroxene hornfels (Plate 1). In the subsurface this endoskarn occurs as 2 to 4 foot thick margins on sills in contact with skarn and hornfels, and as 1 to 2 inch zones in granodiorite adjacent to inclusions of pyroxene hornfels.

Epidote-quartz endoskarn is characterized by the conversion of all primary minerals in the intrusive, except quartz, to epidote (Figure 23). Local accumulations of fine-grained sphene and zircon crystals in quartz probably represent original mafic minerals which were replaced by quartz. Epidote in these rocks is locally strongly zoned, as shown in Figure 24.

The relatively localized occurrence of epidote-quartz endoskarn, near igneous contacts, suggests that it formed by small scale diffusion of calcium into the intrusive from adjacent calc-silicate wall rocks.

Figure 23. Hand specimens of epidote-quartz endoskarn (left) and granodiorite (right) from the Seligman stock.

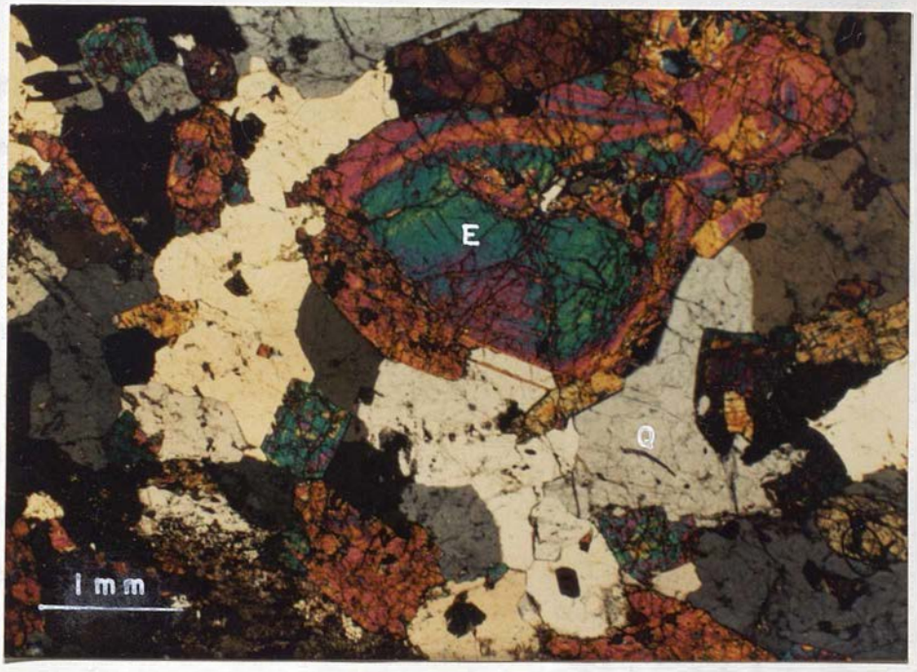

Figure 24. Photomicrograph of zoned epidote (E) and quartz (Q) in epidote-quartz endoskarn. Crossed nicols. (Sample ES-1)

Pyroxene-(Garnet) Endoskarn

Clinopyroxene±garnet endoskarn most commonly occurs in aplite dikes near the contacts of the Seligman stock, and in medium-grained aplitic zones in sills intersected in drill holes PH-10 and PH-22. Clinopyroxene is also common in rhyodacite porphyry sills near the Monte Cristo, where it pseudomorphically replaces prismatic hornblende.

In this type of endoskarn, clinopyroxene pseudomorphically replaces hornblende and also occurs as fine-grained granular crystals rimming biotite, and as clusters of granular crystals embedded in K-feldspar. It is commonly partially altered to calcite or prehnite.

Garnet is a less common constituent of these endoskarns, but where present it tends to occur as coarse grained (as much as 5 cm across) rounded crystals embedded in K-feldspar (Figure 25). These garnets range from isotropic to anisotropic and are commonly concentrically zoned.

The common association of clinopyroxene±garnet with aplitic rocks, suggests that these minerals formed by local diffusion of calcium from wall rocks into the late stage potassium-rich melts which crystallized as aplite.

Figure 25. Drill core specimens of garnet-bearing endoskarn developed in aplite. Sample on left (P22-2, 364 ft.) consists of garnet in sericitically altered K-feldspar (?) and quartz. Sample on right (P10-12, 1405 ft.) consists of garnet and pyroxene in K-feldspar.

Plagioclase-Pyroxene-(Garnet) Endoskarn

Plagioclase-clinopyroxene±garnet endoskarn which has replaced granodiorite and possibly dacite porphyry in the subsurface has been observed only in drill core from holes located south and southwest of the Seligman stock outcrop (Plates 2 and 3). At the surface this type of endoskarn is present as a replacement of rhyodacite porphyry north of the Monte Cristo stock (samples MD-7 and MD-9; Plate 1).

Plagioclase-clinopyroxene±garnet endoskarn consists of calcic plagioclase (50-80%), clinopyroxene (1-35%), quartz (5-40%) and garnet (0-30%). Calcic plagioclase presumably replaced primary plagioclase (andesine) and K-feldspar, although no textural evidence of this was observed in the thin sections studied. Primary hornblende is locally pseudomorphically replaced by clinopyroxene, and biotite is replaced by quartz. Garnet is sometimes present as coarse-grained masses, isolated rounded crystals or veinlets. The rock is generally light gray-green to white, with an equigranular granitoid texture, and it lacks the mafic minerals which characterize the granodiorite which it usually replaces (Figure 26). Where the endoskarn has replaced rhyodacite porphyry, it possesses a porphyritic texture (Figure 27).

Thin sills (.5 to 10 feet thick) tend to be totally replaced by the endoskarn, whereas thicker sills (35-45

Figure 26. Drill core specimens of plagioclase-pyroxene+garnet endoskarn which replaced granodiorite. From left, samples P27-6, 1020 ft.; P11-7, 1594 ft.; P30-9, 1018 ft.; P27-8, 1035 ft.; P51-8, 1876 ft. Compare with unaltered granodiorite above (sample P64-3, 936 ft.)

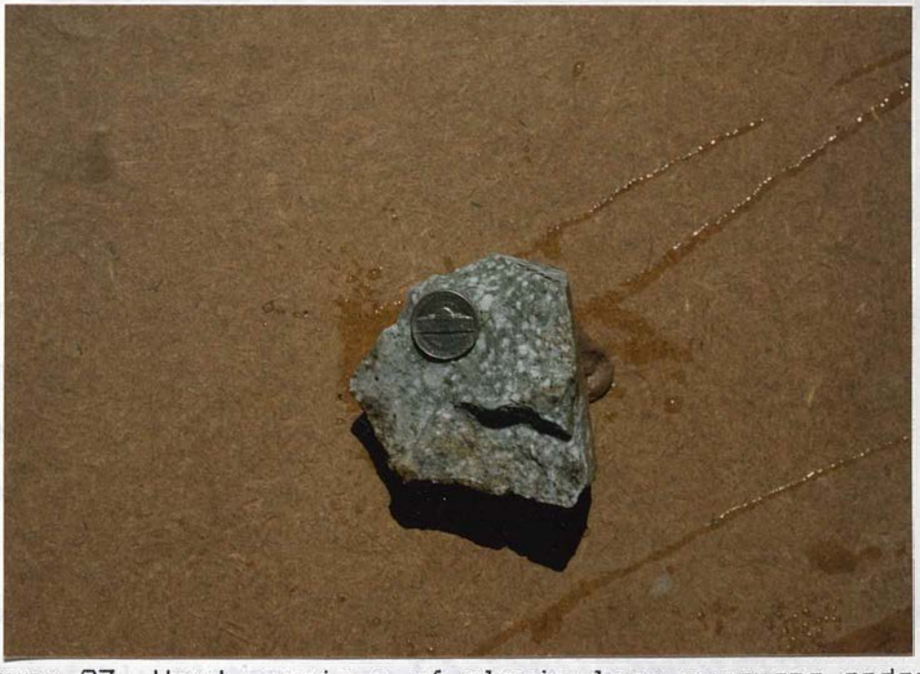

Figure 27. Hand specimen of plagioclase pyroxene endoskarn which replaced rhyodacite porphyry (sample MD-7).

feet thick) may have cores of relatively fresh granodiorite. In some cases sills in the deeper parts of the drill holes are altered to endoskarn whereas sills intersected farther up the hole are relatively fresh, and in other cases all sills intersected have been altered to endoskarn. The contact of the Seligman stock, where it has been intersected in drill holes, southwest of the stock outcrop, is variably altered to plagioclase-clinopyroxene endoskarn, which may be up to 40 feet thick. There appears to be no direct relationship between the occurrence of endoskarn and the presence of skarn in adjacent wall rock, as endoskarn occurs in contact with both skarn and hornfels.

Plagioclase in endoskarn generally occurs as a mosaic of medium grained interlocking anhedral crystals (Figure 28), but it locally possesses crystal faces where it projects into areas of optically-continuous quartz. Where the endoskarn has replaced rhyodacite porphyry, calcic plagioclase presumably has replaced primary plagioclase (andesine) phenocrysts, and fine-grained calcic plagioclase has probably replaced original groundmass quartz and K-feldspar (Figure 29).

Plagioclase in endoskarn differs from primary plagioclase in the intrusives in its lack of zoning and its notably higher An content. An contents of plagioclase in endoskarn range from An 59 to An 72 , and albite twins

Figure 28. Photomicrograph showing calcic plagioclase (P), clinopyroxene (PX), and quartz (Q) in endoskarn. Crossed nicols. (Sample P51-3, 1835 ft.)

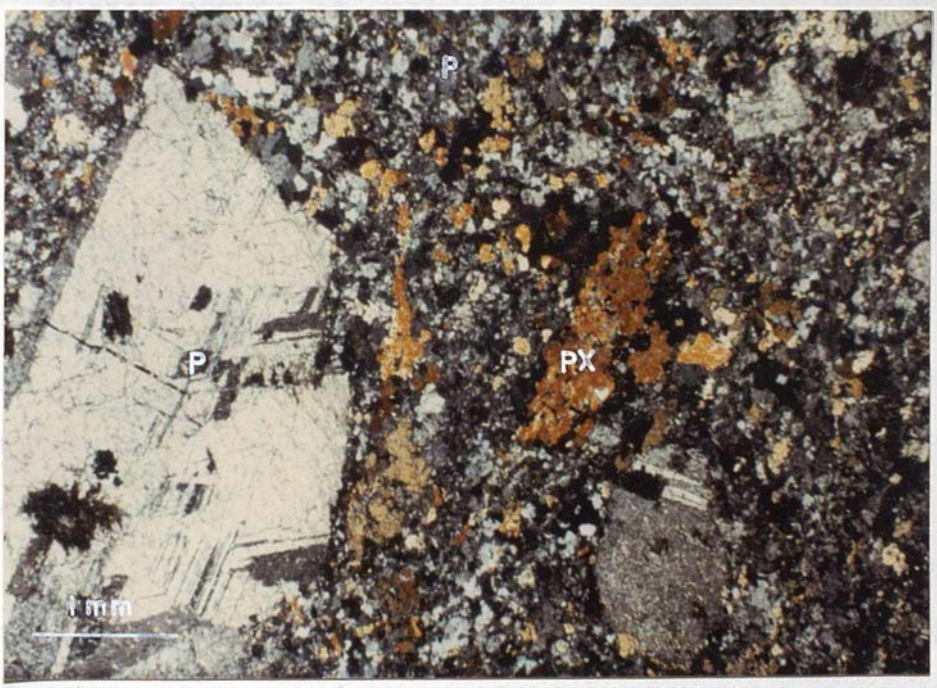

Figure 29. Photomicrograph showing plagioclase-pyroxene endoskarn which has formed from rhyodacite porphyry. Calcic plagioclase (P) has replaced plagioclase phenocrysts and groundmass K-feldspar, and pyroxene (PX) has replaced hornblende. Crossed nicols. (Sample MD-7)

tend to be broader and more diffuse than in primary plagioclase.

Plagioclase in endoskarn is typically partially altered to zoisite, clinozoisite, epidote, sericite prehnite and calcite.

Clinopyroxene occurs as fine-grained rounded crystals in optically continuous quartz and as medium grained subhedral crystals intergrown with plagioclase. In porphyritic endoskarn it occurs as pseudomorphic replacements of hornblende in the groundmass of the rock. Clinopyroxene is typically altered to calcite along cleavages.

Quartz occurs as unstrained, optically-continuous vug-fillings in plagioclase-pyroxene mosaics or as polygonalized anhedral grains. This quartz commonly contains abundant inclusions of granular pyroxene, sphene, and apatite crystals, and euhedral plagioclase. Quartz in endoskarn formed later than plagioclase and pyroxene, as evidenced by its tendency to invade broken crystals of these minerals (Figure 30) and to fill in around euhedral crystals.

Garnet is locally present in this type of endoskarn, generally near the margins of altered sills, and is brown in hand specimen, and is weakly to strongly anisotropic in thin section. Anisotropic garnets typically display sector twinning and concentric zoning. Garnet was probably

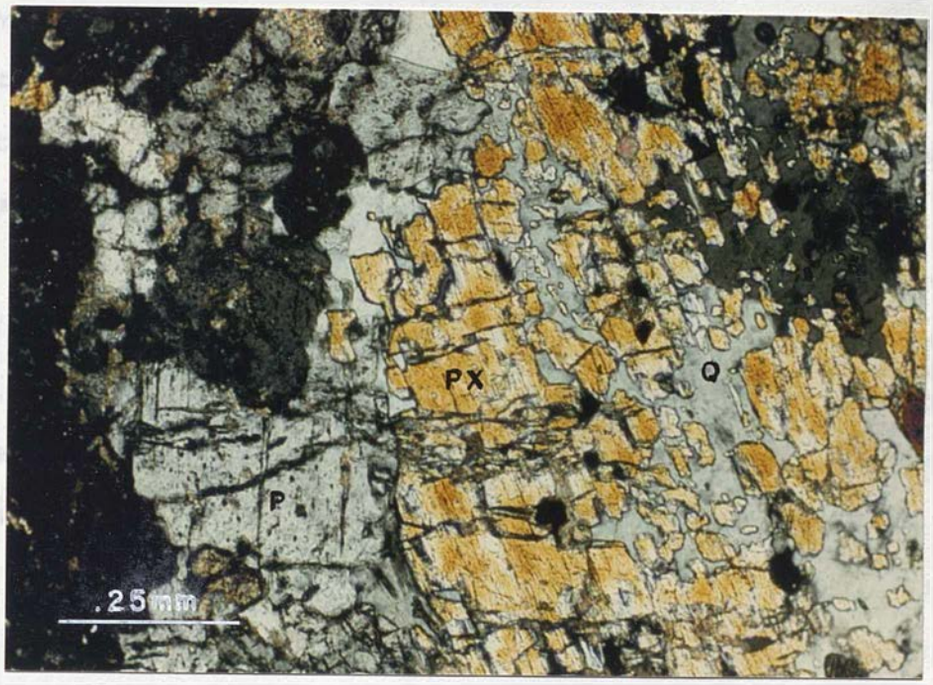

Figure 30. Photomicrograph showing quartz (Q) filling in around fractured pyroxene (PX) and plagioclase (P) in plagioclase-pyroxene endoskarn. Crossed nicols. (Sample P51-3, 1835 ft.)

originally subhedral to euhedral, but intense alteration to epidote, clinozoisite, calcite, and quartz has generally made crystal rims ragged. Garnet locally occurs in veinlets which cut plagioclase (Figure 31), indicating that it formed later than plagioclase.

Sphene is common in the endoskarn as fine-grained crystals included in quartz. In some cases these crystals occur in rectangular arrangements, which may represent the locations of primary biotite books that were replaced by quartz during endoskarn formation (Figure 32).

Plagioclase-pyroxene endoskarn, in intrusives related to the Seligman stock, commonly contains disseminated molybenite, which is associated with clinozoisite-altered areas in plagioclase and quartz-rich zones. Scheelite was observed in one sample of endoskarn (Figure 21).

Plagioclase-pyroxene endoskarn apparently formed by calcium metasomatism of granodiorite, rhyodacite porphyry, and possibly dacite porphyry. The total replacement of sills up to 70 feet thick, suggests that these endoskarns formed by infiltration of metasomatic fluid into the rock rather than by local diffusion of components between adjacent intrusives and carbonates.

The presence of plagioclase-pyroxene endoskarn only in the area southwest of the Seligman stock (Plates 2 and 3) suggests that the formation of these endoskarns may be related to the intrusion of the Monte Cristo. The Monte

Figure 31. Photomicrograph of garnet veinlet (G) cutting plagioclase (P) and pyroxene (PX) in endoskarn. Garnet is weakly anisotropic. Crossed nicols. (Sample P11-7, 1594 ft.)

Figure 32. Photomicrograph showing oriented sphene crystals (SP) in quartz (Q). Arrangement of sphene crystals suggests that quartz replaced a biotite phenocryst in granodiorite during the formation of plagioclase endoskarn. Clouded grains are altered plagioclase. Uncrossed nicols. (Sample P11-1, 723 ft.)

Cristo stock may have been the source of the fluids which produced the endoskarns.

LATE STAGE ALTERATION

Late stage alteration of intrusives and endoskarns includes pervasive and veinlet-related prehnite, calcite, and laumontite. These alteration types most commonly affect sills and dikes peripheral to the two stocks, and are considered late stage based on the presence of minerals which form at relatively low temperatures, and their common occurrence in veinlets which cross-cut all high temperature mineral assemblages.

Prehnite occurs as globular masses of dusty anhedral crystals which show incomplete extinction and second order interference colors. It occurs as patchy replacements of primary plagioclase and K-feldspar in granodiorite, aplite, and rhyodacite porphyry, and also locally partially replaces plagioclase in endoskarns, and pyroxene in calcic-altered aplites. In some cases alteration to prehnite totally obscures the original texture of the rock (Figure 33).

Calcite occurs as patches replacing plagioclase, mafic minerals, and locally quartz, and as narrow veinlets which typically cross-cut the other alteration minerals present.

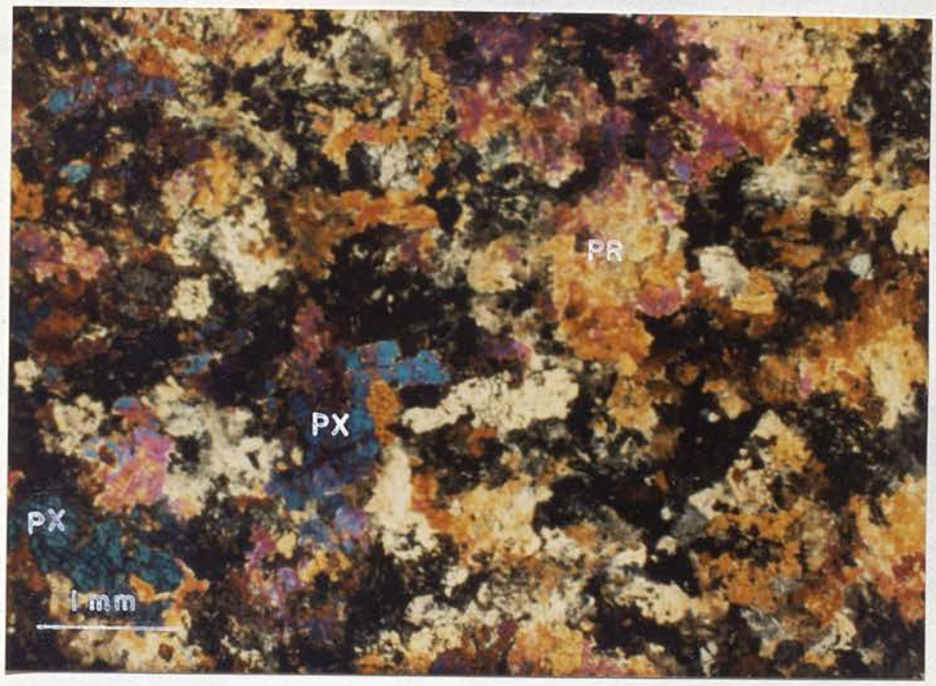

Figure 33. Photomicrograph showing prehnite (PR) and pyroxene (PX) in altered aplite (?). Crossed nicols. (Sample P19-2, 1328 ft.)

The latest stage of alteration identified in the study area is the local deposition of laumontite as thin fracture fillings, which cross-cut all minerals in the samples in which they occur (Figure 34). Laumontite exhibits simple twinning and low first order interference colors in thin section, and occasionally coexists with calcite in the same veinlets.

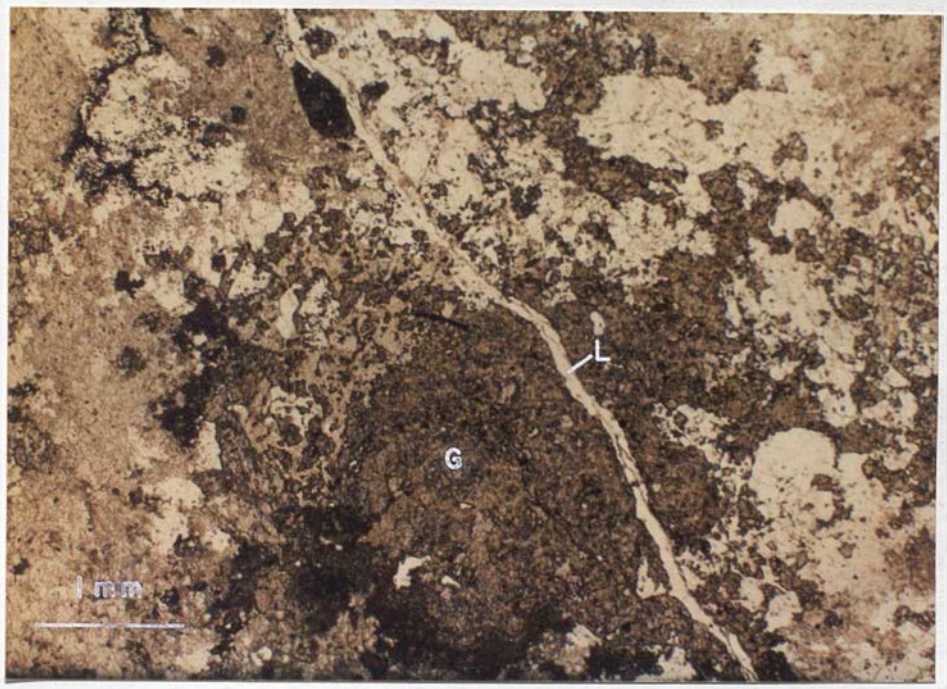

Figure 34. Photomicrograph of laumontite veinlet (L) cutting garnet (G) in plagioclase-pyroxene-garnet endoskarn. Uncrossed nicols. (Sample P27-6, 1020 ft.)

GEOCHEMISTRY OF INTRUSIVE ROCKS

The geochemistry of the intrusives and their altered equivalents was studied using major and trace element analyses. The elements analysed, detection limits and method of analysis are shown in Table 4. Whole rock and trace element analyses by inductively-coupled plasma emission spectroscopy (ICP) were done by Barringer Magenta Ltd., Toronto, Canada, and other trace element analyses were done by Barringer Resources Inc., Sparks, Nevada. Complete analyses for all samples, grouped by rock or alteration type, are listed in Appendix A.

PETCAL, a BASIC language computer program, which is described by Bingler and others (1976), was used to calculate CIPW norms and petrologic indices for the intrusives from major element data. Major element values, normalized to 100%, were used in norm calculations and variation diagrams. The program also calculated FeO from total iron, which was reported as Fe_2O_3. CLUSTR, a FORTRAN program written by Davis (1973) and modified by Don Hudson, was used to investigate relationships between major and trace elements in the intrusives and in plagioclase-pyroxene endoskarns.

TABLE 4. DETECTION LIMITS AND METHODS OF GEOCHEMICAL ANALYSES

OXIDE OR TRACE ELEMENT	METHOD OF ANALYSIS	DETECTION LIMIT
SiO_2	ICP	.05 %
Al_2O_3	ICP	.01 %
K_2O	ICP	.02 %
Na_2O	ICP	.02 %
CaO	ICP	.01 %
MgO	ICP	.01 %
Fe_2O_3 (Total Fe)	ICP	.01 %
MnO	ICP	.001 %
P_2O_5	ICP	.02 %
TiO_2	ICP	.001 %
Ba	ICP	30 ppm
Sr	ICP	1 ppm
Cu	ICP	.5 ppm
Pb	ICP	5 ppm
Zn	ICP	2 ppm
Ni	ICP	2 ppm
Co	ICP	3 ppm
Cd	ICP	7 ppm
Be	ICP	.1 ppm
Cr	ICP	5 ppm
Ag	ICP	5 ppm
V	ICP	1 ppm
Th	ICP	6 ppm
Zr	ICP	3 ppm
Mo	ICP	30 ppm
WO_3	Colorimetric	2 ppm
Rb	AA	1 ppm
F	Spec. ion electrode	4 ppm

MAJOR ELEMENT GEOCHEMISTRY

Average major element values and CIPW norms for intrusive rocks from the study area are listed in Table 5, along with average values for biotite granite and hornblende biotite granodiorite from Nockolds (1954).

An effort was made to obtain fresh samples for chemical analysis in order to characterize the primary geochemistry of the intrusives. However, petrographic studies indicate that all samples have been altered to some extent. Values from endoskarns were not included in the average chemistry of the intrusives, but samples of rhyodacite porphyry and granite porphyry display potassic and sericitic alteration, and dacite porphyry samples display sericitic and propylitic alteration. Therefore, the values presented in Table 5 probably reflect some alteration affects, especially those for the porphyries.

Seligman Stock and Related Intrusives

Inspection of Table 5 reveals that granodiorite of the Seligman stock is chemically similar to the "average" granodiorite, but has slightly higher Al_2O_3, Fe_2O_3, FeO, and CaO, and slightly lower SiO_2, Na_2O, and MgO. Granite from the Seligman area is much closer in chemistry to the average granodiorite than to the average granite. Seligman

TABLE 5 AVERAGE MAJOR ELEMENT ANALYSES AND CIPW NORMS OF INTRUSIVE ROCKS

Oxides (Wt. %)*	Seligman Area					Monte Cristo Area			Nockolds, 1954	
	Granod.	Granite	Q. Mzd., Diorite	Aplite	Dacite Porphyry	Granite Porphyry	Granod. Porphyry	Rhyodac. Porphyry	Average Granod.	Average Granite
SiO_2	64.02	63.87	51.61	73.08	64.46	71.28	66.00	60.73	65.50	73.28
Al_2O_3	16.43	16.39	19.97	13.70	15.20	14.13	16.34	16.28	15.65	13.33
Fe_2O_3	2.07	2.10	2.05	1.66	2.23	1.92	2.16	2.10	1.63	.87
FeO**	4.22	3.45	8.18	1.06	4.88	1.71	3.60	2.97	2.79	1.38
MgO	1.61	1.51	2.95	.51	2.05	.96	1.73	1.80	1.86	.50
CaO	5.04	4.73	7.86	2.94	6.04	2.98	4.76	6.19	4.10	1.17
Na_2O	2.62	2.51	2.62	1.32	1.62	1.06	1.52	1.90	3.84	2.96
K_2O	3.13	4.53	3.06	5.48	2.70	5.42	3.14	7.09	3.01	5.52
TiO_2	.55	.59	1.08	.14	.61	.33	.54	.60	.61	.30
P_2O_5	.22	.23	.48	.05	.15	.14	.14	.19	.23	.14
MnO	.09	.09	.16	.05	.07	.07	.07	.15	.09	.05
No. of Samples	37	6	3	4	4	17	6	4	65	37
CIPW Norms										
Q	21.8	18.9	----	37.3	26.9	36.4	31.0	8.9	20.0	31.2
or	18.5	26.7	18.1	32.4	15.9	32.0	18.5	41.9	17.8	32.8
ab	22.2	21.3	22.2	11.2	13.7	9.0	12.8	16.1	32.5	25.2
an	23.6	20.1	33.7	14.3	26.3	13.9	22.7	15.0	16.4	5.0
c	.1	----	----	.4	----	1.4	2.1	----	----	.5
wo	----	.8	.9	----	1.1	----	----	6.1	.9	----
en	4.0	3.8	7.2	1.3	5.1	2.4	4.3	4.5	4.6	1.3
fs	5.3	3.8	11.6	.4	6.2	1.2	4.1	3.0	2.9	1.3
fo	----	----	.1	----	----	----	----	----	----	----
fa	----	----	.2	----	----	----	----	----	----	----
mt	3.0	3.1	3.0	2.4	3.3	2.8	3.1	3.0	2.3	1.2
il	1.1	1.1	2.1	.3	1.2	.6	1.0	1.1	1.2	.6
ap	.5	.5	1.1	.1	.4	.3	.3	.4	.6	.3
Diff. Index	63	67	40	81	57	77	62	67	70	89

* Values normalized to 100 % by PETCAL program
** Calculated from total Fe (reported as Fe_2O_3) by PETCAL program

granite has lower values of FeO, MgO, and CaO, and higher K_2O than the average granodiorite. Rocks which were classified modally as diorite and quartz monzodiorite have higher FeO, Al_2O_3, MgO, CaO, TiO_2, P_2O_5, and MnO, and lower SiO_2 than granodiorite, reflecting their high modal percentages of mafic minerals and plagioclase compared to granodiorite. Dacite porphyry has higher Fe_2O_3, FeO, MgO, CaO, and TiO_2, and lower Al_2O_3, Na_2O, K_2O, and P_2O_5 than granodiorite, but these differences probably reflect the affects of sericitic and propylitic alteration. Aplite displays values very similar to those of the average granite, but has less Na_2O, TiO_2, and P_2O_5, and more CaO. The low Na_2O values may result from sericitic alteration of albitic plagioclase and high CaO values may result from minor assimilation of Ca from adjacent wall rock.

A plot of normative orthoclase, quartz, and plagioclase (albite + anorthite) with rock type fields according to Streckheisen (1973, 1979) is presented in Figure 35. The rock names indicated by major element chemistry generally agree with those assigned to the rocks based on modes. The average values for modal diorite and quartz monzodiorite plot as monzodiorite on this diagram due to the lack of normative quartz.

Alkali-lime and AFM plots (Figures 36 and 37), indicate that intrusives from the Seligman area have a calc-alkaline trend, and that they represent a trend of

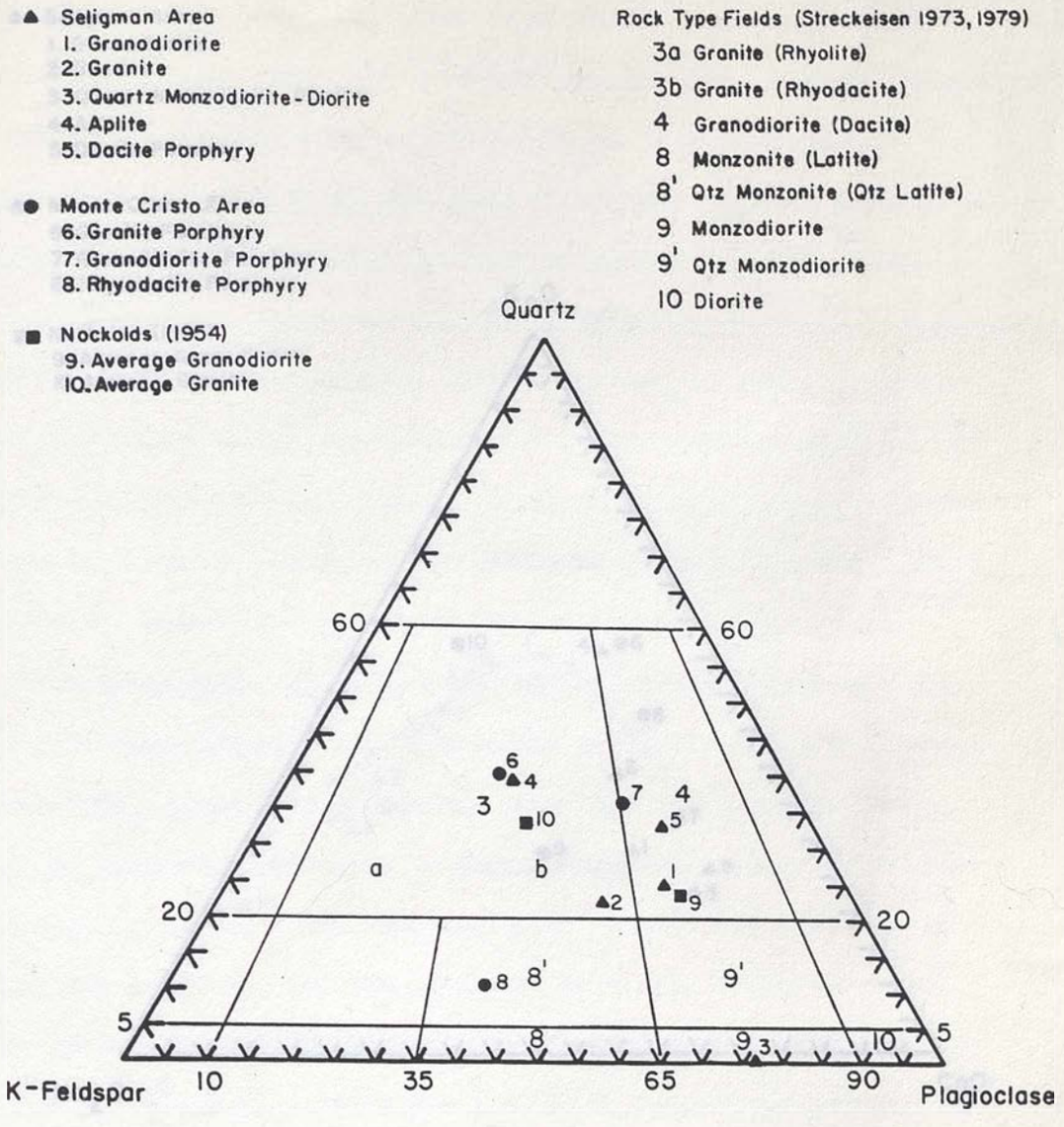

Figure 35. Plot of normative quartz, orthoclase, and plagioclase with rock type fields according to Streckheisen (1973, 1979).

▲ Seligman Area
1. Granodiorite
2. Granite
3. Quartz Monzodiorite - Diorite
4. Aplite
5. Dacite Porphyry

● Monte Cristo Area
6. Granite Porphyry
7. Granodiorite Porphyry
8. Rhyodacite Porphyry

■ Nockolds (1954)
9. Average Granodiorite
10. Average Granite

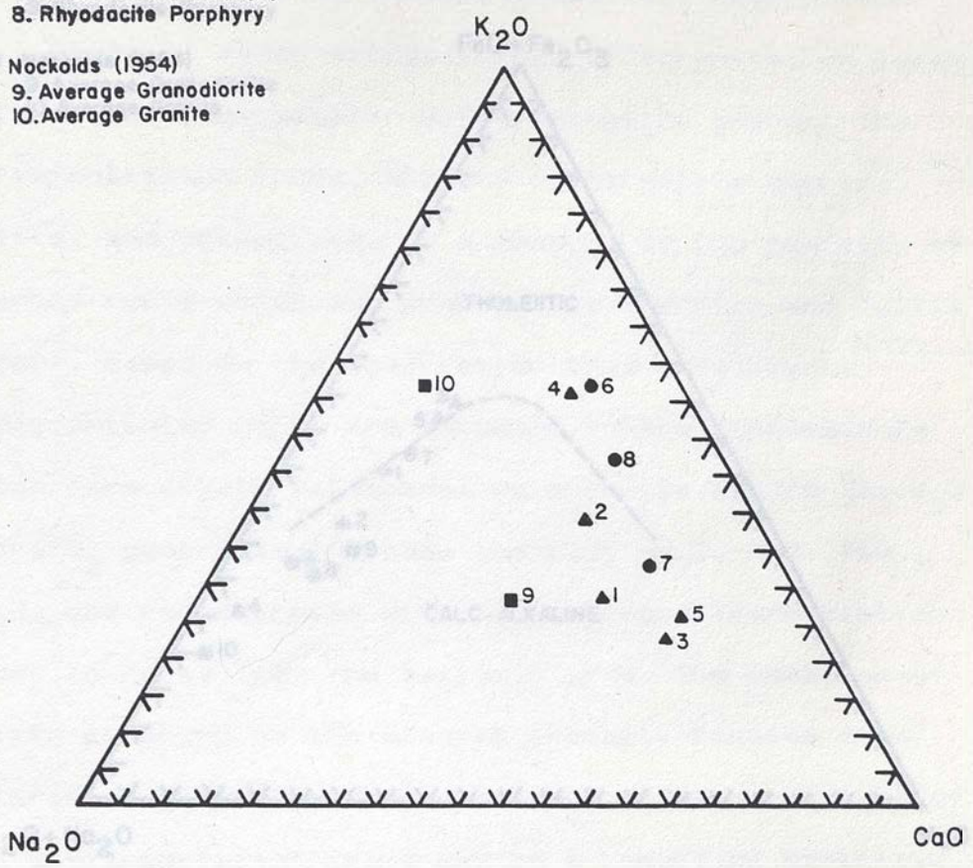

Figure 36. Alkali-lime plot for intrusive rocks.

▲ Seligman Area
1. Granodiorite
2. Granite
3. Quartz Monzodiorite - Diorite
4. Aplite
5. Dacite Porphyry

● Monte Cristo Area
6. Granite Porphyry
7. Granodiorite Porphyry
8. Rhyodacite Porphyry

■ Nockolds (1954)
9. Average Granodiorite
10. Average Granite

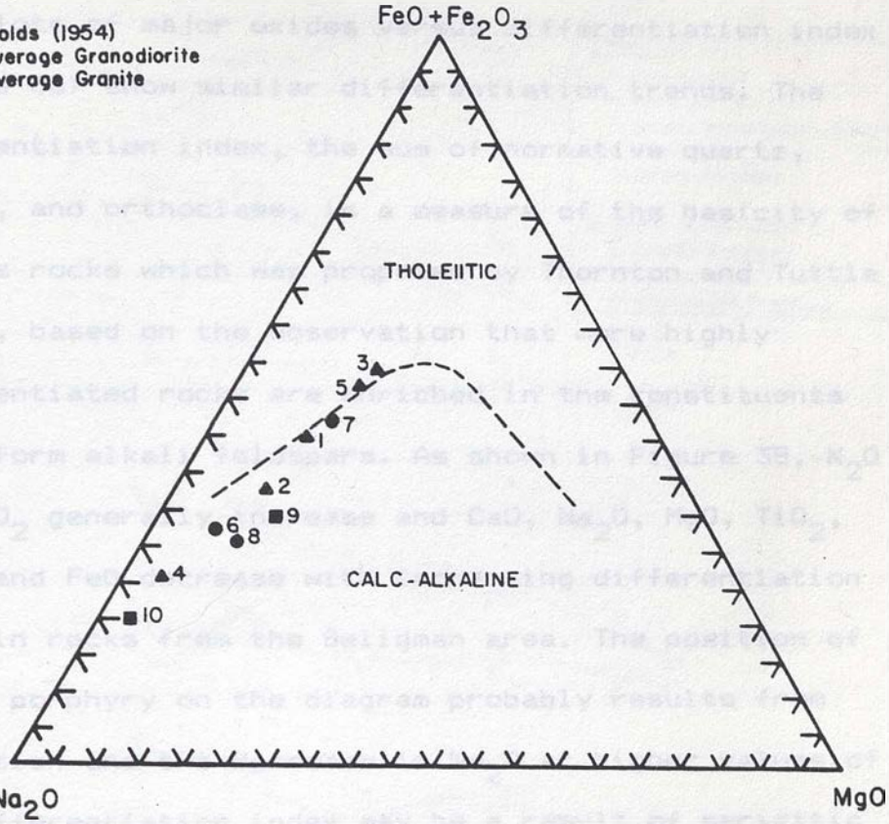

Figure 37. A-F-M diagram for intrusive rocks. Tholeiitic - calc-alkaline field boundary from Irvine and Barager (1971).

increasing differentiation from quartz monzodiorite-diorite to aplite. The plotted position of dacite porphyry near quartz monzodiorite-diorite on the diagrams is probably a result of K_2O depletion and CaO enrichment in these rocks caused by intense propylitic alteration.

Plots of major oxides versus differentiation index (Figure 38) show similar differentiation trends. The differentiation index, the sum of normative quartz, albite, and orthoclase, is a measure of the basicity of igneous rocks which was proposed by Thornton and Tuttle (1960), based on the observation that more highly differentiated rocks are enriched in the constituents which form alkali feldspars. As shown in Figure 38, K_2O and SiO_2 generally increase and CaO, Na_2O, MgO, TiO_2, Al_2O_3 and FeO decrease with increasing differentiation index in rocks from the Seligman area. The position of dacite porphyry on the diagram probably results from alteration and the decrease in Na_2O at higher values of the differentiation index may be a result of sericitic alteration. The trends shown in this diagram agree quite well with those depicted in Thornton and Tuttle (1960) for 5,000 analyses of igneous rocks. The major difference is in their Na_2O curve which is essentially horizontal from differentiation index values of 40 to 95.

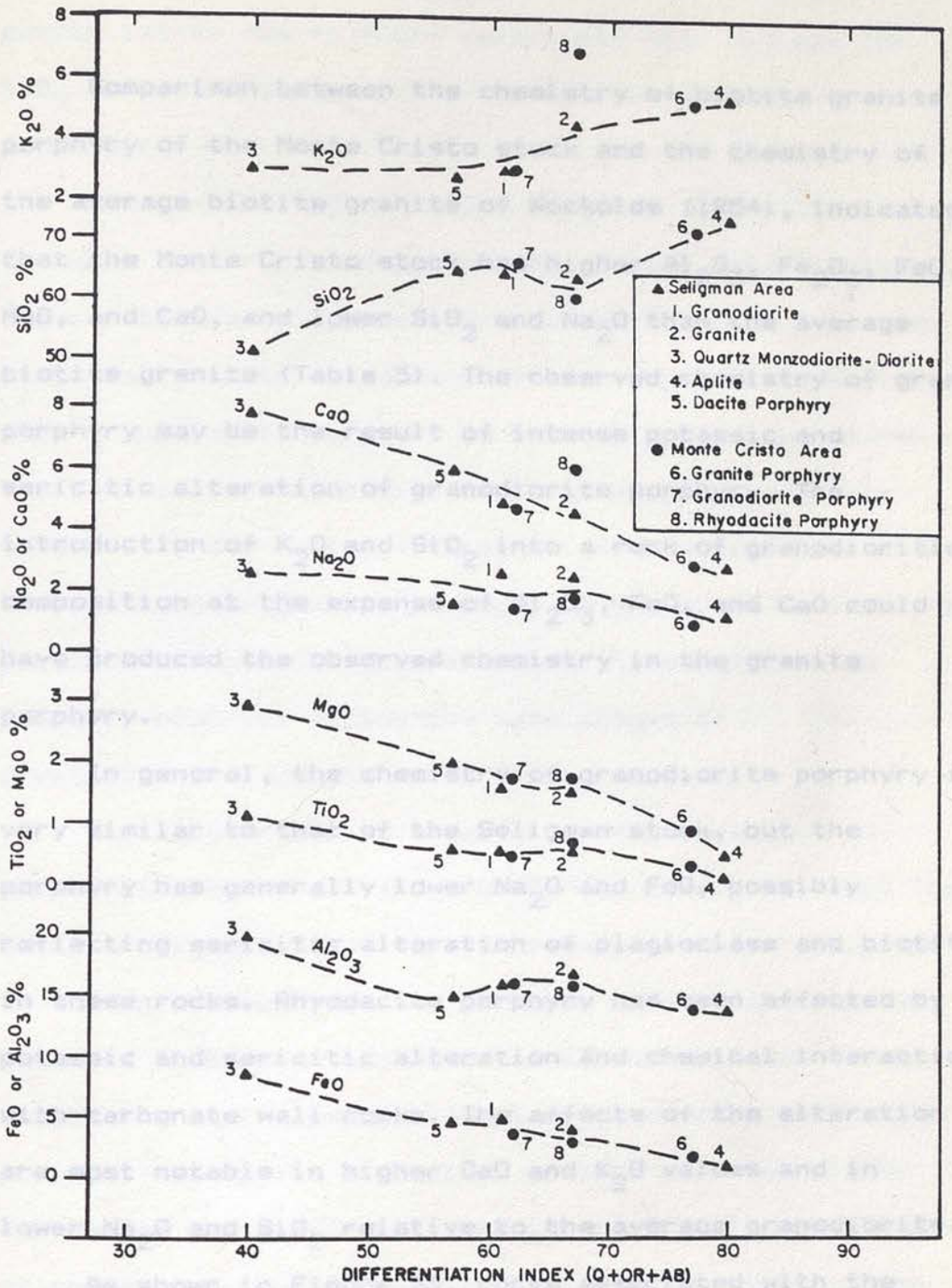

Figure 38. Variation diagram with major elements plotted versus differentiation index.

Monte Cristo Stock and Related Intrusives

Comparison between the chemistry of biotite granite porphyry of the Monte Cristo stock and the chemistry of the average biotite granite of Nockolds (1954), indicates that the Monte Cristo stock has higher Al_2O_3, Fe_2O_3, FeO, MgO, and CaO, and lower SiO_2 and Na_2O than the average biotite granite (Table 5). The observed chemistry of granite porphyry may be the result of intense potassic and sericitic alteration of granodiorite porphyry. The introduction of K_2O and SiO_2 into a rock of granodioritic composition at the expense of Al_2O_3, FeO, and CaO could have produced the observed chemistry in the granite porphyry.

In general, the chemistry of granodiorite porphyry is very similar to that of the Seligman stock, but the porphyry has generally lower Na_2O and FeO, possibly reflecting sericitic alteration of plagioclase and biotite in these rocks. Rhyodacite porphyry has been affected by potassic and sericitic alteration and chemical interaction with carbonate wall rocks. The affects of the alteration are most notable in higher CaO and K_2O values and in lower Na_2O and SiO_2 relative to the average granodiorite.

As shown in Figure 35, rocks associated with the Monte Cristo stock plot in the granite, granodiorite, and quartz latite fields. Rocks assigned the name rhyodacite

on the basis of modal analysis plot on the diagram as quartz latite due to their relatively high K_2O and low SiO_2 values, which probably result from potassic alteration.

Alkali-lime and AFM plots (Figures 36 and 37) indicate that rocks from the Monte Cristo area display similar trends to intrusives from the Seligman area. The diagrams indicate a sequence of increasing differentiation from granodiorite porphyry to biotite granite porphyry. The position of rhyodacite on these plots is probably unrealistic due to the alteration affects described above. The position of granite porphyry on the plots reflects the presence of potassic alteration in these rocks which probably occurred during the late stages of crystallization of the Monte Cristo stock.

Variation diagrams of major oxides versus differentiation index (Figure 38) for intrusives from the Monte Cristo area show similar trends to those exhibited by the intrusives from the Seligman area. Granodiorite porphyry plots near granodiorite of the Seligman stock, indicating their chemical similarity, whereas granite porphyry and aplite plot close to each other at higher values for the differentiation index. The altered nature of the rhyodacite porphyry is indicated by its position well above the inferred trend lines for CaO and K_2O.

Summary

Variation diagrams based on major element chemistry demonstrate the overall chemical similarity between the intrusives of the Seligman and Monte Cristo stocks, and indicate that these rocks may have been derived from the same calc-alkaline parent magma. Rocks from the Seligman area show a trend of increasing differentiation from quartz monzodiorite-diorite, to granodiorite, to granite, to aplite, and rocks from the Monte Cristo area show a trend of increasing differentiation from granodiorite porphyry to granite porphyry. The exact position of dacite porphyry and rhyodacite porphyry in the sequence is unknown due to chemical changes which affected these rocks during alteration.

Mafic-rich rocks of quartz monzodiorite to diorite composition may represent the earliest products of fractional crystallization, which may have been injected from the deeper parts of the magma chamber. Further crystallization produced a melt of granodiorite composition which was intruded into the Seligman area. Porphyritic granite formed as a chilled margin on this stock, and granite sills and aplite crystallized from increasingly differentiated melt as the stock crystallized. Granodiorite porphyry associated with the Monte Cristo stock may be the result of relatively rapid

crystallization of a more water-rich granodioritic magma which probably originated from the same magma chamber which produced the Seligman stock. As crystallization of this magma proceeded, violent release of a potassium and silica-rich aqueous phase, which was localized in the area of the Monte Cristo stock, may have produced intense fracturing and quartz-K-feldspar veining in granodiorite porphyry, producing 'granite' porphyry.

TRACE ELEMENT GEOCHEMISTRY

Mean trace element analyses for the intrusives are listed in Table 6. Average trace element analyses for high Ca (granodiorite) and low Ca (granite) granitic rocks from Turekian and Wedepohl (1961) are also included in this table. Trace element analyses which were less than the detection limit for a given element were arbitrarily assigned a value of one half the detection limit, and these values were incorporated into the listed means. An examination of Appendix A reveals that in the complete data set greater than 30% of values for Th, WO_3, Co, Pb and Mo are below detection limit. Therefore mean values listed for these elements are not an accurate reflection of the actual means of these rocks. Detection limits for Mo and WO_3 are unacceptibly high for these analyses to be useful in characterizing their primary abundances in the

TABLE 6 MEAN TRACE ELEMENT ANALYSES OF INTRUSIVE ROCKS

Element (ppm)	Seligman Area					Monte Cristo Area			Turekian and Wedepohl, 1961	
	Granod.	Granite	Q. Mzd., Diorite	Aplite	Dacite Porphyry	Granite Porphyry	Granod. Porphyry	Rhyodac. Porphyry	Granitic Rocks High Ca	Low Ca
Cu	69±4	71±17	219±63	56±13	492±92	140±19	336±39	69±13	30	10
Pb	57±3	31±15	-5	-5	-5	8±2	-5	36±20	15	19
Zn	53±1	84±29	66±2	12±2	41±6	55±7	23±2	41±4	60	39
Mo	-30	-30	-30	-30	-30	-30	165±80	-30	1.0	1.3
WO_3	7±1	4±3	5±4	12±3	10±3	10±2	2±.3	21±14	1.6	2.8
Ba	1022±17	1267±91	1020±274	573±276	595±188	1099±80	443±73	1727±636	420	840
Be	2.0±.02	2.0±.1	2.2±.1	2.4±.3	2.0±.3	1.8±.2	2.2±.2	2.4±.3	2	3
Cr	55±.4	48±4	68±1	39±4	57±6	36±1	64±4	71±6	22	4.1
Co	13±1	11±6	29±3	-3	33±10	3±1	-3	-3	7	1.0
F	701±11	781±69	923±116	255±114	1512±67	603±32	698±85	433±44	520	850
Ni	23±0	20±2	26±1	19±6	29±1	17±1	23±1	26±3	15	4.5
Rb	69±1	79±5	101±18	109±43	102±32	89±5	109±18	163±5	110	170
Sr	725±18	756±54	861±181	402±171	530±64	332±30	620±63	1379±338	440	100
Th	14±1	20±5	44±15	26±2	20±4	7±1	-6	15±7	8.5	17
V	63±1	64±4	129±1	11±3	112±1	52±4	93±3	92±3	88	44
Zr	22±0	24±2	35±4	27±4	37±6	27±1	25±1	41±3	140	175
No. of Samples	37	6	3	4	4	17	6	4	Not Reported	

Mean ± Error

$$\text{Error} = \frac{(1.96)(\text{Standard Deviation})}{\text{No. of Samples}}$$ at 95% Significance Level

(Beus and Grigorian, 1977)

intrusives, as indicated by their average abundances in granite and granodiorite. Samples were analysed for Ag and Cd, but analyses for these elements are not listed because all of them were below detection limit.

Trace elements in the studied intrusives are similar to those associated with granites and granodiorites (Table 6) reported by Turekian and Wedepohl (1961). In general the granite and granodiorite contain higher amounts of Cu, Ni, Ba, and Sr, and lesser amounts of Rb and Zr than the average granite or granodiorite.

Trends in trace element content in rocks from the Seligman area appear to be related to differentiation trends in the rocks. Cu,Cr,F,Ni,Rb,Sr,and V, which are commonly present in ferromagnesian silicates (biotite and hornblende) and accessory minerals (sphene and apatite) are more abundant in mafic-rich quartz monzodiorite-diorite than in granite, granodiorite, and aplite. Ba, a common trace element in K-feldspar increases with increasing differentiation, except in the case of aplite which has an unusually low average Ba content. Dacite porphyry has higher values of F,Cu,Cr,Ni,Rb,V, and Zr, and lower values of Ba and Sr than the Seligman granodiorite.

Similar trends in trace element abundances with respect to degree of differentiation are present in rocks from the Monte Cristo area. Cu,Cr,F,Ni,Rb,Sr, and V decrease and Ba increases with increasing differentiation

from granodiorite porphyry to granite porphyry. Rhyodacite porphyry has higher values of Ba,Ni,Rb,Sr, and Zr, and lower F than granodiorite and granite porphyry.

GEOCHEMISTRY OF ALTERED INTRUSIVES

Major and trace element analyses of altered intrusive rocks are presented in Table 7. Where several analyses for an alteration type were available, the values presented in the table are averages. In some cases only one representative analysis for an alteration type is presented.

Relative chemical enrichments and depletions for potassic and sericitic alteration and endoskarns are shown in Figures 39 through 43. Values for these diagrams were derived by dividing chemical values for altered rocks by the corresponding values in the fresh rock. These diagrams are intended to give a general indication of which components were enriched or depleted in the intrusives during alteration, but they do not indicate the actual amounts of material that was gained or lost, because volume changes which may have occurred during alteration are not considered. Careful sampling of precursor and altered lithologies is necessary for quantitative mass balance calculations to be meaninigful. Samples analysed for this study were not collected for the purpose of calculating mass balances, and therefore a quantitative

TABLE 7 GEOCHEMISTRY OF ALTERED INTRUSIVE ROCKS

Oxides (Wt. %)	Granodiorite			Aplite	Rhyodacite Porphyry	
	Sericitic	Epidote-Qtz Endoskarn	Plag-Px±Gar Endoskarn	Pyroxene Endoskarn	Potassic	Plag-Px Endoskarn
SiO_2	61.2±1.2	61.5 —	46.8±.5	58.5±2.0	59.8 —	54.7 —
Al_2O_3	17.1±.9	11.5 —	19.8±.2	17.1±.1	16.8 —	19.8 —
Fe_2O_3	3.5±.3	6.3 —	4.8±.1	5.1±.3	4.0 —	6.0 —
MgO	1.1±.3	.2 —	2.4±.1	1.5±.1	1.7 —	1.9 —
CaO	3.8±1.2	9.5 —	15.2±.3	7.0±.9	5.7 —	13.8 —
Na_2O	.2±.1	.1 —	1.0±.03	1.5±.7	.9 —	1.9 —
K_2O	3.5±.4	2.4 —	1.1±.1	7.4±1.4	11.8 —	.8 —
TiO_2	.53±.03	.17 —	.84±.03	.66±.03	.59 —	.76 —
P_2O_5	.15±.03	.07 —	.33±.01	.28±.01	.22 —	.21 —
MnO	.08±.03	.14 —	.20±.01	.15±.02	.10 —	.31 —
LOI	6.50±.6	1.24 —	4.09±.3	.25±.03	.25 —	-.01 —
Total	97.7	93.1	96.6	99.4	101.9	100.2
Element (ppm)						
Cu	967±361	94 —	169±19	48±10	44 —	62 —
Pb	-5	-5	14±4	-5	-5	-5
Zn	121±35	17 —	48±2	71±38	34 —	76 —
Mo	-30	-30	197±55	-30	-30	-30
WO_3	8±4	7 —	73±13	4±3	-2	-2
Ba	367±74	230 —	192±15	3100±249	3010 —	20 —
Be	2.7±.8	1.6 —	5.1±.1	1.9±.1	1.7 —	6.1 —
Cr	34±1	55 —	57±1	46±4	62 —	75 —
Co	14±5	8 —	15±1	-3	4 —	-3
F	687±117	125 —	646±22	446±92	460 —	370 —
Ni	18±3	24 —	35±1	24±6	25 —	51 —
Rb	205±38	91 —	77±7	56±9	66 —	42 —
Sr	98±16	542 —	764±48	1230±62	2180 —	1170 —
Th	24±5	31 —	34±2	33±6	31 —	38 —
V	44±5	18 —	59±2	62±9	84 —	76 —
Zr	27±3	46 —	50±1	39±4	42 —	56 —
No. of Samples	4	1	23	3	1	1

Mean ± Error

$$\text{Error} = \frac{(1.96)(\text{Standard Deviation})}{\text{No. of Samples}} \cdot \text{ at 95\% Significance Level}$$

(Beus and Grigorian, 1977)

treatment of the data would probably not be valid.

Potassic Alteration

Relative chemical changes resulting from potassic alteration are shown on Figure 39. This figure compares the chemistry of the freshest sample of rhyodacite porphyry (sample MD-5) with that of sample MD-3, which displays intense potassic alteration. The altered sample also contains clinopyroxene, which replaces primary hornblende, therefore it also exhibits some chemical characteristics of the endoskarns described below.

As shown in Figure 39, alteration of rhyodacite has apparently enriched the rock in K_2O, Ba, Sr, CaO, P_2O_5, Ni, and Zr, and has produced relative depletions in Fe_2O_3, Na_2O, MnO, Cu, Zn, Be, Rb, and V. Enrichment in K_2O and Ba, and depletion of Na_2O probably reflect the production of large amounts of K-feldspar at the expense of plagioclase. Enrichment of CaO, Sr, P_2O_5, Ni, and Zr and depletion of Fe_2O_3, Cu, Zn, Be, and Rb may be related to the conversion of hornblende to pyroxene in these rocks.

Sericitic Alteration

Figure 40 shows relative enrichments and depletions in sericitically altered granodiorite. The diagram was

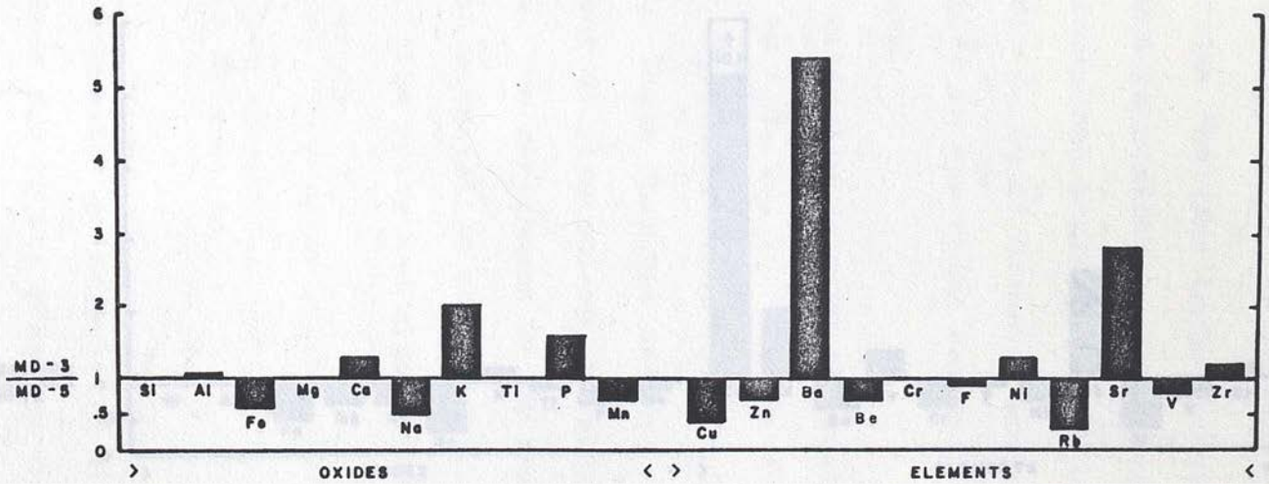

Figure 39. Graph of enrichment-depletion ratio for potassic alteration in rhyodacite porphyry. Values greater than 1 are relative enrichments; values less than 1 are relative depletions.

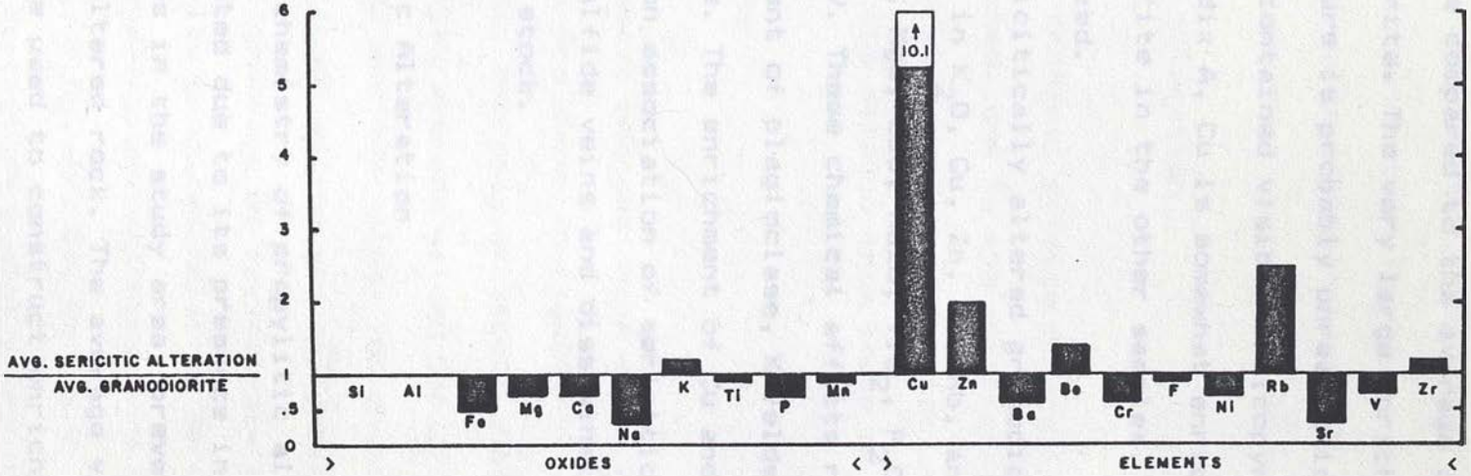

Figure 40. Graph of enrichment depletion ratio for sericitic alteration in granodiorite. Values greater than 1 are relative enrichments; values less than 1 are relative depletions.

derived using the average chemical values for 5 samples of granodiorite which exhibited intense sericitic alteration, which are compared to the average chemical values in granodiorite. The very large enrichment in Cu shown on this figure is probably unrealistic, because two of the samples contained visible chalcopyrite. However, as shown in Appendix A, Cu is somewhat enriched relative to fresh granodiorite in the other samples, which are not visibly mineralized.

Sericitically altered granodiorite is relatively enriched in K_2O, Cu, Zn, Be, Rb, and Zr, and is depleted in Fe_2O_3, MgO, CaO, Na2O, TiO_2, P_2O_5, MnO, Ba, Cr, F, Ni, Cr, and V. These chemical affects result from the replacement of plagioclase, K-feldspar and biotite by muscovite. The enrichment of Cu and Zn is consistent with the common association of sericitic alteration with quartz-sulfide veins and disseminated chalcopyrite in the Seligman stock.

Propylitic Alteration

The chemistry of propylitic alteration could not be investigated due to its presence in almost all the intrusives in the study area, preventing comparison with truly unaltered rock. The average values for granodiorite, which were used to construct enrichment-depletion

diagrams, are actually indicative of weak propylitic alteration, but they probably approximate the original chemistry of the rock. Titley and Beane (1981) noted that propylitic alteration in intrusives hosting porphyry copper deposits probably involves the rearrangement of original chemical components in the rock.

Argillic Alteration

The chemical affects of argillic alteration were not investigated, due to the occurrence of this alteration type with other alteration types, making it impossible to separate its affects from those of the other types.

Endoskarns

Chemical changes which occurred during endoskarn formation are shown in Figures 41, 42, and 43. In Figures 41 and 43B, averages or single analyses of endoskarn are ratioed with average values for granodiorite, and in Figures 42 and 43A values for endoskarns are ratioed to those of fresh aplite and rhyodacite, respectively.

The formation of epidote-quartz endoskarn in granodiorite produced relative enrichments in CaO, MnO, Cu, Rb, and Zr, and depletions in Al_2O_3, Fe_2O3, MgO, Na_2O, K_2O, TiO_2, P_2O_5, Zn, Ba, Be, F, Sr, and V (Figure 41). The observed depletions probably resulted from the destruction

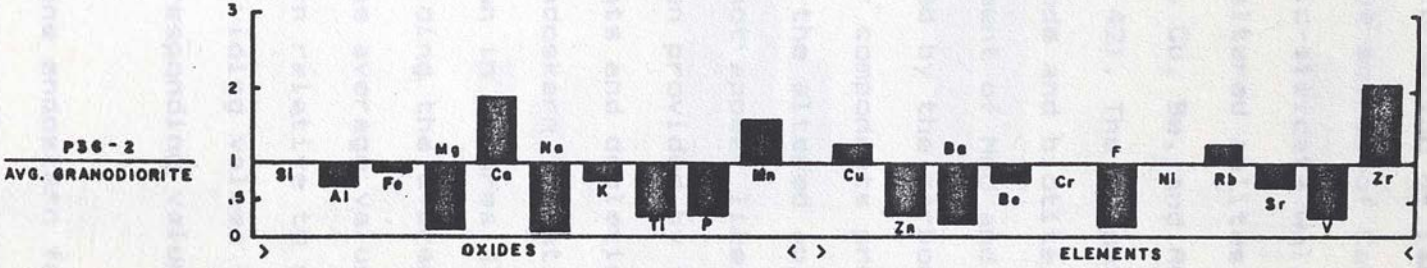

Figure 41. Graph of enrichment-depletion ratio for epidote-quartz endoskarn in granodiorite. Values greater than 1 are relative enrichments; values less than 1 are relative depletions.

of primary plagioclase, K-feldspar, biotite, and hornblende during the formation of large amounts of epidote in the rock. The source of CaO to form epidote was apparently adjacent calc-silicate wall rock.

Pyroxene-bearing altered aplites are enriched in all components except SiO_2, Cu, Be, and Rb, which are depleted in these rocks (Figure 42). The formation of pyroxene at the expense of hornblende and biotite in these rocks could account for the enrichment of MgO and CaO. These elements could have been provided by the carbonate wall rocks. The enrichment of the other components probably reflects primary differences in the altered aplites relative to fresh aplite. It does not appear likely that these elements could have been provided by the wall rock.

Chemical enrichments and depletions present in plagioclase-pyroxene endoskarn, relative to granodiorite and rhyodacite are shown in Figures 43A and 43B. Figure 43A was derived by dividing the average values of 23 endoskarn samples by the average values in granodiorite. The values for endoskarn relative to rhyodacite (Figure 43B) were derived by dividing values for sample MD-7 (endoskarn) by the corresponding values in sample MD-5 (fresh rhyodacite).

Plagioclase-pyroxene endoskarn formation produced similar changes in all elements except Cu, Zn, V, and Rb, in both rhyodacite and granodiorite. This endoskarn is

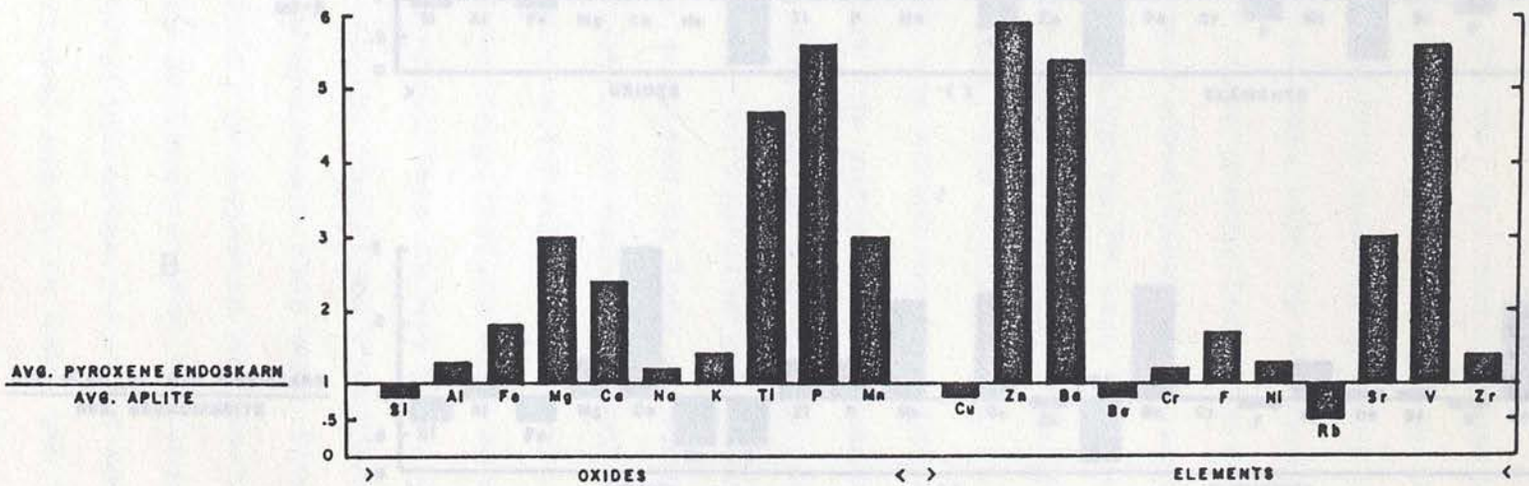

Figure 42. Graph of enrichment-depletion ratio for pyroxene endoskarn in aplite. Values greater than 1 are relative enrichments; values less than 1 are relative depletions.

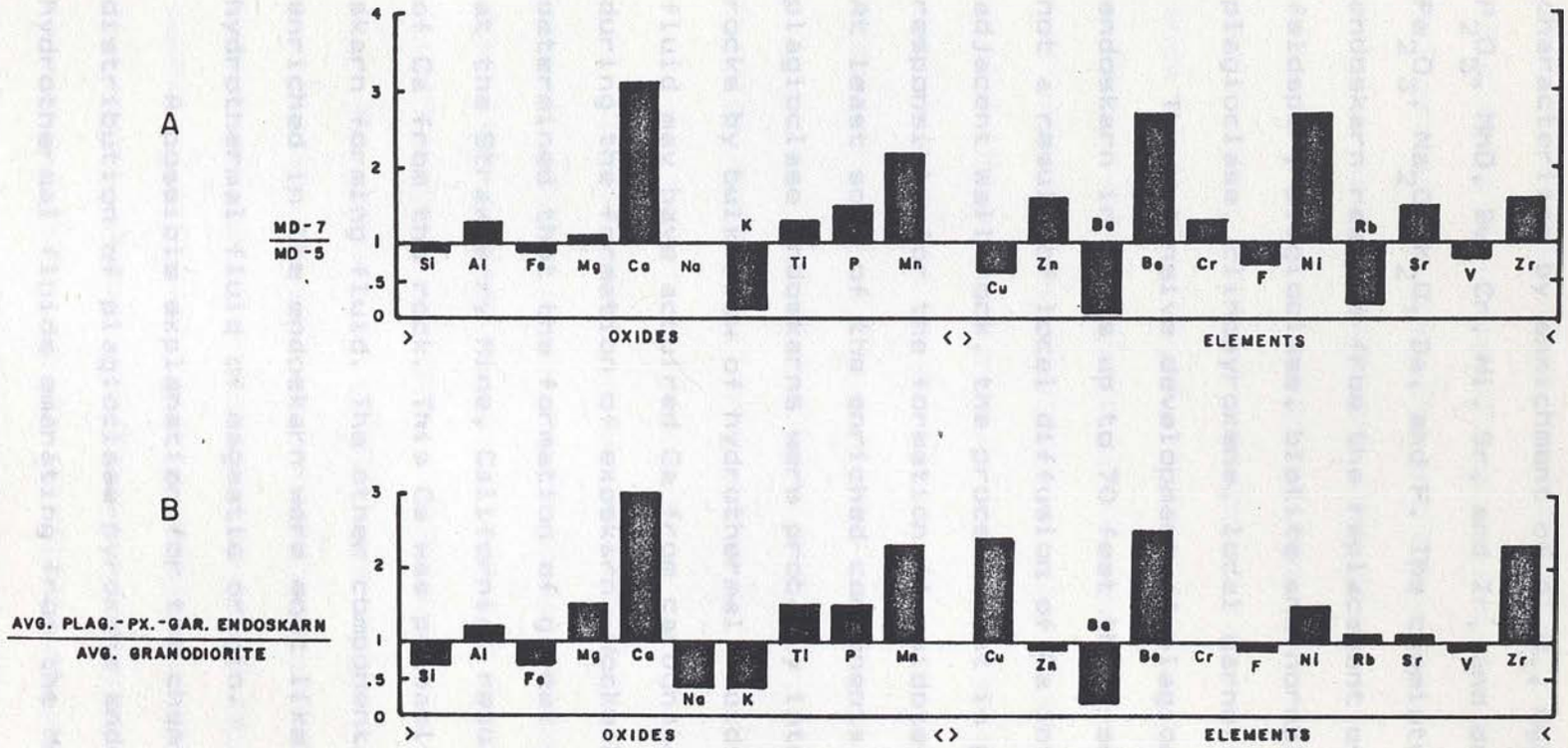

Figure 43. Graphs of enrichment-depletion ratio for plagioclase-pyroxene±garnet endoskarn in rhyodacite porphyry (A) and granodiorite (B). Values greater than 1 are relative enrichments; values less than 1 are relative depletions.

characterized by enrichment of Al_2O_3, MgO, CaO, TiO_2, P_2O_5, MnO, Be, Cr, Ni, Sr, and Zr, and depletion in SiO_2, Fe_2O_3, Na_2O, K_2O, Ba, and F. The chemistry of the endoskarn results from the replacement of primary K-feldspar, plagioclase, biotite and hornblende by calcic plagioclase, clinopyroxene, local garnet, and quartz.

The extensive development of plagioclase-pyroxene endoskarn in sills up to 70 feet thick suggests that it is not a result of local diffusion of Ca into the rock from adjacent wall rock, the process that is probably responsible for the formation of epidote-quartz endoskarn. At least some of the enriched components in the plagioclase endoskarns were probably introduced into these rocks by bulk flow of hydrothermal fluids. The altering fluid may have acquired Ca from carbonate wall rocks during the formation of exoskarn. Nockelberg (1981) determined that the formation of garnet skarn from marble at the Strawberry Mine, California, resulted in a net loss of Ca from the rock. This Ca was probably removed by the skarn forming fluid. The other components which are enriched in the endoskarn were most likely provided by a hydrothermal fluid of magmatic origin.

A possible explanation for the chemistry and spatial distribution of plagioclase-pyroxene endoskarn is that hydrothermal fluids emanating from the Monte Cristo stock produced skarn in wall rock surrounding the stock, and

became enriched in Ca during the skarn forming process. This fluid may have flowed toward the Seligman stock along sill-carbonate contacts and the contact of the Seligman stock, reacting with the intrusives and producing plagioclase-pyroxene endoskarn. This scenario could explain the observed enrichment in endoskarn of components such as Al, Mg, Ti, P, Mn, Be, Cr, Ni, Sr, and Zr, which probably were provided by a magmatic fluid, and Ca, which was probably provided by the wall rocks. It may also explain the occurrence of this type of endoskarn only in intrusive rocks on the southwest side of the Seligman stock.

CLUSTER ANALYSIS

Cluster analysis was performed on the major and trace element values in an effort to determine which elements exhibited similar chemical behavior in the intrusives. The CLUSTR program of Davis (1973) was used.

The version of CLUSTR used in this study uses the correlation coefficient (r) as a measure of similarity between elements and oxides in the data sets. The correlation coefficient is defined as the ratio of the covariance of two variables to the product of their standard deviations. It is a unitless number which ranges from -1 to +1, with a value of +1 indicating a perfect

linear relationship between the variables, and a value of -1 indicating a perfect inverse relationship between the variables. A value of 0 indicates that there is no linear relationship between the variables.

The program constructs a matrix of correlation coefficients which gives an indication of the degree of similarity between all possible pairs of elements and oxides in the data set. Weighted pair group averaging is then performed which groups the elements with the highest mutual correlations into clusters. After two elements are clustered their correlations with all other elements are averaged and a similarity matrix of the mutually highest correlations between variables is produced. The program then prints a dendrogram which is a graphic presentation of the similarity matrix.

Significance testing was done to determine which similarity values on the dendrograms were statistically significant. The null hypothesis (H:0) for these tests is H:0 r=0, or that there is no correlation between the variables. The alternate hypothesis is H:1 r<0 or r>0, because the variables can be positively or negatively correlated. A 90% significance level (alpha = 10%) was chosen for this test. The significance level (alpha) indicates the probability of rejecting the null hypothesis when it is true, which is referred to as a type I error. The critical value of r at alpha = 10%, and for the

appropriate number of samples used in the cluster analysis was obtained from a table in Koch and Link (1971, p.419). This value was then plotted as a line on the dendrograms. Similarity values which fall to the right of this line are significantly positively correlated at the 90% significance level.

Results

Cluster analysis was performed on two data sets; one which contains all analyses of 'fresh' inrusive rock (Figures 44 and 45), and another which contains analyses of plagioclase-pyroxene endoskarn (Figures 46 and 47). Plagioclase-pyroxene endoskarn was chosen for cluster analysis due to the relatively large number of analysed samples of this endoskarn (25) compared to the other alteration types. In general Mo, WO_3, Co, Th, and Pb were eliminated from cluster analysis due to the relatively large number of samples with values below detection limit for these elements. WO_3 was included in the endoskarn cluster analysis, because only two samples had WO_3 below detection limit. Correlation coefficients and similarity values greater than .184 in Figures 44 and 45, and greater than .337 in Figures 46 and 47, are considered significant at the 90% significance level.

The dendrogram for relatively fresh intrusive rocks

from the study area (Figure 45) displays three significant clusters; SiO_2-K_2O-Ba, Al_2O_3-Sr-Na_2O-Fe_2O_3-P_2O_5-MgO-TiO_2-V-CaO-MnO-Cr-Ni-Be, and Cu-F-Zr.

The first cluster consists of components which form K-feldspar, and which are generally associated with the late, more differentiated products of magmatic crystallization. The second cluster mostly contains components which are associated with mafic minerals (hornblende and biotite), accessory minerals (apatite and sphene), and calcic plagioclase, which are generally the early products of fractional crystallization of a magma. The third cluster contains components which have mafic affinities (Cu) and felsic affinities (Zr and F).

The association of Be and Na_2O with the 'mafic' cluster is unexpected because these components are typically enriched in late stage pegmatites (Boyle, 1974). However, this clustering probably reflects the trend in the intrusives of the study area of generally decreasing Na_2O and Be with increasing differentiation (Table 6 and Figure 38). The apparent depletion of Na in the more differentiated rocks (aplite and granite porphyry) may be due to intense sericitic alteration of plagioclase in these rocks. Depletion of Be in granite porphyry relative to granodiorite porphyry may be a result of partitioning of Be into late stage aqueous fluid which was exsolved from the magma during its crystallization. This aqueous

CORRELATION COEFFICIENTS

	SIO2	AL203	FE203	MGO	CAO	NA20	K20	TIO2	P205	MNO	CU	ZN	BA	BE	CR	F	NI	RB	SR	V	ZR
SIO2	1.000																				
AL203	-.541•	1.000																			
FE203	-.621•	.601•	1.000																		
MGO	-.701•	.578•	.725•	1.000																	
CAO	-.607•	.567•	.603•	.559•	1.000																
NA20	-.135	.614•	.576•	.339•	.489•	1.000															
K20	.305•	-.213•	-.603•	-.419•	-.537•	-.410•	1.000														
TIO2	-.724•	.648•	.795•	.926•	.611•	.450•	-.405•	1.000													
P205	-.676•	.719•	.744•	.711•	.614•	.520•	-.311•	.842•	1.000												
MNO	-.500•	.535•	.515•	.581•	.677•	.483•	-.241•	.643•	.652•	1.000											
CU	-.341•	-.054	.269•	.358•	.044	-.328•	-.261•	.257•	-.049	-.069	1.000										
ZN	.023	.182	-.011	.004	.021	.049	.185	.093	.213•	.192•	-.161	1.000									
BA	.115	.052	-.150	-.063	-.122	-.011	.619•	-.010	.116	.094	-.405•	.171	1.000								
BE	-.090	.311•	.218•	.228•	.341•	.446•	-.259•	.211•	.171	.503•	.071	-.006	-.275•	1.000							
CR	-.422•	.358•	.458•	.492•	.613•	.410•	-.350•	.536•	.415•	.584•	.206•	-.148	-.046	.303•	1.000						
F	-.420•	.218•	.412•	.502•	.265•	.035	-.236•	.453•	.325•	.038	.479•	.097	-.083	-.023	.169	1.000					
NI	-.384•	.323•	.423•	.410•	.596•	.209•	-.321•	.348•	.341•	.346•	.198•	-.015	-.025	.244•	.587•	.407•	1.000				
RB	-.242•	-.175	-.144	.010	-.178	-.381•	.218•	-.022	-.211•	-.054	.221•	-.131	-.130	-.048	-.013	.044	-.167	1.000			
SR	-.419•	.671•	.320•	.334•	.636•	.444•	.029	.404•	.466•	.500•	-.190•	.087	.324•	.207•	.462•	.011	.390•	-.170	1.000		
V	-.690•	.445•	.685•	.815•	.491•	.113	-.371•	.774•	.547•	.438•	.621•	.005	-.171	.182	.476•	.531•	.375•	.084	.284•	1.000	
ZR	-.155	.198•	.033	.241•	.138	-.167	.187•	.215•	.112	.311•	.375•	.128	.062	.289•	.062	.198•	.249•	.027	.216•	.441•	1.000

NUMBER OF SAMPLES USED IN MATRIX • 81

Figure 44. Matrix of correlation coefficients for fresh intrusive rocks. Significant correlations at 90% significance level ($r > .184$ or $r < -.184$) are denoted by • to right of values.

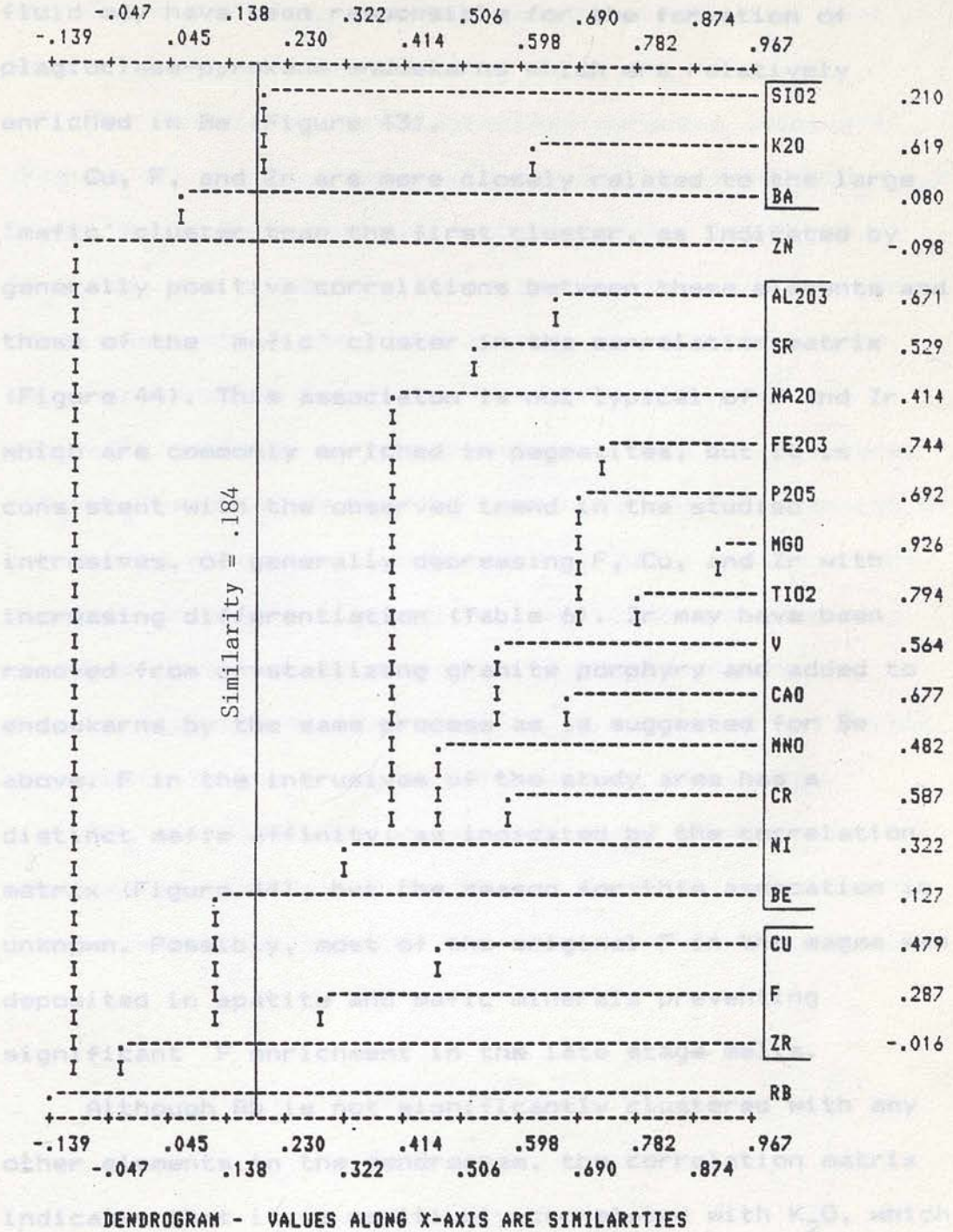

DENDROGRAM - VALUES ALONG X-AXIS ARE SIMILARITIES

Figure 45. Cluster diagram for fresh intrusive rocks based on correlation coefficients. Significant clusters at 90% significance level (similarity values > .184) are in brackets.

fluid may have been responsible for the formation of plagioclase-pyroxene endoskarns which are relatively enriched in Be (Figure 43).

Cu, F, and Zr are more closely related to the large 'mafic' cluster than the first cluster, as indicated by generally positive correlations between these elements and those of the 'mafic' cluster in the correlation matrix (Figure 44). This associaton is not typical of F and Zr which are commonly enriched in pegmatites, but it is consistent with the observed trend in the studied intrusives, of generally decreasing F, Cu, and Zr with increasing differentiation (Table 6). Zr may have been removed from crystallizing granite porphyry and added to endoskarns by the same process as is suggested for Be above. F in the intrusives of the study area has a distinct mafic affinity, as indicated by the correlation matrix (Figure 44), but the reason for this assocation is unknown. Possibly, most of the original F in the magma was deposited in apatite and mafic minerals preventing significant F enrichment in the late stage melts.

Although Rb is not significantly clustered with any other elements in the dendrogram, the correlation matrix indicates that it is positively correlated with K_2O, which is consistent with the observed similarity in chemical behavior between Rb and K (Boyle, 1974). Zn is also not clustered with any other elements, but it is positively

correlated with P_2O_5 and MnO, possibly indicating that it occurs in the mafic minerals.

The dendrogram for plagioclase-pyroxene endoskarn (Figure 47) contains seven significant clusters; SiO_2-Na_2O, Cr-Ni, Fe_2O_3-Cu-V, MgO-TiO_2-P_2O_5-F-MnO-Zn, CaO-Sr-Zr, Al_2O_3-Be, and K_2O-Ba-Rb. These associations are similar to those observed in the fresh intrusives. The components which are present in alkali feldspars, and which are generally depleted in the endoskarns, form two clusters, SiO_2-Na_2O and K_2O-Ba-Rb. The remaining clusters consist of components which are associated with mafic and accessory minerals or calcic plagioclase, and which are generally enriched in the endoskarns. The cluster analysis demonstrates the similar behavior of the mafic and felsic components in the fresh and endoskarned intrusives.

WO_3 is not clustered with any other elements and shows no statistically significant correlations with any other elements at the 90% significance level (Figure 46).

CORRELATION COEFFICIENTS

	SIO2	AL203	FE203	MGO	CAO	NA2O	K2O	TIO2	P2O5	MNO	CU	ZN	WO3	BA	BE	CR	F	NI	RB	SR	V	ZR
SIO2	1.000																					
AL203	-.073	1.000																				
FE203	.124	-.223	1.000																			
MGO	-.590 •	-.282	.050	1.000																		
CAO	-.594 •	.022	.159	.383 •	1.000																	
NA2O	.416 •	.035	.219	-.321	-.171	1.000																
K2O	-.029	.117	-.516 •	-.083	-.479 •	.006	1.000															
TIO2	-.514 •	-.272	.223	.681 •	.431 •	-.128	-.317	1.000														
P2O5	-.585 •	-.222	.110	.758 •	.438 •	-.211	-.160	.898 •	1.000													
MNO	-.173	-.348 •	-.002	.471 •	.280	.216	.157	.556 •	.531 •	1.000												
CU	-.090	-.097	.744 •	-.028	.033	-.165	-.347 •	.031	-.033	-.437 •	1.000											
ZN	-.356 •	-.359 •	.445 •	.433 •	.137	.142	.011	.541 •	.487 •	.479 •	.376 •	1.000										
WO3	-.086	.261	.174	.039	.268	-.217	-.218	.243	.132	-.152	.171	-.106	1.000									
BA	-.084	-.051	-.397 •	.018	-.231	.046	.701 •	-.059	.080	.354 •	-.315	.078	-.282	1.000								
BE	-.141	.384 •	.073	.260	.037	.201	.052	.257	.245	.243	.063	.320	-.043	.035	1.000							
CR	.383 •	-.111	.603	-.180	.178	.552 •	-.611 •	.074	-.059	.091	.112	-.020	.046	-.473 •	-.160	1.000						
F	-.705 •	.045	.030	.569 •	.420 •	-.238	.093	.726 •	.746 •	.299	.127	.501 •	.163	.090	.375 •	-.322	1.000					
NI	.176	-.346 •	.409 •	.104	.183	.105	-.268	.215	.164	.308	.067	.114	-.138	-.132	-.164	.562 •	-.086	1.000				
RB	-.104	-.030	-.477 •	.064	-.553 •	-.099	.627 •	-.305	-.244	.055	-.319	-.109	-.240	.458 •	-.043	-.424 •	.023	-.150	1.000			
SR	-.219	-.000	-.077	-.038	.419 •	.251	-.221	.071	.132	.004	-.185	-.007	-.087	-.010	-.257	.144	-.101	-.040	-.291	1.000		
V	.083	-.425 •	.618 •	.195	.122	.008	-.207	.495 •	.290	.187	.526 •	.473 •	.230	-.102	.129	.148	.273	.359 •	-.380 •	-.213	1.000	
ZR	-.317	-.253	-.043	.117	.367 •	.081	-.309	.137	.029	-.037	-.018	-.008	-.256	-.089	-.297	.192	-.073	.315	-.095	.409 •	.028	1.000

NUMBER OF SAMPLES USED IN MATRIX = 25

Figure 46. Matrix of correlation coefficients for plagioclase-pyroxene±garnet endoskarns. Significant correlations at 90% significance level ($r > .337$ or $r < -.337$) are denoted by • to right of values.

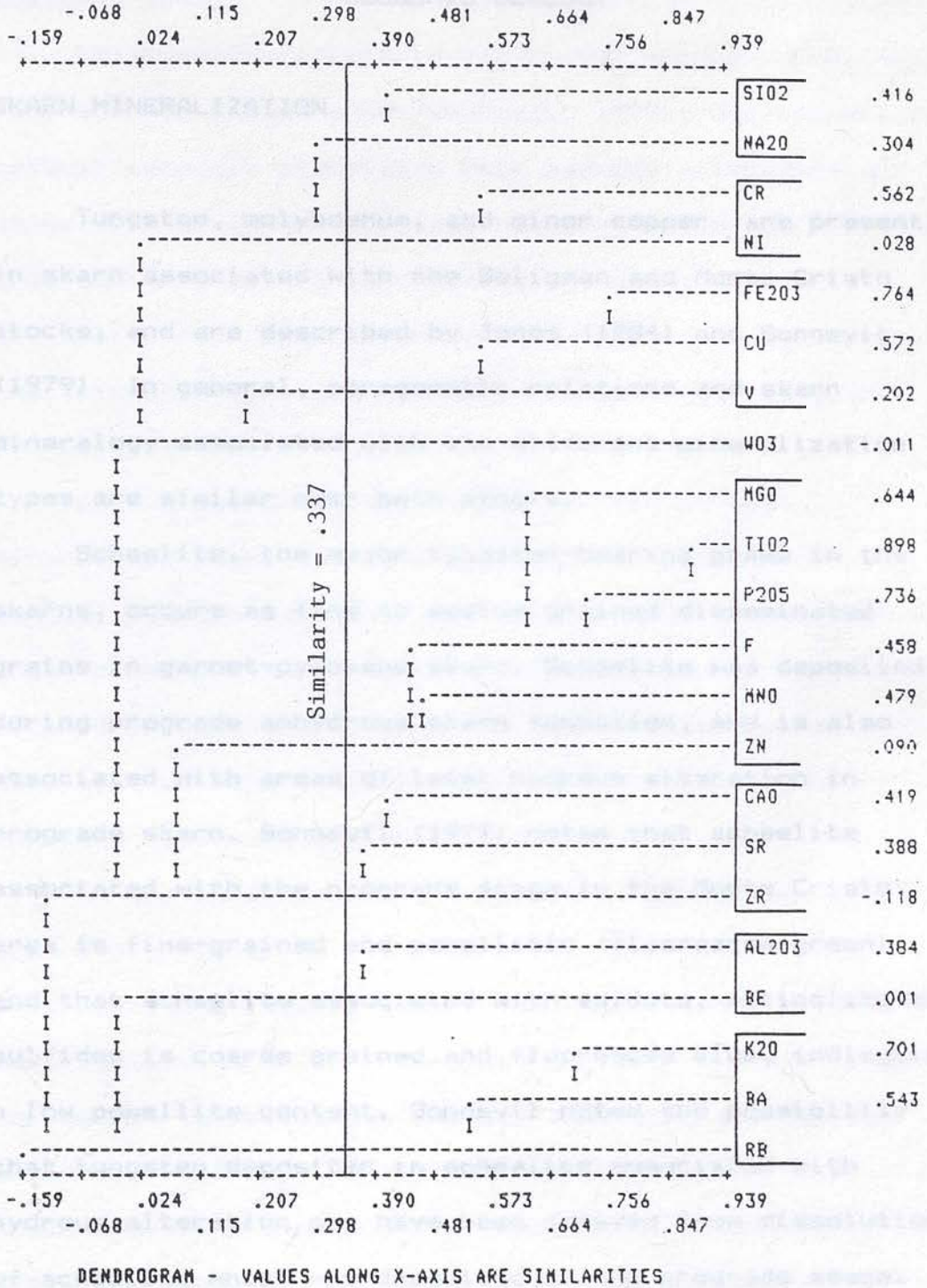

Figure 47. Cluster diagram for plagioclase-pyroxene±garnet endoskarn based on correlation coefficients. Significant clusters at 90% significance level (similarity values > .337) are in brackets.

ECONOMIC GEOLOGY

SKARN MINERALIZATION

Tungsten, molybdenum, and minor copper are present in skarn associated with the Seligman and Monte Cristo stocks, and are described by Jones (1984) and Sonnevil (1979). In general, paragenetic relations and skarn mineralogy associated with the different mineralization types are similar near both stocks.

Scheelite, the major tungsten-bearing phase in the skarns, occurs as fine to medium grained disseminated grains in garnet-pyroxene skarn. Scheelite was deposited during prograde anhydrous skarn formation, and is also associated with areas of later hydrous alteration in prograde skarn. Sonnevil (1979) noted that scheelite associated with the prograde stage in the Monte Cristo area is fine-grained and powellitic (fluoresces green), and that scheelite associated with epidote, actinolite and sulfides is coarse grained and fluoresces blue, indicating a low powellite content. Sonnevil noted the possibility that tungsten deposited in scheelite associated with hydrous alteration may have been derived from dissolution of scheelite which was deposited in the prograde stage. Jones (1984) noted similar relationships between fluorescence in scheelite and associated mineralogy in the

Seligman area.

Molybdenite is locally associated with prograde skarn in the Monte Cristo area (Sonnevil, 1979), but appears to be most commonly associated with hydrous alteration and deposition of other sulfides. Molybdenite in the Seligman area commonly occurs in chlorite, epidote, and actinolite-rich altered areas in garnet-pyroxene skarn, and in quartz-pyrite-chalcopyrite-epidote veinlets (Jones,1984).

Late stage oxidation of molybdenite in some mineralized zones near the Seligman stock has produced powellite which pseudomorphically replaces molybdenite. In these zones pyrite is converted to limonite and garnet is altered to biotite, epidote and iron oxides (Jones, 1984). This type of late stage alteration was not noted by Sonnevil (1979) in the Monte Cristo area.

In the Seligman area, relatively high grade (greater than 0.1 % WO_3 or Mo) tungsten and molybdenum mineralization locally occur in the same interval, but in most cases mineralized intervals exhibit values of .X % for one of the elements, whereas the other element is present at the .0X % level or lower. This could indicate that tungsten and molybdenum were deposited during different stages by different fluids, as is suggested by associated gangue mineralogy, or that these metals were carried by the same fluid and deposited under different

chemical conditions at different places in the system. It is unknown whether these elements display similar relatonships in mineralized zones in the Monte Cristo area.

MINERALIZATION IN INTRUSIVE ROCKS

Weak molybenum and copper mineralization is present in most of the intrusives in the study area. Scheelite was observed only in plagioclase-pyroxene endoskarn. Silver and lesser amounts of gold are contained in quartz-sulfosalt veins in both stocks.

Molybdenite occurs in isolated veinlets and as local disseminations in granodiorite, dacite porphyry, granite porphyry, granodiorite porphyry and endoskarns. Molybdenite is present as disseminated fine to medium grained rosettes and streaks in 0.5 to 2 cm thick quartz-pyrite$\pm$epidote veinlets. Veinlets which lack epidote commonly have sericitic alteration selvages, while epidote-bearing veins have epidote-clinozoisite alteration selvages. Disseminated molybdenite usually occurs in areas which also contain molybdenite-bearing quartz veins.

In plagioclase-pyroxene endoskarn, disseminated molybenite is commonly rimmed by clinozoisite suggesting that it was deposited during hydrous alteration of endoskarn. In drill hole PH-40, plagioclase endoskarn has

been altered to prehnite and disseminated molybdenite is locally altered to powellite, suggesting that late stage fluids which altered molybdenite to powellite were also responsible for alteration of endoskarn to prehnite. Prehnite-altered endoskarn at the surface locally contains powellite after molybdenite (Figure 48). Disseminated molybdenite and powellite also occur in drill hole PH-22 associated with intensely sericitically altered garnet endoskarn in an aplitic zone.

Molybdenum mineralization in the intrusives appears to be too discontinuous and too low grade to be economic. Specific assay data from the Monte Cristo area are not available, but molybdenite in granite porphyry and granodiorite porphyry appears to be limited to isolated veinlets and minor disseminations. The best intercepts of molybdenum mineralization in intrusives in the Seligman area occur in endoskarn in holes PH-51 and PH-22. In PH-51 a 20 foot interval within a 70 foot thick plagioclase-pyroxene endoskarn sill averages 0.13 % Mo, and in PH-22 a 29 foot interval in sericitically altered garnet endoskarn averages 0.36 % Mo.

Tungsten in the form of scheelite is virtually absent from the intrusive rocks. However, scheelite was observed in one thin section of plagioclase-pyroxene endoskarn (Figure 21), where it occurs disseminated in a quartz-rich zone in association with molybdenite and clinozoisite.

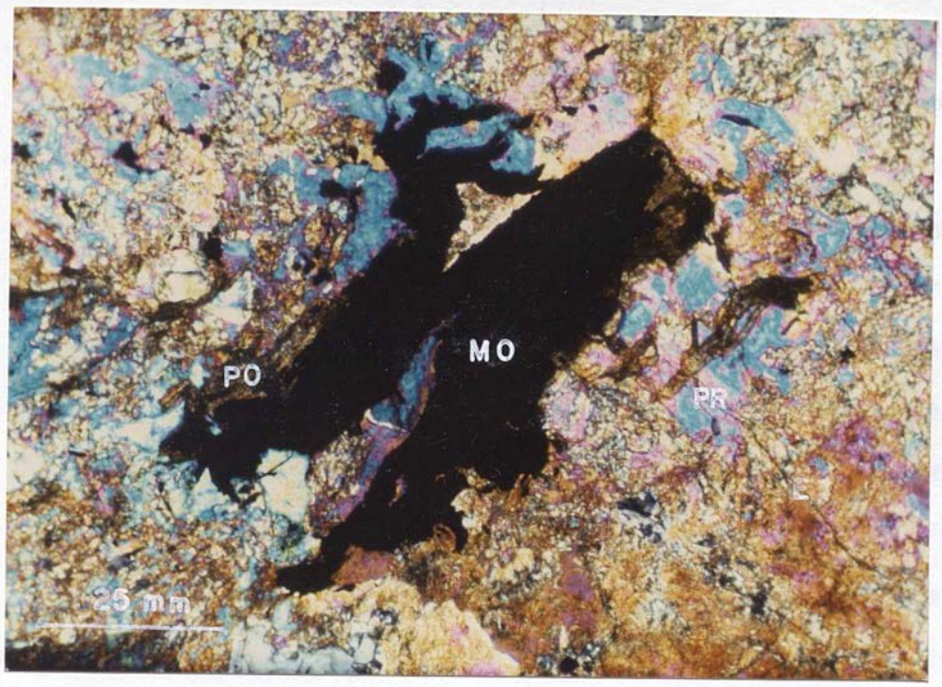

Figure 48. Photomicrograph of powellite (PO) replacing molybdenite (MO) in prehnite (PR)-altered epidote (E) endoskarn. Crossed nicols. (Sample SD-7)

Scheelite, without associated molybdenite, has also been observed in hand specimen with the aid of a black light in endoskarn. Geochemical analyses of endoskarn (Appendix A) indicate that tungsten is enriched in the plagioclase endoskarns relative to fresh granodiorite, suggesting that tungsten was introduced during endoskarn formation. Molybdenite deposition in these endoskarns appears to be associated with later alteration of endoskarn to epidote-clinozoisite.

Copper mineralization is locally present in the Seligman and Monte Cristo stocks as quartz-pyrite-chalcopyrite veinlets and local zones of disseminated chalcopyrite. In granodiorite these veinlets range in thickness from 3 mm to 2 cm and they typically have sericitic alteration selvages. Disseminated blebs of medium grained chalcopyrite$\pm$pyrite$\pm$molybdenite are generally limited to areas of intense sericitic alteration in the granodiorite.

Copper assays up to 0.3 % for a 2 foot interval have been obtained from mineralized zones in granodiorite. This copper mineralization appears to be most common in the buried portion of the Seligman stock, in the vicinity of holes PH-4, PH-5, PH-28, PH-39, PH-45, and PH-49. Sonnevil (1979) reports similar copper grades (up to 0.2 %) in the Monte Cristo stock.

Precious metal mineralization in the Seligman and

Monte Cristo stocks occurs in quartz-sulfosalt veins. Sonnevil (1979) reported the presence of 0.5 to 6 cm quartz-tetrahedrite veins in the Monte Cristo area which carry silver and small amounts of gold. Precious metal veins in the Seligman area are apparently more extensive than those associated with the Monte Cristo stock (Jones, 1984). These veins are up to 6 ft thick at the surface, and generally trend northwest and dip to the northeast (Plate 1). According to Jones the most common assemblage in these veins is sphalerite-pyrite-stibnite±tetrahedrite-bournonite-jamesonite. Granodiorite wall rock adjacent to these veins is intensely altered to sericite.

RELATION OF SKARN MINERALIZATION TO INTRUSIVES

Both the Seligman and Monte Cristo stocks were capable of producing tungsten and molybdenum mineralization, as indicated by the presence of these metals in skarn peripheral to both stocks. Unfortunately the high detection limits for Mo and WO_3 used in this study make it impossible to determine whether one stock was significantly enriched in these elements relative to the other. The similarity in type and style of mineralization associated with both stocks suggests that the magmas they crystallized from had similar W and Mo contents.

Unlike tungsten skarns which developed in relatively massive marble, such as Pine Creek, California (Bateman, 1965; Newberry, 1982) and Tem Piute, Nevada (Buseck, 1967), skarn and mineralization in the study area is generally not limited to a relatively narrow zone along the stock contacts. The well-bedded nature of the carbonate wall rock has apparently allowed mineralized fluids, which probably were produced by both stocks, to flow outward and produce mineralized zones in skarn up to 1500 ft laterally from the intrusives. Sonnevil (1979) and Jones (1984) attributed the extensive development of skarn away from intrusive contacts to the presence of highly permeable siltstone-limestone interbeds which acted as conduits for metasomatic fluids. Therefore, the location of skarn and associated mineralization is more related to wall rock bedding attitude than it is to variations in the stock contact.

An examination of cross sections with assay values from the Seligman area indicates that mineralized skarn intersected in drill holes southwest of the Seligman stock is more continuous than that which occurs on the northeastern side of the stock. Mineralization in this area may be a result of remobilization of pre-existing tungsten and molybdenum mineralization, which was produced during intrusion of the Seligman stock by fluids which were expelled from the Monte Cristo stock. The presence of

plagioclase-pyroxene endoskarn in sills and in the buried Seligman stock southwest of the stock outcrop, may be an indication of fluid input from the Monte Cristo stock.

Detailed study of skarn and mineralization paragenesis in drill core from the area between the two stocks would be necessary to determine the presence of overlapping stages of mineralization, which may have been produced by multiple intrusion.

INTRUSIVE AND ALTERATION HISTORY

The Seligman and Monte Cristo stocks are the surface expression of an apparently much larger granodioritic intrusive system which underlies the west flank of Pogonip Ridge. The stocks exhibit similarities in geochemistry, mineralogy and associated mineral deposits, and a close spatial relationship, all of which are features which suggest that the stocks were derived from the same magma chamber. However, the stocks are markedly different in alteration and texture, indicating differences in their cooling histories and style of emplacement. The Monte Cristo stock appears to be younger than the Seligman stock although crosscutting relationships between them have not been observed. This inference is based on the presence of plagioclase-pyroxene endoskarn in granodiorite only on the southwest side of the Seligman stock. K-Ar dates on the stocks are inconclusive due to overlapping error brackets, but are permissive of the inferred age relationships.

The intrusive history of the area began in Early Cretaceous time with the passive emplacement of a large body of granodioritic magma (Seligman stock) into a thick section of Cambrian carbonates, at a depth of 6 to 8 km. As temperatures rose in the contact zone of the stock, limestone and calcareous siltstone wallrocks were converted to marble and hornfels. A narrow 'chilled' margin of

porphyritic granite formed where the magma was in contact with cooler wall rocks, and sills and minor dikes of granodiorite, granite and diorite were emplaced into the carbonates. Local diffusion of Ca from adjacent wallrocks produced small bodies of epidote-quartz endoskarn in granodiorite near intrusive contacts.

As crystallization of the stock proceeded, the remaining melt became saturated with water resulting in exsolution of an aqueous phase which migrated out from the stock along permeable beds, producing metasomatic garnet-pyroxene skarn and local tungsten mineralization in marble and hornfels. Aqueous phase saturation in the Seligman stock may have occurred when the stock was 80 to 90 % crystallized, as indicated by the modal percentage of late-crystallizing K-feldspar in the granodiorite. This K-feldspar fills in around plagioclase crystals which locally display myrmekitic overgrowths of quartz and oligoclase. According to Hibbard (1979), myrmekite in granitic rocks serves as a marker between pre- and post-aqueous phase saturation. Relatively minor amounts of late stage K-rich fluids crystallized as local aplite-pegmatite dikes and veinlets in granodiorite and fractured hornfels near the stock contacts. Aplite adjacent to hornfels commonly contains metasomatic pyroxene and/or garnet presumably due to diffusion of calcium from adjacent wallrocks.

After crystallization of the Seligman stock, narrow

dacite porphyry dikes were locally emplaced along steep fractures along the southwestern flank of the Seligman stock. These dikes are texturally similar to the intrusives of the Monte Cristo area, and their emplacement may have been temporally related to the intrusion of the Monte Cristo stock.

Intrusive activity in the Monte Cristo area apparently began with the emplacement of rhyodacite porphyry sills and dikes, which was followed by the intrusion of the Monte Cristo stock (granite porphyry) and granodiorite porphyry sills and dikes. The presence of potassic alteration in rhyodacite porphyry, the source of which was probably the Monte Cristo stock, suggests that rhyodacite predates the Monte Cristo stock.

The Monte Cristo stock and associated granodiorite porphyry may have crystallized from a relatively water-rich magma which was derived from the magma which produced the Seligman stock. Intense fracturing and quartz-K-feldspar veining, which generally were limited to the Monte Cristo stock, may have occurred due to relatively violent release of a potassium and silica-rich aqueous fluid from the stock as it crystallized to the point of aqueous phase saturation. Aqueous phase release may have caused quenching of the remaining melt, producing the fine-grained quartz-K-feldspar groundmass of granite and granodiorite porphyry.

As the released magmatic fluid migrated from the stock along silty carbonate beds, it produced garnet-pyroxene skarn and local tungsten mineralization in carbonates peripheral to the Monte Cristo stock. This fluid may have travelled northeastward along sill-carbonate contacts and the Seligman stock contact, producing plagioclase-pyroxene±garnet endoskarns in rhyodacite porphyry and granodiorite by calcium metasomatism. Calcium may have been added to these fluids during the formation of exoskarns in the carbonates.

As temperatures declined in the contact aureole of the stocks, quartz-sulfide and quartz-sulfosalt veins with sericite or epidote selvages were emplaced along fractures in the solidified intrusives. Hydrous alteration and molybdenite, chalcopyrite, and pyrite deposition in prograde exoskarns adjacent to the stocks may have occurred contemporaneously with this alteration and mineralization. Meteoric water may have been a major component in the solutions responsible for retrograde alteration. Isotopic studies by Taylor and O'Neil (1977) indicated that significant amounts of meteoric water were present during hydrous alteration of tungsten skarns in the Osgood Mountains, Nevada.

With further decrease in temperature in the contact zones, prehnite, and locally kaolinite, were deposited in the intrusives, possibly by encroaching meteoric waters.

These waters may have been responsible for oxidation of molybdenite to powellite in some mineralized exoskarn and endoskarn peripheral to the Seligman stock. The final stage of alteration, which probably occurred at very low temperature, was the deposition of laumontite as narrow fracture fillings in the intrusives.

RECOMMENDATIONS FOR FURTHER STUDY

Although several studies related to tungsten-molybdenum skarns in the Seligman-Monte Cristo area have been undertaken, more detailed studies are necessary to unravel the history of this magmatic/hydrothermal system. Major element geochemical analyses of the various types of hornfels and skarn and correlative precursor lithologies could be used to delineate the role of metasomatism in the formation of hornfels and skarn. Microprobe study of chemical zonation in skarn minerals from the Seligman area could indicate what changes occurred in the hydrothermal solutions during skarn formation. Oxygen and hydrogen isotopic study of skarn and intrusives could determine the sources for fluids involved in different stages of skarn formation and alteration.

REFERENCES

Adair, D.H., and Stringham, B., 1960, Intrusive igneous rocks of east-central Nevada: in Guidebook to the Geology of East-Central Nevada: Intermountain Assoc. Petrol. Geol., 11th Annual Field Conference, Salt Lake City, Utah, p. 229-311.

Armstrong, R.L., 1970, K-Ar dating using neutron activation for Ar analysis: comparison with isotope dilution Ar analyses: Geochim. et Cosmochim. Acta, vol. 34, p.233-236.

Bateman, P.C., 1965, Geology and tungsten mineralization of the Bishop District, California: U.S. Geol. Survey, Prof. Paper 470, 208 p.

Beus, A.A., and Grigorian, S.V., 1977, Geochemical exploration methods for mineral deposits: Applied Publishing Co., Wilmette, Illinois, 287 p.

Bingler, E.C., Trexler, D.T., Kemp, W.R., and Bonham, H.F., Jr., 1976, PETCAL: A BASIC language computer program for petrologic calculations: Nevada Bur. Mines and Geol., Rept. 28, 27 p.

Boyle, R.W., 1974, Elemental associations in mineral deposits and indicator elements of interest in geochemical prospecting: Canadian Geol. Survey, Pap. 74-45, 40 p.

Brand, S.R., 1980, Structure and alteration map of the Mt. Hamilton-Monte Cristo area, Nevada: unpub. map, Phillips Petroleum Co.

Burnham, C.W., and Ohmoto, H., 1980, Late stage processes of felsic magmatism, Mining Geol., Spec. Issue 8, p. 1-11.

Buseck, P.R., 1967, Contact metasomatism and ore deposition: Tem Piute, Nevada: Econ. Geol., v. 62, p.331-353.

Carroll, D., 1970, Clay minerals: A guide to their x-ray identification, Geol. Soc. America, Spec. Pap. 126, 80 p.

Dalrymple, G.B., 1979, Critical tables for conversion of K-Ar ages from old to new constants, Geol., v. 7, p.558-560.

Davis, J.C., 1973, Statistics and data analysis in geology: John Wiley & Sons, 550 p.

Edwards, G., and McLaughlin, W.A., 1972, Shell list no. 1, K-Ar and Rb-Sr age determinations of California, Nevada, and Utah rocks and minerals: Isochron/West, no. 3, p.1-7.

Einaudi, M.T., Meinert, L.D., and Newberry, R.J., 1981, Skarn deposits, Econ. Geol., 75th anniv. vol., p 317-391.

Einaudi, M.T., and Burt, D.M., 1982, Introduction: Terminology, classification, and composition of skarn deposits: Econ. Geol., v. 77, p. 745-754.

Hague, A., 1870, Geology of the White Pine District, Nevada: U.S. Geol. exploration 40th parallel (King), v. 3, p. 409-444.

Hewett, D.F., and Radtke, A.S., 1967, Silver-bearing black calcite in western mining districts: Econ. Geol., v. 62, no.1, p. 1-21.

Hibbard, M.J., 1979, Myrmekite as a marker between preaqueous and postaqueous phase saturation in granitic systems: Geol. Soc. America Bull., v. 90, p. 1047-1062.

Hose, R.K., Blake, M.C. Jr., and Smith, R.M., 1976, Geology and mineral deposits of White Pine County, Nevada: Nevada Bur. Mines and Geol., Bull. 85, 105 p.

Houghton, J.G., Sakamoto, C.M., and Gifford, R.O., 1975, Nevada's weather and climate: Nevada Bur. Mines and Geol., spec. pub. 2, 78 p.

Irvine, T.N., and Barager, W.R.A., 1971, A guide to the classification of the common volcanic rocks: Canadian Jour of Earth Sci., v. 8, p. 523-543.

Jackson, W.T., 1963, Treasure Hill: portrait of a silver mining camp: Tuscon, Ariz., Univ. Arizona Press, 251 p.

Jones, S.K., 1984, Geology and mineralization in the zone of contact metamorphism associated with the Seligman Stock, White Pine Mining District, White Pine County, Nevada: unpub. M.S. thesis, Univ. Nevada Reno, 93 p.

Keys, W.S., 1955, The geology of the Mary Ellen Mine, Hamilton District, White Pine County, Nevada: unpub. M.A. thesis, Univ. California Los Angeles, 63 p.

Koch, G.S., and Link, R.F., 1970, Statistical analysis of geological data Volume II: John Wiley & Sons, 438 p.

Langenheim, R.L., and Larson, E.R., 1973, Correlation of Great Basin stratigraphic units: Nevada Bur. Mines and Geol., Bull. 72, 36 p.

Larsh, W.S., 1909, Mining at Hamilton, Nevada: Mines and Minerals, v. 29, p. 521-523.

Levinson, A.A., 1974, Introduction to exploration geochemistry: Wilmette, Ill., Applied Publishing Ltd., 614 p.

Meyer, C., and Hemley, J.J., 1967, Wall rock alteration, in Barnes, H.L., ed., Geochemistry of hydrothermal ore deposits: New York, Holt, Rinehart and winston, p. 166-235.

Moores, E.M., Scott, R.B., and Lumsden, W.W., 1968, Tertiary tectonics of the White Pine-Grant Range region, east-central Nevada, and some regional implications: Geol. Soc. America Bull., v. 79, p. 1703-1726.

Newberry, R.J., 1982, Tungsten-bearing skarns of the Sierra Nevada I - the Pine Creek Mine, California: Econ. Geol.,v. 77, p. 823-844.

Newberry, R.J., and Einaudi, M.T., 1981, Tectonic and geochemical setting of tungsten skarn mineralization in the Cordillera: Arizona Geol. Soc. Digest, v. 14, p. 99-111.

Nockelberg, W.J., 1981, Geologic setting, petrology, and geochemistry of zoned tungsten-bearing skarns at the Strawberry Mine, central Sierra Nevada, California: Econ. Geol., v. 76, p. 111-133.

Nockolds, S.R., 1954, Average chemical compositions of some igneous rocks: Geol. Soc. America Bull., v. 65, p. 1007-1032.

Nolan, T.B., Merriam, C.W., and Williams, J.S., 1956, The stratigraphic section in the vicinity of Eureka, Nevada: U.S. Geol. Survey Prof. Pap. 276, 77 p.

Smith, R.M., 1970, Treasure Hill reinterpreted: Econ. Geol., v. 65, p. 538-540.

Sonnevil, R.A., 1979, Evolution of skarn at Monte Cristo, Nevada, unpub. M.S. thesis, Stanford Univ., 84 p.

Stewart, J.H., 1980, Geology of Nevada: Nevada Bur. Mines and Geol. Spec. Pub. 4, 136 p.

Streckheisen, A.L., 1973, Plutonic rocks - classification and nomenclature by the IUGS subcommission: Geotimes, v. 18, no. 16, p. 26-30.

----------, 1979, Classification and nomenclature of volcanic rocks, lamprophyres, carbonatites, and mellilitic rocks - Recommendations and suggestions of the IUGS subcommision on the systematics of igneous rocks: Geol., v. 7, p. 331-335.

Taylor, B.E., and O'Neil, J.R., 1977, Stable isotope studies of metasomatic Ca-Fe-Al-Si skarns and associated metamorphic and igneous rocks, Osgood Mountains, Nevada: Contrib. Mineral. Petrol., v. 63, p. 1-49.

Thornton, C.P., and Tuttle, O.F., 1960, Chemistry of igneous rocks I - Differentiation index: Am. Jour. Sci., v. 258, p. 664-684.

Titley, S.R., and Beane, R.E., 1981, Porphyry copper deposits: Econ. Geol., 75th anniversary vol., p. 214-269.

Tracy, W.C., 1980, Structure and stratigraphy of the central White Pine Range, east-central Nevada: unpub. M.S. thesis, California State Univ. Long Beach, 66 p.

Turekian, K.K., and Wedepohl, K.H., 1961, Distribution of the trace elements in some major units of the earth's crust: Geol. Soc. America Bull., v.72, p.175-192.

APPENDIX A.

Major and Trace Element Analyses of Intrusive Rocks

Rock Type Codes

GRDI = Hornblende Biotite Granodiorite
GRAN = Hornblende Biotite Granite
MZDI = Quartz Monzodiorite, Diorite
APLT = Aplite
APLA = Pyroxene Endoskarn in Aplite
DACP = Biotite Dacite Porphyry
RDAP = Biotite Hornblende Rhyodacite Porphyry
GRNP = Biotite Granite Porphyry
GRDP = Biotite Granodiorite Porphyry
ESK1 = Plagioclase-Pyroxene-(Garnet) Endoskarn in Granodiorite
ESK2 = Prehnite-altered Endoskarn
ESK3 = Epidote-Quartz Endoskarn
ESK4 = Plagioclase-Pyroxene Endoskarn in Rhyodacite Porphyry
GRDS = Sericitically Altered Granodiorite

SAMPLE	ROCK >	OXIDES IN %										< >					ELEMENTS IN PPM										<
NUMBER	TYPE	SI	AL	FE	MG	CA	NA	K	TI	P	MN	CU	PB	ZN	MO	WO3	BA	BE	CR	CO	F	NI	RB	SR	TH	V	ZR
P4-2	GRDI	63.2	16.6	7.0	2.0	5.5	2.0	3.6	.58	.20	.10	229	-5	79	-30	5	1230	2.0	53	39	100	27	68	762	10	76	38
P4-3	GRDI	63.9	16.6	6.7	1.6	5.0	2.7	2.4	.50	.20	.10	38	5	81	-30	12	1400	1.7	40	37	750	27	46	839	14	71	29
P5-2	GRDI	69.9	15.9	6.0	1.2	4.4	2.7	3.1	.46	.19	.09	32	-5	48	-30	-2	1300	1.6	52	49	620	28	50	634	14	56	30
P5-4	GRDI	64.2	16.0	7.0	2.2	5.2	2.5	2.4	.58	.22	.12	69	25	104	-30	10	1380	2.8	54	49	1050	32	50	738	16	82	31
P5-7	GRDI	68.4	16.0	5.4	1.2	3.7	2.8	3.9	.43	.19	.06	32	5	60	-30	5	1880	1.9	48	39	630	29	45	737	18	47	19
P7-1	GRDI	68.2	15.4	6.4	1.3	3.7	2.5	3.6	.46	.18	.07	43	140	35	-30	5	968	2.2	58	-3	680	21	110	607	-6	45	22
P7-4	GRDI	60.9	15.7	6.7	1.5	4.1	2.6	3.8	.51	.19	.08	42	200	36	-30	-2	977	2.2	54	3	690	22	73	605	13	50	18
P10-3	GRDI	63.3	17.8	6.1	1.5	5.6	2.8	3.4	.60	.24	.08	50	5	50	-30	12	1180	1.2	51	51	730	28	33	825	25	59	23
P10-10	GRDI	69.3	15.2	6.0	1.3	4.1	2.7	3.3	.50	.19	.06	45	-5	49	-30	7	1080	1.8	56	51	920	28	62	572	12	52	23
P10-11	GRDI	53.9	22.7	6.3	1.4	9.7	3.0	1.7	.54	.28	.10	58	5	84	-30	15	513	1.6	56	37	760	33	32	2600	9	71	29
P11-4	GRDI	61.0	15.5	5.9	1.9	7.0	1.8	3.3	.68	.25	.08	58	-5	44	-30	12	1030	1.2	56	33	900	31	58	665	12	82	25
P17-6	GRDI	64.7	15.9	7.0	1.4	4.1	2.7	4.0	.53	.21	.09	71	5	41	-30	-2	1060	2.6	66	-3	600	28	68	790	28	64	27
P22-7	GRDI	66.3	16.1	7.1	1.6	4.9	2.9	3.2	.59	.23	.11	35	110	74	-30	-2	1080	1.5	53	-3	890	20	78	625	-6	59	18
P23-6	GRDI	64.8	15.9	6.2	1.3	4.3	2.7	3.2	.46	.18	.06	57	150	33	-30	-2	860	2.2	49	3	700	20	104	570	-6	47	16
P24-3	GRDI	63.7	15.9	6.4	1.5	4.8	3.0	3.6	.58	.23	.06	67	-5	35	-30	-2	1040	2.1	54	-3	880	28	54	803	25	58	33
P25-4	GRDI	59.5	16.5	8.7	2.0	5.2	2.8	3.1	.69	.27	.12	50	-5	64	-30	-2	1370	2.7	64	-3	910	36	86	800	33	86	26
P26-1	GRDI	62.8	16.0	5.9	1.3	4.9	2.6	3.5	.54	.24	.09	25	-5	38	-30	-2	1190	2.5	37	-3	600	17	38	608	33	59	25
P27-7	GRDI	60.9	17.0	7.6	1.8	5.8	2.6	2.8	.64	.30	.10	70	-5	52	-30	7	1030	1.5	66	20	720	25	106	755	16	72	21
P27-15	GRDI	68.2	15.8	6.7	1.4	4.5	2.8	2.9	.46	.19	.06	71	80	35	-30	-2	1120	1.8	67	-3	600	22	75	644	-6	56	14
P30-1	GRDI	62.8	15.4	6.3	1.5	6.0	2.6	2.7	.53	.20	.09	36	90	65	-30	-2	944	1.8	42	3	680	15	70	609	-6	61	14
P30-5	GRDI	50.0	18.1	8.5	2.7	8.3	2.8	.5	.88	.36	.19	310	-5	60	-30	2	350	2.0	70	20	820	27	29	763	21	106	32
P30-8	GRDI	61.6	15.8	5.8	1.2	4.2	2.6	3.3	.46	.23	.06	76	25	31	-30	7	300	2.4	54	-3	720	21	123	588	-6	48	23
P33-3	GRDI	69.1	16.1	6.5	1.5	4.7	2.5	3.1	.49	.17	.09	29	80	53	-30	-2	1070	1.6	56	3	620	19	83	624	10	60	18
P35-3	GRDI	65.7	15.9	6.3	1.6	4.1	2.8	3.0	.47	.18	.07	27	180	64	-30	15	1280	2.0	55	3	720	16	68	692	-6	53	15
P39-4	GRDI	61.2	16.7	8.1	1.9	5.8	2.7	2.6	.59	.23	.11	44	-5	73	-30	-2	956	2.7	53	-3	610	18	50	913	32	87	31
P39-6	GRDI	62.2	16.0	7.2	1.7	4.7	2.6	3.4	.55	.23	.11	47	-5	61	-30	-2	1260	2.5	76	13	610	39	56	771	34	77	28
P42-3	GRDI	62.7	15.8	7.1	1.9	6.7	2.5	1.2	.59	.26	.11	64	-5	44	-30	20	120	2.7	60	-3	540	22	32	555	26	64	21
P45-2	GRDI	66.8	15.6	4.9	1.2	4.2	2.3	3.7	.46	.18	.06	47	170	40	-30	15	1120	3.0	47	-3	345	18	106	565	-6	38	19
P48-2	GRDI	67.3	15.5	6.3	1.4	4.0	2.3	3.5	.48	.18	.08	30	70	47	-30	7	1070	1.7	55	7	650	19	96	575	-6	52	14
P54-1	GRDI	56.6	16.0	7.5	2.2	5.0	1.6	3.9	.72	.25	.09	405	-5	3	-30	-2	670	2.1	69	34	1400	34	141	497	54	85	25
P57-3	GRDI	64.1	16.0	7.2	1.7	5.0	2.9	2.4	.57	.22	.07	42	80	38	-30	12	942	1.8	65	-3	760	21	57	757	8	60	12
P64-2	GRDI	62.9	16.1	7.2	1.6	4.9	2.7	2.7	.57	.20	.10	33	80	62	-30	7	1040	1.8	58	-3	640	17	67	658	-6	66	12
P64-3	GRDI	61.2	16.3	7.4	1.7	4.8	2.7	3.2	.59	.22	.10	33	110	62	-30	10	985	1.8	55	-3	740	20	58	645	-6	67	12
U52-2	GRDI	63.8	14.6	7.0	.8	3.5	3.0	3.7	.28	.10	.07	107	160	31	-30	52	971	1.7	52	-3	405	20	77	508	-6	29	15
U52-3	GRDI	65.0	16.4	8.1	2.0	5.0	2.7	2.8	.68	.24	.13	36	160	75	-30	12	1070	1.8	63	-3	680	22	63	619	-6	71	12
SB-3	GRDI	64.7	16.6	6.1	1.5	4.9	2.9	3.3	.56	.20	.08	22	160	49	-30	15	920	1.8	38	-3	660	15	100	667	12	54	18
SI-9	GRDI	65.4	17.1	6.5	1.3	3.7	2.8	4.4	.55	.22	.09	58	-5	61	-30	-2	1070	2.5	56	4	640	14	45	656	30	71	38
MEANS	GRDI	63.5	16.3	6.7	1.6	5.0	2.6	3.1	.55	.22	.09	69	57	53	-30	7	1022	2.0	55	13	701	23	69	725	14	63	22
P11-14	GRAN	65.6	16.3	5.1	.9	3.4	1.8	6.6	.39	.15	.06	166	5	31	-30	22	1380	1.7	51	49	700	29	69	543	16	42	30
P14-2	GRAN	61.7	16.3	5.7	2.0	5.9	2.7	3.8	.70	.24	.10	40	110	37	-30	2	1140	1.8	60	-3	920	23	88	857	-6	67	20
P18-9	GRAN	62.2	16.1	7.5	1.7	4.6	2.3	4.2	.64	.24	.10	96	-5	49	-30	-2	1760	2.6	52	13	1100	18	108	766	31	70	29
P28-6	GRAN	60.7	16.9	7.8	2.0	5.3	2.6	2.7	.65	.27	.11	56	70	66	-30	-2	955	1.8	54	-3	810	19	75	696	-6	73	12
SI-7	GRAN	65.0	16.1	4.9	1.4	4.6	3.0	3.9	.59	.23	.09	25	-5	57	-30	-2	1140	1.9	23	-3	500	14	64	656	24	63	25
SI-14	GRAN	65.5	16.3	4.4	1.3	4.5	2.5	6.0	.55	.23	.10	43	-5	265	-30	-2	1230	2.4	51	3	660	18	71	1020	44	70	29
MEANS	GRAN	63.5	16.3	5.9	1.5	4.7	2.5	4.5	.59	.23	.09	71	31	84	-30	4	1267	2.0	48	11	781	20	79	756	20	64	24

SAMPLE NUMBER	ROCK TYPE	OXIDES IN % SI	AL	FE	MG	CA	NA	K	TI	P	MN	ELEMENTS IN PPM CU	PB	ZN	MO	WO3	BA	BE	CR	CO	F	NI	RB	SR	TH	V	ZR
P27-3	MZDI	50.0	16.0	10.0	2.7	6.3	2.3	3.2	1.11	.43	.16	298	-5	70	-30	2	1450	2.3	69	25	1000	25	109	597	22	128	37
P51-9	MZDI	47.1	18.6	8.7	4.0	6.3	2.3	3.4	1.18	.43	.15	250	-5	63	-30	12	1000	2.2	65	33	1050	25	126	838	44	131	40
P51-10	MZDI	44.9	20.4	11.8	1.5	9.0	2.6	1.9	.68	.47	.13	110	-5	67	-30	-2	610	2.2	70	30	720	29	70	1150	68	129	28
MEANS	MZDI	47.3	18.3	10.2	2.7	7.2	2.4	2.8	.99	.44	.15	219	-5	66	-30	5	1020	2.2	68	29	923	26	101	861	44	129	35
P36-1	APLT	62.3	15.4	3.1	.6	2.9	1.0	7.2	.23	.08	.06	90	-5	16	-30	15	1410	2.6	37	8	270	18	240	918	23	16	23
SB-2	APLT	77.9	11.5	3.3	.2	2.0	.9	4.7	.06	.02	.04	65	5	8	-30	15	406	2.0	52	-3	110	29	48	182	23	5	26
SB-5	APLT	77.7	12.9	2.2	.1	.7	2.3	6.8	.08	.02	.03	27	10	9	-30	17	270	2.0	31	-3	62	1	70	198	30	6	41
SI-5	APLT	70.2	14.0	2.5	1.1	6.2	.9	2.9	.20	.09	.06	43	-5	18	-30	-2	208	3.1	38	-3	580	28	81	313	28	20	20
MEANS	APLT	72.0	13.5	2.8	.5	2.9	1.3	5.4	.14	.05	.05	56	-5	12	-30	12	573	2.4	39	-3	255	19	109	402	26	11	27
SB-1	APLA	60.4	17.2	5.0	1.5	6.4	2.7	5.2	.62	.28	.14	66	5	33	-30	-2	2800	2.0	47	3	360	28	46	1290	45	49	42
SB-10	APLA	58.3	17.1	4.6	1.5	5.9	1.2	9.4	.65	.26	.13	37	5	43	-30	10	3530	1.8	40	-3	610	14	73	1120	28	63	32
SB-11	APLA	56.9	17.1	5.6	1.6	8.7	.7	7.8	.72	.30	.19	41	-5	139	-30	2	2970	1.8	53	-3	370	31	51	1280	28	76	45
MEANS	APLA	58.5	17.1	5.1	1.5	7.0	1.5	7.4	.66	.28	.15	48	-5	71	-30	4	3100	1.9	46	-3	446	24	56	1230	33	62	39
P13-1	DACP	63.8	14.5	6.8	2.0	5.4	1.8	1.4	.55	.13	.06	523	10	54	-30	20	250	2.6	54	51	1650	33	49	492	8	112	47
P13-2	DACP	64.5	14.5	6.3	1.9	5.8	1.5	2.0	.61	.17	.08	253	5	50	-30	12	1130	1.6	43	51	1350	28	56	690	19	116	49
P54-3	DACP	54.8	13.6	8.4	1.7	6.3	1.6	2.8	.56	.14	.06	713	-5	29	-30	10	400	2.1	72	17	1600	29	113	563	28	112	24
P54-5	DACP	55.9	13.9	7.0	1.9	4.7	1.0	3.8	.55	.13	.05	480	-5	31	-30	-2	600	1.7	62	15	1450	26	190	377	27	111	30
MEANS	DACP	59.8	14.1	7.1	1.9	5.6	1.5	2.5	.57	.14	.06	492	-5	41	-30	10	595	2.0	57	33	1512	29	102	530	20	112	37
MB-3	RDAP	59.8	16.8	4.0	1.7	5.7	.9	11.8	.59	.22	.10	44	-5	34	-30	-2	3010	1.7	62	4	460	25	66	2180	31	84	42
MB-4	RDAP	55.5	17.7	6.2	1.9	8.4	2.1	6.5	.62	.24	.23	76	-5	48	-30	8	2680	2.5	89	-3	420	32	119	1730	25	96	51
MB-5	RDAP	60.5	15.7	6.7	1.7	4.4	1.9	5.8	.60	.14	.14	104	80	49	-30	10	556	2.3	60	-3	535	19	250	765	-6	102	35
MB-6	RDAP	67.5	15.0	4.9	1.7	6.1	2.7	4.4	.58	.15	.14	52	60	35	-30	65	665	3.0	75	-3	320	28	217	841	-6	89	36
MEANS	RDAP	60.8	16.3	5.4	1.8	6.2	1.9	7.1	.60	.19	.15	69	36	41	-30	21	1727	2.4	71	-3	433	26	163	1379	15	92	41
P56-1	GRNP	61.9	15.0	7.5	2.6	1.8	.2	1.8	.68	.19	.08	705	-5	41	-30	80	114	1.9	28	-3	810	16	116	30	-6	151	42
P56-7	GRNP	65.9	13.7	7.0	1.4	7.9	1.6	.5	.51	.16	.10	344	-5	18	-30	-2	115	2.6	69	-3	640	35	23	525	-6	99	36
U9-1	GRNP	59.1	14.1	2.9	.6	6.0	.1	3.4	.26	.10	.08	77	40	131	-30	-2	200	1.6	29	-3	930	20	181	54	-6	45	33
U9-3	GRNP	67.3	15.5	3.9	.7	3.3	2.3	5.2	.23	.13	.08	214	5	36	-30	-2	836	2.7	28	4	810	22	124	368	28	50	35
U9-4	GRNP	65.0	7.4	2.1	.2	.2	.2	4.2	.12	.05	.02	65	-5	11	-30	15	270	.6	31	-3	290	15	170	86	-6	14	14

SAMPLE	ROCK >	OXIDES IN %										< >	ELEMENTS IN PPM																<
NUMBER	TYPE	SI	AL	FE	MG	CA	NA	K	TI	P	MN	CU	PB	ZN	MO	W03	BA	BE	CR	CO	F	NI	RB	SR	TH	V	ZR		
U9-5	GRNP	65.8	16.8	4.4	1.1	3.9	3.2	5.6	.39	.14	.10	70	5	29	-30	-2	1660	3.1	54	-3	560	22	54	830	27	47	35		
U11-1	GRNP	60.6	9.1	2.5	.7	3.5	.2	4.4	.24	.10	.04	31	-5	14	-30	10	1650	.3	32	-3	450	20	134	231	-6	36	12		
U11-3	GRNP	63.0	15.0	2.4	1.6	2.6	.5	9.9	.37	.17	.05	13	-5	32	-30	15	2280	.3	22	27	1150	19	90	513	11	54	28		
U16-2	GRNP	68.2	14.8	4.4	1.6	3.6	2.1	4.4	.43	.17	.05	129	-5	22	210	-2	1130	2.5	40	-3	880	17	69	714	-6	103	25		
U16-3	GRNP	60.7	16.3	4.1	1.6	.5	.2	4.3	.43	.13	.04	209	-5	20	-30	-2	1110	1.3	31	-3	495	13	118	191	-6	68	23		
M9-8	GRNP	65.8	14.6	3.6	1.3	6.8	3.0	2.4	.46	.20	.22	42	-5	62	-30	4	521	5.3	48	-3	360	22	55	770	18	38	29		
M1-2	GRNP	72.3	12.9	3.1	.3	.7	.6	8.7	.26	.11	.04	68	5	89	-30	4	1830	.9	43	-3	580	15	88	429	-6	39	23		
M1-3	GRNP	69.9	14.7	3.6	.7	.4	1.6	6.7	.28	.12	.06	110	-5	31	-30	4	797	2.0	23	-3	100	4	34	257	-6	60	28		
M1-4	GRNP	72.4	10.5	3.2	.2	2.6	.3	6.2	.11	.10	.04	45	5	18	-30	30	1850	.8	47	-3	450	14	76	228	-6	24	18		
M1-5	GRNP	77.3	9.7	3.0	.2	2.4	.3	5.0	.13	.09	.04	42	5	12	-30	-2	1490	.8	43	-3	340	10	40	187	-6	18	18		
M1-6	GRNP	69.7	15.2	2.6	.6	.5	.4	8.2	.21	.18	.06	52	10	164	-30	4	1050	2.3	30	-3	900	24	88	125	-6	36	32		
M1-10	GRNP	76.6	11.1	1.9	.3	.6	.2	6.6	.17	.06	.03	168	55	208	-30	10	1790	.8	23	14	520	14	67	111	10	18	30		
MEANS	GRNP	67.1	13.3	3.6	.9	2.8	1.0	5.1	.31	.13	.07	140	8	55	-30	10	1099	1.8	36	3	603	17	89	332	7	52	27		
U23-1	GRDP	56.0	15.0	4.5	1.9	4.0	1.1	3.7	.47	.13	.05	152	-5	20	-30	2	210	2.1	44	-3	860	25	120	617	-6	93	23		
U41-1	GRDP	67.2	15.6	7.2	1.5	4.5	2.7	3.2	.48	.16	.07	362	-5	22	-30	-2	771	3.0	73	-3	1000	25	36	783	-6	98	38		
U50-1	GRDP	59.5	17.0	5.2	1.5	2.2	.2	4.1	.64	.16	.05	519	-5	36	-30	5	450	1.7	52	-3	900	17	178	387	-6	96	34		
U51-1	GRDP	61.4	13.8	5.8	1.6	4.3	1.5	2.8	.36	.11	.06	330	-5	20	650	-2	640	2.0	74	-3	580	26	136	510	-6	80	19		
U51-2	GRDP	60.7	14.6	6.2	1.8	4.7	1.5	2.5	.54	.11	.07	367	-5	27	160	-2	350	2.1	73	-3	510	20	142	518	-6	109	19		
U51-3	GRDP	61.4	14.6	5.7	1.3	6.7	1.6	1.0	.50	.10	.07	291	10	18	140	2	240	2.5	73	-3	340	25	45	908	-6	82	20		
MEANS	GRDP	61.0	15.1	5.7	1.6	4.4	1.4	2.9	.50	.13	.06	336	-5	23	165	2	443	2.2	64	-3	698	23	109	620	-6	93	25		
P11-6	ESK1	37.0	18.3	3.0	5.1	12.9	.7	2.1	.91	.41	.25	9	-5	61	-30	2	140	6.2	33	-3	870	18	229	380	-6	34	49		
P11-7	ESK1	37.1	18.3	3.4	2.5	18.7	.9	.8	.94	.39	.15	36	-5	44	-30	7	300	2.4	51	-3	580	26	42	2960	-6	40	77		
P11-8	ESK1	41.1	17.8	4.3	2.1	21.1	1.3	.9	.83	.39	.25	60	-5	51	30	52	110	4.0	70	47	690	42	56	1350	61	28	65		
P11-9	ESK1	37.7	17.6	3.5	3.0	19.2	.9	.8	1.76	.51	.34	43	-5	74	-30	286	130	6.2	45	19	1250	28	68	504	39	104	55		
P11-10	ESK1	41.3	17.8	9.5	2.2	13.3	1.0	.6	.87	.32	.09	1030	-5	118	-30	82	90	5.6	55	28	880	28	46	522	45	104	43		
P13-7	ESK1	46.1	22.7	2.9	.8	12.1	.7	2.8	.11	.04	.15	52	-5	14	50	58	280	4.6	39	-3	260	21	218	551	16	23	46		
P13-8	ESK1	48.9	21.4	2.1	1.6	10.9	.8	4.9	.53	.29	.19	13	-5	54	-30	12	465	4.4	18	33	820	21	108	274	31	63	34		
P27-6	ESK1	49.5	22.2	5.5	1.9	15.4	1.5	1.2	.71	.29	.23	176	-5	44	-30	30	290	5.4	85	14	520	41	79	800	19	41	41		
P27-8	ESK1	46.0	18.9	6.0	2.5	18.4	1.3	1.0	.94	.38	.37	59	-5	52	-30	15	250	4.9	67	15	800	36	59	743	24	58	44		
P27-10	ESK1	45.4	18.4	5.1	3.3	16.4	.7	.1	1.12	.41	.37	49	5	74	-30	46	110	5.2	66	19	630	43	10	754	25	48	45		
P27-11	ESK1	41.4	22.3	5.8	3.0	19.0	1.6	.2	1.30	.46	.33	71	-5	71	170	5	180	6.0	85	22	840	48	15	1010	36	72	71		
P30-3	ESK1	47.2	18.0	3.6	2.7	12.6	1.1	2.8	.96	.39	.35	25	-5	62	-30	15	810	6.0	33	18	620	29	173	371	25	62	47		
P30-4	ESK1	52.3	21.6	3.9	1.1	12.9	1.5	.7	.51	.27	.12	58	-5	28	-30	-2	110	5.7	64	15	490	35	56	979	28	22	45		
P30-6	ESK1	42.6	22.1	3.8	2.7	13.3	.8	2.5	.89	.37	.19	64	-5	50	270	15	300	5.5	50	11	940	58	232	539	28	38	53		
P42-2	ESK1	45.4	21.9	5.2	2.1	16.0	1.3	.3	.67	.21	.06	406	-5	33	-30	17	150	6.2	56	21	730	32	19	817	68	78	79		
P44-2	ESK1	60.0	17.5	4.1	1.5	12.4	.9	.2	.54	.18	.10	127	5	29	-30	22	70	2.9	67	17	170	37	12	404	41	52	57		
P44-3	ESK1	55.0	17.7	4.1	1.5	9.8	.9	.2	.54	.18	.10	126	-5	27	-30	15	100	2.9	66	6	405	36	210	405	41	50	56		
P44-4	ESK1	53.6	22.3	4.6	1.5	12.7	1.0	.7	.63	.28	.10	173	-5	28	-30	-2	38	6.8	61	-3	480	23	30	517	44	51	34		
P51-1	ESK1	48.9	24.2	6.0	2.2	17.1	.8	.2	.86	.32	.10	273	160	27	3080	725	11	4.6	66	7	620	28	5	762	26	69	32		
P51-2	ESK1	46.5	20.3	4.9	2.4	17.3	.8	.3	.71	.29	.12	253	-5	37	570	104	50	5.1	57	12	245	34	26	709	52	54	69		

SAMPLE NUMBER	ROCK TYPE	OXIDES IN % SI	AL	FE	MG	CA	NA	K	TI	P	MN	ELEMENTS IN PPM CU	PB	ZN	MO	W03	BA	BE	CR	CO	F	NI	RB	SR	TH	V	ZR
P51-3	ESK1	45.8	20.4	6.7	2.9	17.5	.8	.2	1.20	.44	.16	332	130	41	40	120	13	5.1	64	11	930	33	8	499	26	74	37
P51-5	ESK1	49.5	14.2	7.2	3.2	17.2	.4	.4	1.06	.41	.27	401	-5	48	100	55	150	3.9	70	31	560	80	27	400	85	128	61
P64-1	ESK1	57.1	19.5	4.6	2.4	14.2	1.4	1.3	.83	.35	.26	71	-5	53	-30	10	280	6.7	51	-3	540	29	45	1330	32	78	31
MEANS	ESK1	46.8	19.8	4.8	2.4	15.2	1.0	1.1	.84	.33	.20	169	14	48	197	73	192	5.1	57	15	646	35	77	764	34	59	50
P11-11	ESK2	36.1	17.7	6.2	1.3	20.4	.4	.4	.85	.27	.08	449	-5	36	80	20	90	4.8	57	23	2700	27	30	873	54	115	44
P40-1	ESK2	39.0	21.7	7.5	1.1	25.5	.3	.2	.79	.35	.47	51	-5	46	1500	2	30	4.3	70	22	660	43	18	923	76	55	53
P42-1	ESK2	58.1	15.8	7.1	2.2	13.2	.2	.2	.68	.15	.13	549	-5	25	-30	63	110	3.4	70	22	500	35	9	328	47	94	38
P51-6	ESK2	46.2	20.3	4.6	2.1	19.0	.5	.7	.74	.30	.17	97	-5	28	-30	27	90	5.1	73	29	420	55	39	437	75	67	49
P51-7	ESK2	48.4	16.8	4.7	3.7	18.3	.4	.4	1.29	.49	.22	95	-5	42	-30	71	90	4.4	64	29	560	40	23	510	92	122	61
SD-8	ESK2	44.2	17.7	8.1	1.5	25.1	.4	.6	.69	.30	.30	79	5	117	-30	10	92	2.7	85	-3	320	62	5	553	36	54	43
SD-13	ESK2	59.5	12.3	6.8	1.6	20.5	.1	.6	.57	.17	.27	44	-5	110	-30	17	78	1.1	59	36	280	38	10	337	17	48	68
MEANS	ESK2	47.4	17.5	6.4	1.9	20.3	.3	.4	.80	.29	.23	194	-5	57	236	30	82	3.7	68	23	777	42	19	565	56	79	50
P36-2	ESK3	61.5	11.5	6.3	.2	9.5	.1	2.4	.17	.07	.14	94	-5	17	-30	7	230	1.6	55	8	125	24	91	542	31	18	46
MEANS	ESK3	61.5	11.5	6.3	.2	9.5	.1	2.4	.17	.07	.14	94	-5	17	-30	7	230	1.6	55	8	125	24	91	542	31	18	46
MD-7	ESK4	54.7	19.8	6.0	1.9	13.8	1.9	.8	.76	.21	.31	62	-5	76	-30	-2	20	6.1	75	-3	370	51	42	1170	38	76	56
MD-9	ESK4	61.0	15.8	6.8	1.6	9.0	2.2	2.1	.64	.21	.26	92	-5	52	-30	65	215	3.9	95	-3	270	45	123	736	28	84	52
MEANS	ESK4	57.9	17.8	6.4	1.7	11.4	2.1	1.5	.70	.21	.28	77	-5	64	-30	33	117	5.0	85	-3	320	48	82	953	33	80	54
P28-1	GRDS	60.9	19.1	3.2	1.7	4.1	.4	4.6	.59	.11	.12	1700	-5	179	-30	5	210	4.7	35	23	800	23	266	108	26	37	34
P28-3	GRDS	58.6	14.7	2.7	1.1	6.4	.1	3.7	.51	.11	.12	1490	-5	183	-30	22	270	2.6	35	22	740	24	216	127	39	34	18
P39-1	GRDS	60.9	17.6	4.2	.9	4.3	.2	2.7	.46	.17	.05	217	-5	88	-30	5	470	2.5	35	-3	340	14	94	107	19	51	29
P49-1	GRDS	64.4	16.8	3.9	.6	.5	.3	3.2	.56	.20	.02	463	-5	37	-30	2	520	.9	32	12	870	13	246	50	14	56	29
MEANS	GRDS	61.2	17.1	3.5	1.1	3.8	.2	3.5	.53	.15	.08	967	-5	121	-30	8	367	2.7	34	14	687	18	205	98	24	44	27